Rock stability considerations for siting and constructing a KBS-3 repository

Based on experiences from Äspö HRL, AECL's URL, tunnelling and mining

C Derek Martin, University of Alberta

Rolf Christiansson, Svensk Kärnbränslehantering AB

Jörgen Söderhäll, VBB VIAK AB

December 2001

SKB

Rock stability considerations for siting and constructing a KBS-3 repository

Based on experiences from Äspö HRL, AECL's URL, tunnelling and mining

C Derek Martin, University of Alberta

Rolf Christiansson, Svensk Kärnbränslehantering AB

Jörgen Söderhäll, VBB VIAK AB

December 2001

Summary

Over the past 25 years the international nuclear community has carried out extensive research into the deep geological disposal of nuclear waste in hard rocks. In two cases this research has resulted in the construction of dedicated underground research facilities: SKB's Äspö Hard Rock Laboratory, Sweden and AECL's Underground Research Laboratory, Canada. Both laboratories are located in hard rocks considered representative of the Fennoscandian and Canadian Shields, respectively. Prior to the construction of these facilities SKB and AECL were also involved in the research carried out at Stripa Mine (Sweden). This report is intended to synthesize the important rock mechanics findings from these research programs. In particular the application of these finding to assessing the stability of underground openings.

As such the report draws heavily on the published results from the SKB's ZEDEX Experiment in Sweden and and AECL's Mine-by Experiment in Canada. Examples from mining and tunnelling are also used to illustrate the application of these findings to underground excavations in general.

The objectives of this report are to:

1. Describe, using the current state of knowledge, the role rock engineering can play in siting and constructing a KBS-3 repository.

2. Define the key rock mechanics parameters that should be determined in order to facilitate repository siting and construction.

3. Discuss possible construction issues, linked to rock stability, that may arise during the excavation of the underground openings of a KBS-3 repository.

4. Form a reference document for the rock stability analysis that has to be carried out as a part of the design works parallel to the site investigations.

While there is no unique or single rock mechanics property or condition that would render the performance of a nuclear waste repository unacceptable, certain conditions can be treated as negative factors. For example, a highly fractured rock mass such that the overall rock mass permeability is not acceptable or high in-situ stress magnitudes such that construction of the underground openings will create a safety concern for the construction workers. Outlined below are major rock mechanics issues that should be addressed during the siting, construction and closure of a nuclear waste repository in Sweden in hard crystalline rock.

Siting requirements

During the site investigations phase, rock mechanics information will be predominately gathered from examination and testing of the rock core and mapping of the borehole walls. Two major tasks must be accomplished during this period:

1. an assessment of the quality of the rock mass and

2. an assessment of the state of stress within the volume of rock containing the repository.

Empirical methods such as the Q system can be used to establish the domains of rock mass quality and to assess tunnel support requirements during the preliminary design phase.

The laboratory testing should be carried out to determine the crack initiation stress, the long-term strength, peak strength and post-peak response in accordance with the information provided in Section 3.1. The determination of these parameters should be determined from stress-strain data, as well acoustic emission testing techniques, using testing methods based on accepted national standards, such as the ISRM suggested methods or ASTM.

The in-situ stress state must be measured with confidence. The number of measurements and the method(s) used will be a function of the geology of the site.

The stress to strength ratios around the underground openings must also be known with confidence to minimize the potential for localized stress-induced spalling.

Constructibility

In situations where the stability of a tunnel is controlled by discontinuities, traditional approaches using limit equilibrium analysis or numerical tools such as *3DEC* may be appropriate.

Practical experience indicates that stress-induced failure (spalling) will occur on the boundary of an underground opening in hard rocks when the maximum tangential stresses on the boundary of the opening exceed approximately 0.3 to 0.4 of the laboratory uniaxial compressive strength. Hence to assess the potential for spalling, numerical analysis will be required for the various shaped openings planned for the repository. These numerical analysis can be used to optimize the shape of the tunnels, the orientation of the tunnels relative to the far-field stress state, intersection support, and deposition tunnel/borehole spacing.

The support for the tunnels in a repository is expected to range from light support pressure equivalent to standard spot-bolting to local bolts with mesh and fibre-reinforced shotcrete. At major intersections medium to heavy support pressure may be required.

Aspect to consider when choosing construction method

The layout of a repository will be similar to a mine using a room-and-pillar mining method but the extraction ratio will be of the order of $< 30\%$. A drill-and-blast excavation method will provide the maximum flexibility for such an excavation technique. In addition, should spalling be encountered, the shape of the tunnels can be changed to control the extent of spalling as illustrated in Section 5.

Recommendations

The two common modes of failure (structurally controlled and stress-induced spalling) can be analyzed using the approaches outlined in this report. However, it is not clear what

approach should be used when the mode of failure is transitional, i.e., structure/stress. Apart from the ZEDEX experiment, very little rock mechanics research has been carried out with the combined in-situ stress magnitudes and well defined structure such as occurs at the 400 to 450 Level in the Äspö HRL. Because of the likelihood of encountering these transitional conditions at the depth of the proposed repository in Sweden it is recommended that further rock mechanics research be carried out to assess the stress at failure for these transitional conditions. In particular, the strength of the pillars between the emplacement boreholes should be established such that the pillar dimensions can be assessed by means other then empirical formulas developed from mining conditions.

Sammanfattning

De senaste 25 åren har omfattande internationell forskning kring geologisk förvaring av radioaktivt avfall i kristallint berg utförts av kärnkraftsindustrin. Två speciella under-jordsanläggningar för forskning har byggts: SKB:s Äspö Hard Rock Laboratory i Sverige och AECL:s Underground Research Laboratory, Kanada. Båda laboratorierna är anlagda i hårt kristallint berg, representativa för Fennoskandiska respektive Kanadensiska urbergsskölden. Innan dessa anläggningar byggdes var bl.a. SKB och AECL engagerade i forskningen vid Stripagruvan, Sverige. Denna rapport sammanfattar de väsentligaste resultaten från dessa program, speciellt med tillämpning på stabilitet i undermarksutrymmen.

Rapporten utgår främst från publicerade resultaten från SKB:s ZEDEX experiment i Sverige och AECL:s Mine-by experiment i Kanada. Exempel från gruvdrift och tunnelbyggnad i allmänhet är också nyttjade för att illustrera tillämpningen av bergmekaniska forskningsresultat.

Rapportens syfte är att:

1. utifrån dagens kunskapsnivå beskriva bergteknikens betydelse för lokalisering och bygge av ett KBS-3 förvar,

2. definiera de viktigaste bergmekaniska parametrarna som ska bestämmas för att genomföra lokalisering och byggande,

3. diskutera möjliga konstruktionsfrågor angående bergstabilitet som kan uppstå under bygge av ett KBS-3 förvar,

4. utgöra ett referensdokument till de bergmekaniska analyser som ska göras i samband med den projektering som görs parallellt med platsundersökningarna.

Inget enskilt kriterium eller egenskap kan beskriva ett bergrums eller ett under-jordiskt förvars funktion. Det finns inte heller någon enskild bergmekanisk parameter eller förhållande som gör ett underjordiskt förvar oacceptabelt kan det finnas vissa tillstånd som kan betraktas som negativa, till exempel en mycket uppsprucken bergmassa som gör den totala permeabiliteten i berget oacceptabelt hög eller höga in-situ-spänningar som gör att byggandet av bergrummet blir en säkerhetsrisk för anläggningsarbetarna. Nedan presenteras några viktiga bergmekaniska frågeställningar som bör klarläggas under genomförande av platsval, konstruktion och återslutning.

Krav vid platsval

Under plastvalsfasen kommer den bergmekaniska informationen främst att samlas in genom studier av borrkärnor och i borrhål. Två huvudsakliga uppgifter måste utföras under denna period:

1. bestämning av bergmassans kvalitet mot djupet,
2. bestämning av spänningsförhållandena mot djupet.

Empiriska metoder såsom Q-systemet kan användas för att fastställa krav på tunnelförstärkning och för att etablera bergkvalitetsklasser.

Laboratorietester bör utföras för att bestämma sprickinitieringsspänningen, den långsiktiga hållfastheten, den maximala hållfasthet och residualhållfastheten i enlighet med den information som ges i kapitel 3.1. Dessa parametrar bör bestämmas utifrån såväl spänningstöjningsdata som utifrån tester med akustisk emission, i enlighet med accepterade standards såsom ISRM:s föreslagna metoder eller ASTM.

In-situ-spänningarna måste bestämmas med betryggande säkerhet. Antalet mätningar och vilken/vilka metod(er) som kommer att användas kommer att bestämmas av platsens geologi.

Byggbarhet

I situationer där en tunnels stabilitet styrs av diskontinuiteter är ett traditionellt tillvägagångssätt att analysera i brottgränstillståndet eller använda numeriska verktyg som 3DEC.

Innehållet i denna rapport indikerar att spänningsrelaterade brott kommer att uppträda på randen av ett hålrum när den maximala tangentiella spänningen på randen överstiger ungefär 0,3-0,4 av den i laboratorium uppmätta enaxiella tryckhållfastheten. Följaktligen kommer numerisk analyser kommer att krävas för att fastställa risken för avskalningsbrott i de olika tunnelutformningarna i förvaret. Dessa numeriska analyser kan användas för att optimera tunnlarnas form, tunnlarnas läge relativt det storskaliga spänningsfältet, förstärkning vid korsande tunnlar och pelardimensioner.

Förstärkningen av tunnlarna i djupförvaret väntas variera från lättare förstärkning, motsvarande ströbultning med standardbult, till systembultning med nät och sprutbetong. Vid större tunnelkorsningar kan mer omfattande förstärkning komma att krävas.

Överväganden för val av brytningsmetod

Djupförvarets layout kommer att likna en rum- och pelargruva, men brytningens omfattning blir < 30% av total bergvolym på förvarsdjupet. Borrning och sprängning leder till den största flexibiliteten med en sådan brytningsmetod. Dessutom kan eventuella spänningsproblem hanteras genom justering av tunnelkonturens form (se avsnitt 5).

Rekommendationer

De två vanliga brott-typerna (strukturkontrollerade brott och spänningsinducerade avskalningsbrott) kan analyseras med stöd av de strategier som beskrivs i denna rapport. Det finns dock inga tydliga angreppssätt för analys av förhållanden i en övergångszon mellan dessa brott-typer. Förutom ZEDEX –experimentet har mycket lite bergmekanisk forskning utförts under förhållanden med relativt höga spännings-magnituder och distinkta strukturer, såsom är fallet inom 400m- till 450m-nivån vid Äspö HRL. Eftersom SKB kan förväntas stöta på liknande förhållanden i gränszonen mellan strukturkontrollerade brott och rena spänningsinducerade brott i samband med platsundersökningarna i Sverige bör fördjupad forskning ske inom detta område. Speciellt hållfastheten i pelarna mellan deponeringshål måste kunna bestämmas med större säkerhet än med hjälp av empiriska formler som utvecklats under gruv-förhållanden för projektering av pelardimensioner.

Contents

1   Introduction

Over the past 20 years the international nuclear community has carried out extensive research into the deep geological disposal of nuclear waste in hard rocks. In two cases this research has resulted in the construction of dedicated underground research facilities: SKB's[1] Äspö Hard Rock Laboratory (HRL), Sweden and AECL's[2] Underground Research Laboratory (URL), Canada. Both laboratories are located in hard rocks considered representative of the Fennoscandian and Canadian Shields, respectively. Prior to the construction of these facilities SKB and AECL were also involved in the research carried out at Stripa Mine (Sweden). This report is intended to synthesize the relevant rock mechanics findings from these research programs.

As such the report draws heavily on the published results from the the ZEDEX Experiment (Äspö HRL) and the Mine-by Experiment (URL). Examples from mining and tunnelling are used to illustrate the application of these findings to underground excavations in general.

1.1   Current SKB schedule

1.1.1   Site Selection Process

Within a ten-year period, SKB plans to complete the siting of the encapsulation plant and the deep repository (Figure 1).

The key issue is the siting of the deep repository, and the crucial tasks for SKB will be to:

---

[1]Swedish Nuclear Fuel and Waste Management Company
[2]Atomic Energy of Canada Limited
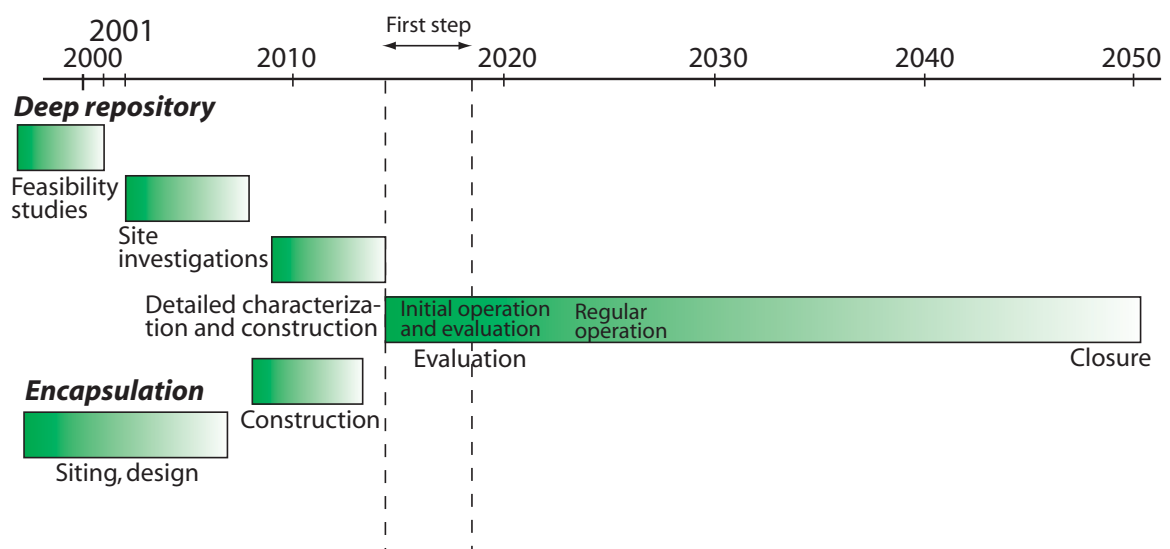
Figure 1: *General time table for the Site Investigation Phase showing the most important Milestones from /1/.*

- Show that a deep repository on the selected site satisfies all requirements for safe long-term disposal. This requires safety assessments, which in turn require extensive investigations of the bedrock.

- Show that a deep repository on the selected site satisfies all technical requirements, as well as health and environmental protection requirements. This requires a number of studies concerning transport prospects, land questions and environmental impact.

- Obtain support for a siting of the deep repository from the municipality in question and from regulatory authorities and the Government.

1.1.2 Siting Requirements

The requirements which the deep repository must satisfy can be described as follows:

- Bedrock

- Industrial establishment

- Societal aspects

The properties of the bedrock help determine the long-term safety of the repository. Andersson *et al.* /6/ lists the bedrock requirements for the repository, advantageous conditions (preferences) and methodology and criteria for determining whether these requirements and preferences are fulfilled. We believe that these requirements should be used in the continued work of selecting sites for site investigations, and in order to evaluate sites during the site investigation phase.

While the key function of the bedrock is to contribute to long-term safety of the repository, the bedrock must also provide a safe working environment that meets occupational health and safety regulations. For example, the strength of the rock, the fracture geometry and the initial rock stresses must be such that the underground facilities are stable and can be constructed using standard construction technology. Stability analyses for the deep geological repository require, in the same way as safety assessments, site-specific geological information. In the early stages of the siting process there is a need for preliminary stability assessments. These assessments can often be supported by actual experience from existing underground rock facilities.

1.2 Objectives

The objectives of this report are to:

1. Describe, using the current state of knowledge, the role rock engineering can play in siting and constructing a KBS-3 repository.

2. Define the key rock mechanics parameters that should be determined in order to facilitate repository siting and construction.

3. Discuss possible construction issues, linked to rock stability, that may arise during the excavation of the underground openings of a KBS-3 repository.

4. Form a reference document for the rock stability analysis that has to be carried out as a part of the design works in parallel with the site investigations.

The rock engineering topics discussed in this report are limited to the siting and construction phase. There is however the implication that good conditions for siting and constructing a KBS-3 repository are also likely to provide an acceptable performance assessment.

This report draws on the international civil and mining experience gained from creating deep excavations. While it is recognized that the KBS-3 is limited to depths of less than 700 m, it is important to consider the experience gained from excavating at great depths, i.e., greater than 2000 m. These deep excavations provide a framework for establishing the upper bound response when other loading conditions may need to be consider, i.e., earthquake or glacial loads. More importantly, when these deep excavations are created the rock mass fails and hence these observations of failure form the basic framework for understanding stress-induced rock mass response. This framework can then be considered when establishing guidelines for siting and constructing a KBS-3 repository.

1.3 The KBS-3 concept

The Swedish system for management of radioactive waste currently consists of the following parts:

- A final repository for short-lived low and intermediate level waste, SFR.

- A central interim storage facility for spent nuclear fuel, CLAB.

- A transport system for shipment of radioactive waste and spent fuel from the power facilities to the CLAB and SFR facilities.

The main disposal facilities that remain to be built are the deep geological repository for spent nuclear fuel and a deep repository for other long-lived radioactive waste, mainly core components that need to be disposed off after decommissioning of the power plants. Two additional surface facilities are also required; a canister factory to produce the cast iron insets and the copper canisters, and an encapsulation plant where the spent fuel will be put into the canisters and the lid sealed. An overview of the Swedish system is given in Figure 2.

In order to achieve long-term safety, the disposal system KBS-3 is based on three safety levels: 1) isolation, 2) retention and 3) dilution. The first, isolation of the spent nuclear fuel from the biosphere, is achieved by encapsulating the spent nuclear fuel in long-lived copper canisters. At the next safety level, the repository has the function to retain and retard the transport of radionuclides should the isolation be broken, thus allowing them to decay before reaching the biosphere. This is achieved by a buffer of highly compacted bentonite surrounding the copper canister, and the host rock surrounding the repository. Thirdly, by proper site selection, transport pathways and dilution conditions in the biosphere can be influenced so that any radionuclides that escape will only reach man in low concentrations.

The deep repository is designed for a capacity of about 9000 tons of spent fuel. This corresponds to about 4500 canisters. The canisters will be put into vertical deposition holes with a diameter of 1.75 m and a depth of 8 m and surrounded by a buffer of highly compacted
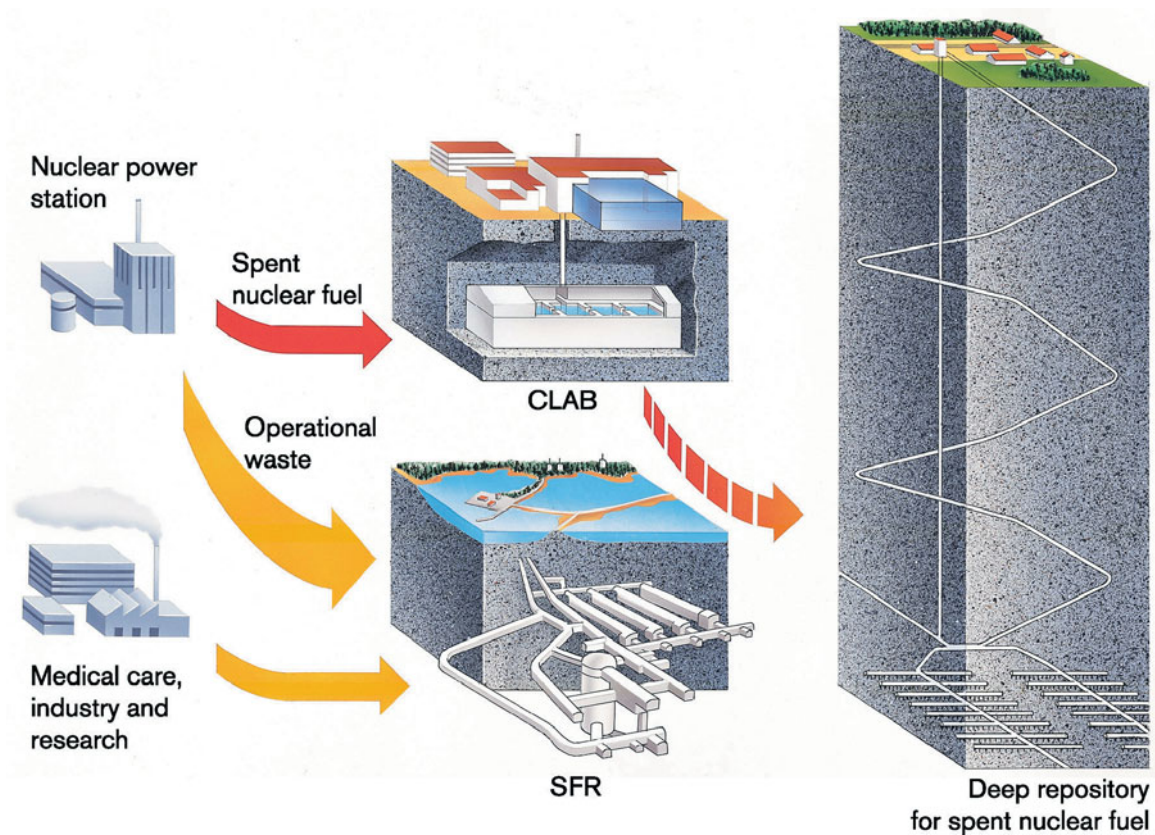
Figure 2: The main components of the Swedish System for final disposal of radioactive waste, from /80/.

bentonite clay. The buffer will provide mechanical protection and prevent groundwater flow around the canister. The planned centre-to-centre distance of the canisters along the deposition tunnels is 6 m and the distance between the tunnels is 40 m. The underground part of the repository is expected to cover an area of 2 - 4 km^2 and will be located at a depth between 400 and 700 m in granitic or gneissic rock. The repository will be built in two steps, an initial test phase involving deposition of about 400 canisters followed by a phase of regular operation when the remainder of the spent fuel will be deposited. A tentative design is indicated in Figure 3.

The dimensions of the tunnels varies depending on the purpose as illustrated in Figure 4. Tunnels for access ramps and communication between different parts of the facilities underground may have a span of 5 to 8 m, depending on traffic requirements. The caverns for central functions such as ventilation, power supply and so on may be 8 to 15 m in span and similar dimensions in height. The tunnels for deposition of the canisters are dependent of
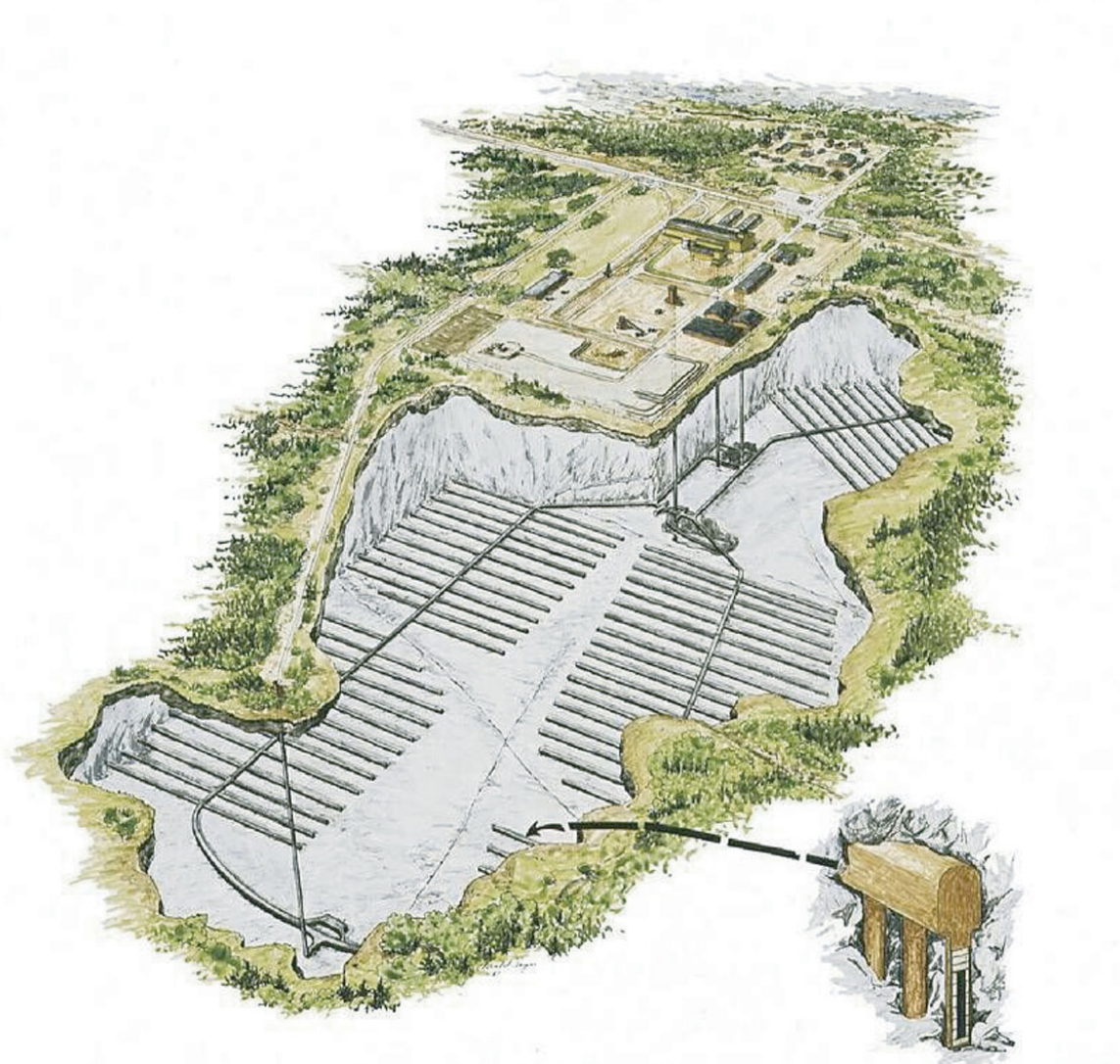
Figure 3: *Possible layout of the KBS-3 deep repository. The actual layout must be adapted to the local site conditions.*
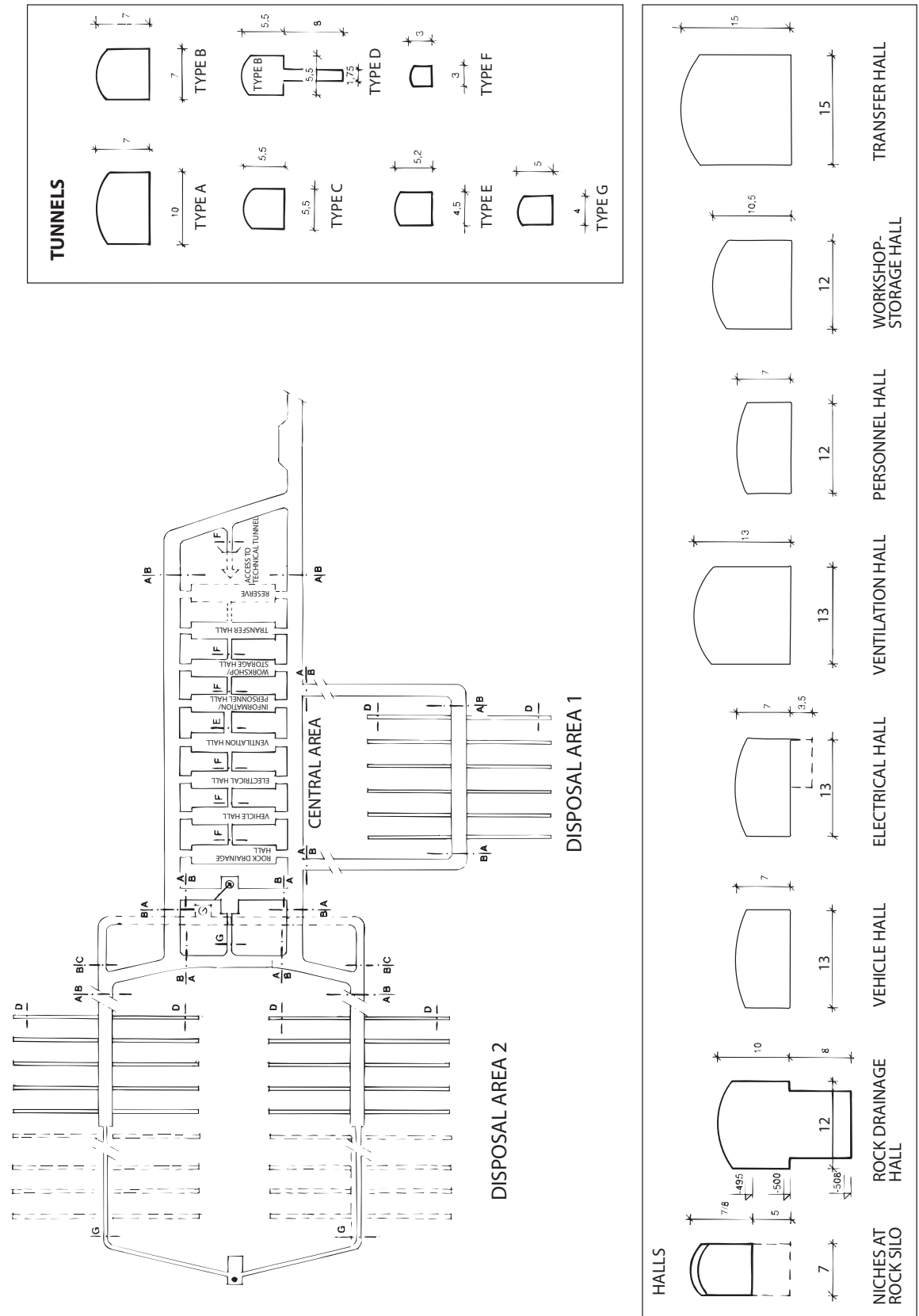
Figure 4: *Typical tunnel profiles proposed for the KBS-3 deep repository. The actual tunnel profiles must be adapted to the local rock mechanics conditions.*

6

the size of the canister and the size of the machine used for placement in the vertical bore hole. The current prototype placement machine that is used at Äspö HRL will need a tunnel that is 5.5 by 5.5 m (Figure 5).

1.4   Key parameters for underground excavations

The preliminary design decisions for the KBS-3 repository that are significantly influenced by rock mechanics factors are:

1. the depth of the facility /52/;

2. the layout of the facility, including access routes and supporting infrastructure;

3. the shape and size of the underground openings;

4. the construction method for the main access routes and the deposition tunnels, i.e., drill and blast versus machine excavation;

5. orientation of the access and deposition tunnels relative to the in-situ stress state; and

6. the width of the pillars (spacing) separating the deposition tunnels and the emplacement boreholes required for mechanical stability.

Figure 5: *The current Prototype Deposition Machine dictate the current dimensions of the tunnels.*

While it is recognized that rock mechanics will play a significant role in the design and construction of the repository, it is also recognized that the rock mechanics criteria are not the only criteria that must be satisfied to meet the overall safety requirements. Nonetheless the single most important rock mechanics issue that must be met for the successful design of the repository is that the underground openings must perform as intended. This normally implies that the underground openings remain stable for their operating life. However, this does not imply that localized failure around the underground openings cannot be accepted; rather the amount of failure must be minimized such that the openings remain functional. Hence, this report attempts to define the modes of failure that are observed around underground openings, techniques that can be used to assess the potential for failure, and the mitigating techniques available to control the failure.

The rock mass around a nuclear waste repository will be subjected to unique stress path(s) created by: the excavation response caused by the construction of the repository; swelling pressure from the buffer; the heat from the emplaced waste; and glaciation (Figure 6). The loading of the repository by these various scenarios will create stress paths that will result in both unloading and loading conditions, as well as stress rotation. Hence when assessing the rock mechanics design issues associated with these various scenarios, two general rock mechanics modes of failure are encountered:

1. structurally controlled gravity-driven failure; and

2. stress-induced slabbing type failure.

While the structurally controlled failure is prevalent at shallow depths, i.e., low in-situ stress magnitudes, and the slabbing failure is commonly observed at great depth, i.e., high in-situ stress magnitudes, mining and tunnelling experience shows that these failure processes can be found at essentially any depth.

As the in-situ stress magnitudes increase, i.e., as the depth increases, the natural fractures become clamped and the failure process becomes brittle and is dominated by new stress-induced fractures growing parallel to the excavation boundary (Figure 7). One of the key parameters characterizing brittle failure in hard rocks is the stress magnitude required to initiate and propagate these stress-induced fractures through intact or tightly clamped fractured rock. Initially, at intermediate depths, these stress-induced fractured regions are localized near the tunnel perimeter but at great depth the fracturing involves the whole boundary of the excavation (Figure 7). Unlike ductile materials in which shear slip surfaces can form while continuity of material is maintained, brittle failure deals with materials for which continuity must first be disrupted through stress-induced fracturing before kinematically feasible failure mechanisms can form.
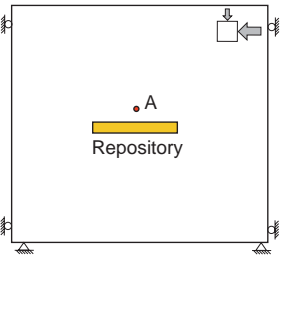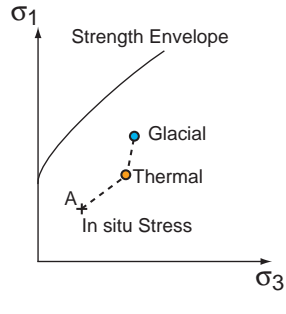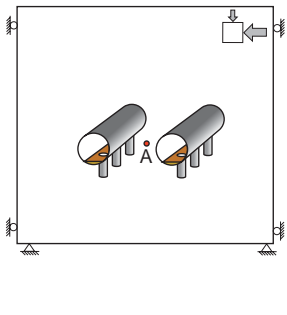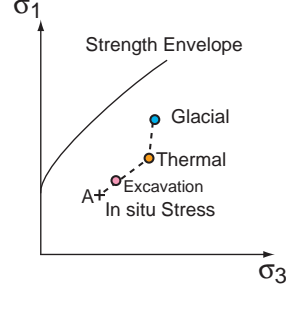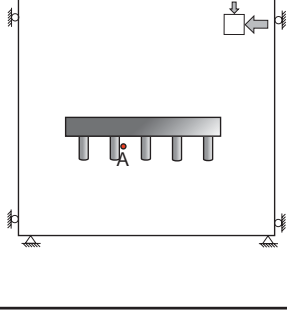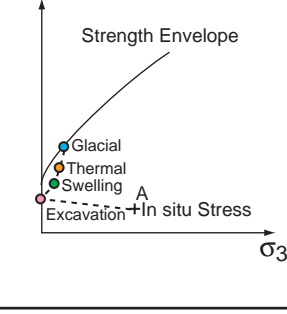
Martin *et al.* /66/ attempted to quantify the potential for stress-induced brittle (spalling) failure by introducing the Damage Index (D_i) given as:

$$D_i = \frac{\sigma_{\max}}{\sigma_c} \qquad (1)$$

where $\sigma_{\max}$ is the maximum tangential stress on the boundary of a circular opening and σ_c is the laboratory uniaxial compressive strength. The correlation between D_i and the ratio of far-field maximum stress (σ_1) to σ_c is given in Figure 7. Note that in Figure 7 stress induced spalling does start until $D_i > 0.4$ or $\sigma_1/\sigma_c > 0.15$.

To evaluate the stability of underground excavations in hard rocks four factors must be known with reasonable confidence:
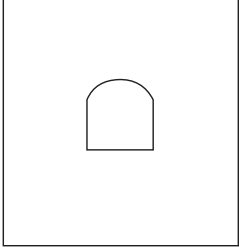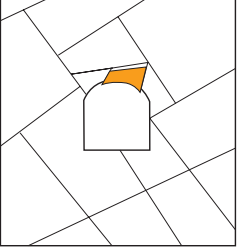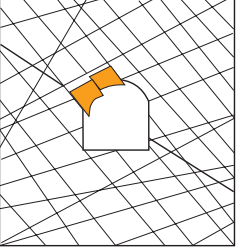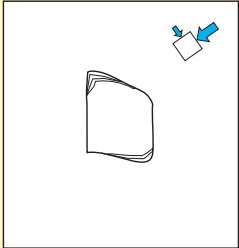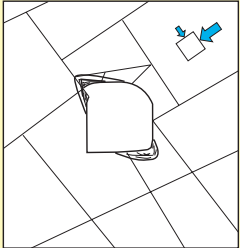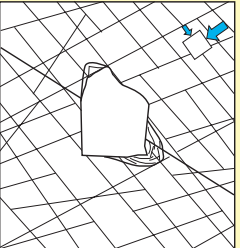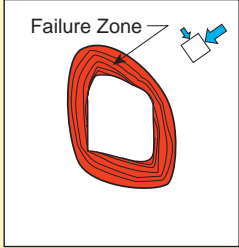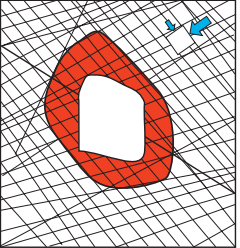
1. The geometry and strength of the discontinuities when the failure mode is structurally controlled gravity-driven failure;

2. The rock mass strength when the failure mode is stress-induced slabbing;

3. The stress magnitudes required to initiate and promote fracture growth; and

4. The in-situ stress magnitudes and orientations and the stress changes that will be

|		Model	Potential Stress Paths	Design Issue
Problem Scale	Repository Scale			1. Change in rock mass properties due to thermal and glacial induced stress changes 2. Stability of rock mass surrounding the repository
	Deposition Rooms Deposition Pillars			1. Stability of deposition pillar 2. Stability of deposition tunnel 3. Construction of underground openings
	Emplacement Borehole & Emplacement Pillar			1. Stability of emplacement borehole 2. Stability of emplacement pillar

Figure 6: *Illustration of the rock mechanics design issues associated with the performance assessment of a nuclear waste repository. Also shown are the potential stress paths that need to be considered when assessing the rock mechanics issues.*

caused by the various loading scenarios.

It is assumed that the KBS-3 repository will be constructed beneath the groundwater table and hence the influence of water and time on these four factors must also be considered.

|	Massive ($GSI > 75$)	Moderately Fractured ($50 > GSI < 75$)	Highly Fractured ($GSI < 50$)	
Low In-Situ Stress ($\sigma_1 / \sigma_c < 0.15$)	Linear elastic response.	Falling or sliding of blocks and wedges.	Unravelling of blocks from the excavation surface.	$D_i < 0.4\ (\pm0.1)$
Intermediate In-Situ Stress ($0.15 > \sigma_1 / \sigma_c < 0.4$)	Brittle failure adjacent to excavation boundary.	Localized brittle failure of intact rock and movement of blocks.	Localized brittle failure of intact rock and unravelling along discontinuities.	$0.4\ (\pm0.1) > D_i < 1.1\ (\pm0.1)$
High In-Situ Stress ($\sigma_1 / \sigma_c > 0.4$)	Failure Zone — Brittle failure around the excavation .	Brittle failure of intact rock around the excavation and movement of blocks.	Squeezing and swelling rocks. Elastic/plastic continuum.	$D_i > 1.1\ (\pm0.1)$

Figure 7: Tunnel instability and modes of failure, modified from Hoek et al. */48/. The Damage Index D_i is defined as the ratio of maximum tangential stress on the boundary of the tunnel (σ_{max}) to the uniaxial compressive strength σ_c.*

10

2 Overview of failure modes around underground openings in hard rocks

Stability issues associated with underground excavations in hard rock can be grouped into three general classes:

1. structurally controlled gravity-driven processes leading to wedge type failures;

2. stress-induced failure causing slabbing and spalling;

3. and, a combination of structurally controlled gravity-driven processes along fractures and stress-induced failure.

A similar classification was proposed by Stille /100/ for Swedish hard rocks. While the wedge-type failure and stress-induced failure are relatively straight-forward to recognize, the combined stress-structure failure is more problematic and harder to identify. For example, a tunnel in a low stress environment where wedge type failures dominant may be supported with only light support such as spot bolts. However, the same tunnel when subjected to stress-structure failure may require much heavier support. In this section, the essential characteristics of Items 1 and 2 above are discussed. Item 3 from above, referred to as fracture/stress failure in this report, is discussed in Section 5.

2.1 Stress path and failure

The notion that there are basically two distinct failure modes around underground openings in hard rocks and the different stress paths that lead to these failure modes, is illustrated in Figure 8. This concept of stress path and related failure modes was used by Martin *et al.* /72/ to assess the potential for ground control problems around underground mine openings. One of the benefits of utilizing stress paths to assess possible failure modes is that if the stress path can be changed so can the failure mode. Stress paths can be changed by:

1. staging and sequencing the excavations,

2. changing the shape of excavations, and

3. changing the alignment of the excavation relative to the principal stress directions.

For example, a circular tunnel parallel to σ_2 will be subjected to a stress path that promotes spalling in the roof. Whereas, a tunnel aligned in the same direction but rectangular in shape will be subjected to a stress path that promotes relaxation in the roof that could lead to structurally controlled wedge type failures. This notion of stress path and associated failure modes will be explored in detail in Section 5.4.

2.2 Structurally-controlled failure

Structurally-controlled failures are common in low stress environments, e.g., at shallow depth, where wedge-type blocks, driven by gravity loading conditions, are able to fall/slide
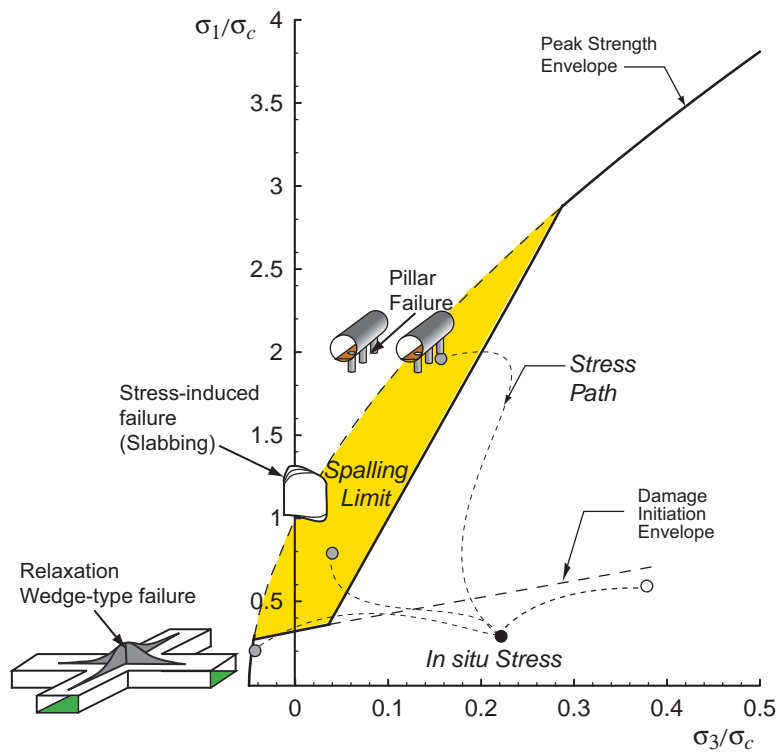
Figure 8: *Illustration of stress path and resulting modes of failure. The shaded region indicates where spalling is likely to be encountered. The damage initiation envelope represents the onset of stress-induced damage.*

from the roofs and sidewalls of tunnels. The shear strength (τ) of these discontinuities can be expressed as:

$$\tau = c + \sigma_n \tan \phi \qquad (2)$$

where c is the cohesion, σ_n is the normal stress acting on the failure plane and ϕ is angle of friction. From equation 2, it can be seen that the strength of these potential wedges is influenced by the confining stress, expressed as the σ_n.

Confinement loss can occur above the roofs of tunnels in the vicinity of large openings or where complex intersection geometries are present. Confinement loss combined with favourably oriented joint sets can form potentially unstable wedges. The stabilizing effect of stress has long been recognized but Diederichs and Kaiser /33/ illustrated that even a small amount of confining stress has a significant impact for such wedges (Figure 9). For example, a wedge with a height to span ratio of 0.6:1, as shown in Figure 9, can be fully stabilized over a span of 10 m by only 1.5 MPa of horizontal stress acting across the roof (friction angle of 45° representative for moderately rough, planar joints). In fact, for any isolated tunnel of standard geometry (circular, rectangular, arched) with a span of 10 m at a depth of more than 40 m in undisturbed or unfaulted ground, a roof wedge with a cone angle of less than the friction angle (average joint dip steeper than friction angle) should be stable when confining stress is included in the analysis /33/.

This stabilizing confinement, however, can be lost in situations where: a large opening is excavated near an existing tunnel; a shallow fault is nearby; or an intersection is created. For tunnel intersections, confinement loss in the roof is induced by a disruption of stress flow in two directions, not just around the initial drift. Intersections at depth also increase
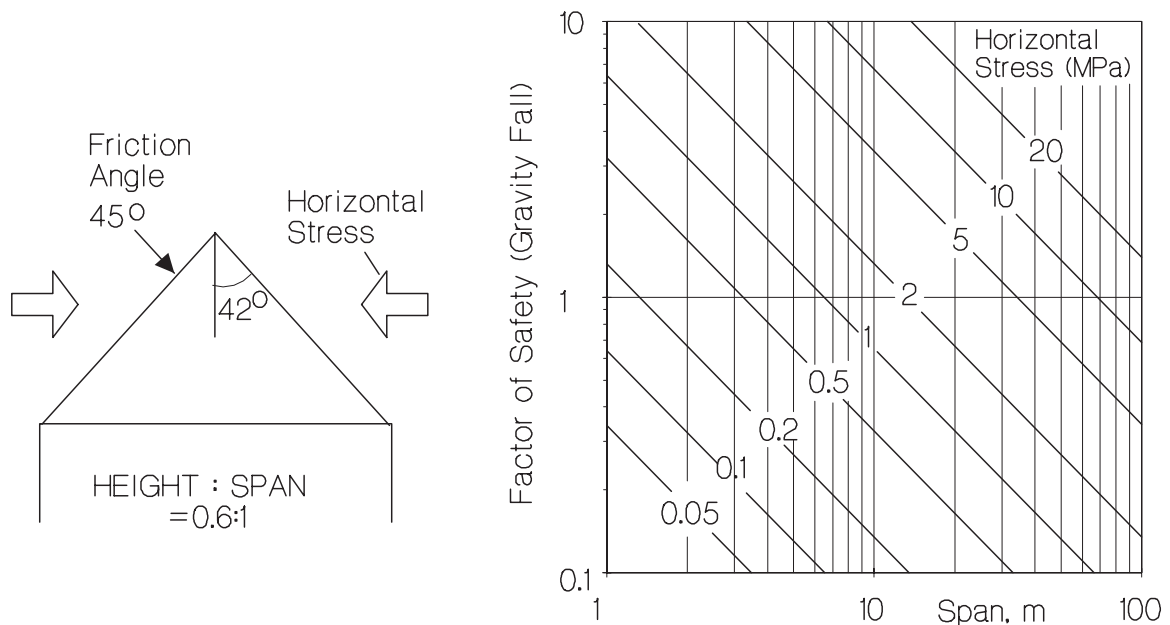

Figure 9: *Effect on wedge stability of small amounts of confining (horizontal) stress, after Diederichs /32/.*

13

midspan displacement, e.g., Diederichs and Kaiser /33/ showed that elastic displacement in an intersection is 1.5 to 2-times the initial roof displacement. This additional deflection increases the zone of tension or relaxation in the roof at midspan allowing larger joint defined blocks to be released. For this reason, intersections often require substantially higher support capacities, i.e., cablebolting. Discrete wedge identification or a semi-empirical approach to structural hazard assessment, taking relaxation into account is a prudent measure when designing intersections /33/.

2.3 Stress-induced brittle failure

The analysis of underground openings for stress-induced brittle (spalling) failure requires knowledge of three variables:

1. the in-situ stress boundary condition,

2. the rock mass strength, and

3. the geometry of the excavation(s).

2.3.1 Intact and rock mass strength

The strength of intact rock is determined from laboratory tests on cylindrical samples using the 'Suggested Testing Methods of the ISRM /18/' and the strength of a rock mass assessed using empirical approaches or by back-analysing case histories where examples of failure have been carefully documented. One of the most widely used empirical failure criteria is the Hoek-Brown criterion /46/. Since its introduction in 1980 the criterion has been modified several times, most recently by Hoek and Brown /47/. The generalized form of the criterion for jointed rock masses is defined by:

$$\sigma_1 = \sigma_3 + \sigma_{ci} \left(m_b \frac{\sigma_3}{\sigma_{ci}} + s \right)^a \tag{3}$$

where σ_1 and σ_3 are the maximum and minimum effective stresses at failure respectively, m_b is the value of the Hoek-Brown constant m for the rock mass, and s and a are constants which depend upon the characteristics of the rock mass, and σ_{ci} is the uniaxial compressive strength of the intact rock. For hard rock masses, Hoek and Brown /47/ recommend a value of 0.5 for a. In order to use the Hoek-Brown criterion for estimating the strength and deformability of jointed rock masses, three properties of the rock mass have to be estimated. These are:

1. uniaxial compressive strength σ_{ci} of the intact rock pieces in the rock mass;

2. Hoek-Brown constant m_i for these intact rock pieces; and

3. Geological Strength Index (*GSI*) for the rock mass.

GSI was introduced by Hoek *et al.* /48/ to provide a system for estimating the rock mass strength for different geological conditions. It can be related to either of the commonly used rock mass classification systems, e.g., the rock mass quality index *Q* or the rock mass

rating *RMR*. According to Hoek *et al.*, once GSI has been estimated the strength parameters for hard rocks (*GSI* > 25) which describe the rock mass are calculated as follows:

$$m_b = m_i \exp\left(\frac{GSI - 100}{28}\right) \qquad (4)$$

and

$$s = \exp\left(\frac{GSI - 100}{9}\right) \qquad (5)$$

The origin of the Hoek-Brown criterion is based on the failure of intact laboratory samples and the reduction of the laboratory strength based on the notion that a jointed rock mass is fundamentally weaker in shear than intact rock. While the concept is sound, the application of the Hoek-Brown criterion to brittle failure has met with limited success /78; 66/. Martin *et al.* /65/ showed that in order to fit the Hoek-Brown criterion to observed brittle failure the value of m_b had to be reduced to unconventionally low values, i.e., close to zero, with a value of $s = 0.11$ ($1/3\sigma_{ci}$). Similar findings have been reported by Stacey and Page /97/; Wagner /105/; Castro *et al.* /22/; Grimstad and Bhasin /36/; Diederichs /32/, who all showed, using back-analyses of brittle failure, that stress-induced fracturing around tunnels initiates at approximately 0.3 to $0.5\sigma_{ci}$ and that it was essentially independent of confining stress. Hence, while the traditional Hoek-Brown parameters may be appropriate for estimating the shear strength of rock masses around tunnels and slopes at shallow depths, there is growing evidence that the same approach is not appropriate for estimating the strength of hard rocks around tunnels at depth. The fundamental difference between the two modes of failure is that in a low stress environment slip along discontinuities dominates the failure process, while at depth stress-induced fracturing dominates the failure process.

Since the early work of Brace *et al.* /16/ laboratory studies have shown that in unconfined compression tests, damage initiation occurs at 0.3 to 0.5 of the peak strength. The microscope work by Tapponnier and Brace /103/ has shown that the length of the cracks, at the initiation stage in the damage process, is approximately equal to the grain size of the rock. Hence, to track the failure process numerical models should be able to simulate the grain scale. Cundall *et al.* /29/ developed the particle flow code *PFC* that can be used to represent rock by considering particles as mineral grains. *PFC* treats the rock as a heterogeneous material bonded together at contacts points with each contact point acting like a pair of elastic springs allowing normal and shear relative motion. When either a tensile normal-force or a shear-force limit is reached the bonds break and cannot carry tension thereafter. Broken contacts, which remain in contact, can generate frictional shear resistance in response to normal stress. Diederichs /32/ used *PFC* to explore the damage initiation in simulated samples of Lac du Bonnet granite. In this work, the accumulation of both tensile-bond breaking and bond slip were tracked as loads were applied.

A typical axial stress versus axial strain curve from these simulations is shown in Figure 10. The stress-strain curve shows the characteristic damage initiation at about 0.3 to 0.4 of the peak strength and the rapid strain weaking immediately after peak. Also shown in Figure 10 are the incremental snap-shots of crack growth. Note that even though the sample is confined

15

with 20 MPa, the total amount of tensile cracking dominates shear cracking by a ratio of approximately 50:1 and that there is very little new crack growth after the macro-scale failure zone has formed. Diederichs /32/ also showed that heterogeneity (both grain size and material properties) is key in generating tensile stresses in a compressive stress field.

2.3.2 Rock mass failure envelope for stress-induced brittle failure

In conventional usage, the Hoek-Brown and the Mohr-Coulomb strength envelopes assume that both cohesion and friction contribute to the peak strength, and are mobilized instantaneously and simultaneously. This is certainly valid at high confinement levels, when the rock behaves in a ductile manner ($\sigma_1/\sigma_3 < 3.4$ according to Mogi /76/) and cohesion and frictional strength components can be mobilized simultaneously. However, Martin *et al.* /66/ argue that the assumption of instantaneously and simultaneously mobilized cohesion and friction is not correct for brittle rocks in a compressive stress field at low confinement. In these conditions, cracks dilate or open after initiation and this inhibits the coincidental
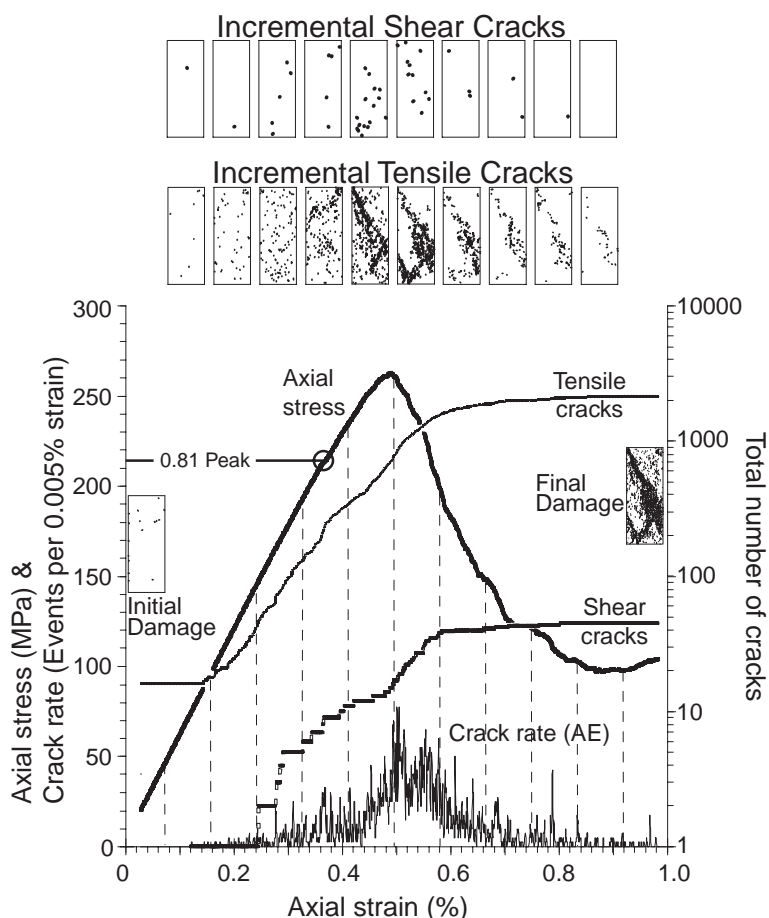

Figure 10: Example of axial stress versus axial strain from a bonded disc model (after /32/). Also shown are the number of tensile and shear cracks, as well as the crack rate per unit strain (after Martin et al. */64/. Note that even though the sample is confined with 20 MPa, the total amount of tensile cracking dominates shear cracking by a ratio of approximately 50:1 and that there is very little new crack growth after the macro-scale failure zone has formed.*

mobilization of friction and cohesion. This notion is also supported by the laboratory findings of Martin and Chandler /62/. Hajiabdolmajid *et al.* /37/ suggested that brittle strength mobilization can be reasonably represented as a two-stage process, with the pre-peak behaviour dominated by the cohesive strength of the rock material, and the residual strength controlled by the mobilized frictional strength within the damaged rock. In short, frictional strength cannot be mobilized until the rock is sufficiently damaged to become essentially cohesionless. At low confinement levels, the accumulation of significant rock damage, equivalent to loss of cohesion, occurs when the principal stress difference, $\sigma_1 - \sigma_3 = 1/3$ to $1/2\sigma_c$, is reached and exceeded. This is equivalent to a bi-linear failure criterion with $\phi = 0$ (Mohr-Coulomb) or $m = 0$ (Hoek and Brown) at low confinement levels.

The concept of a bi-linear failure envelope is not unknown to the soil mechanics community, e.g., for over-consolidated clays. In brittle rock, the strength envelope can also be represented by a bi-linear failure envelope as illustrated schematically by Figure 11. Below a damage threshold ($m = 0$), the rock around underground openings is not damaged and remains undisturbed. When this threshold is exceeded, seismicity (acoustic emissions) are observed and damage accumulates. This damage if unconfined leads to spalling with preferential surface parallel fractures (or fractures parallel to the maximum principal stress; axial splitting) and the in-situ rock mass strength is significantly lower than that predicted by laboratory tests where this mode of failure is retarded due to the particular state of stress in cylindrical samples. If tension is generated, rock fails due to tensile failure of rock bridges and unravelling mechanisms dominate. The stress space for underground openings, therefore, can be divided into three commonly observed rock mass responses (Figure 11):
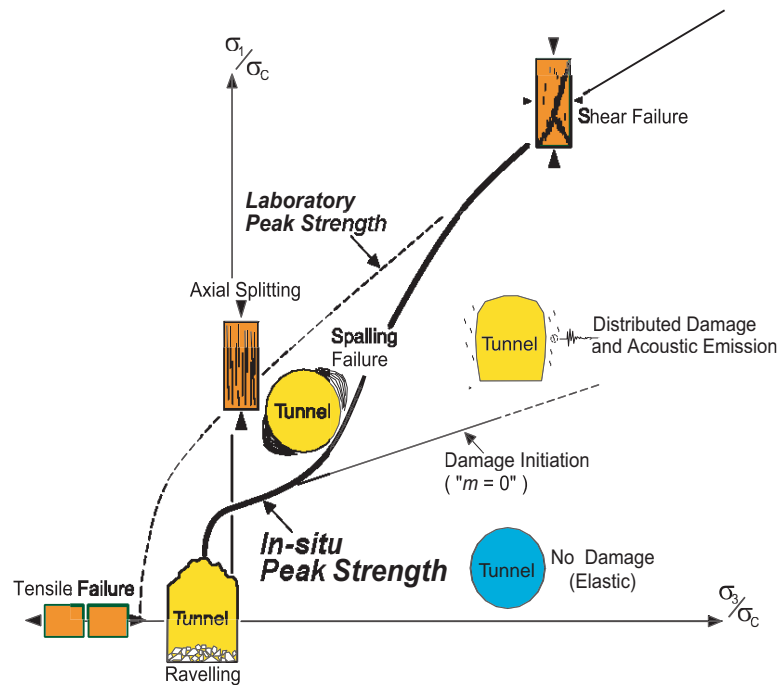

Figure 11: Schematic of failure envelope for brittle failure, showing four zones of distinct rock mass failure mechanisms: no damage, shear failure, spalling, and unravelling (after Diederichs /32/). Around underground openings spalling and unravelling type failures dominate.

17

1. no damage (elastic),

2. spalling failure, and

3. tensile (ravelling) failure.

Martin *et al.* /66/ showed that the concept of the damage initiation threshold ($m = 0$) could be used to establish the boundary between the elastic and damaged rock mass and that the concept is applicable to a wide range of rock mass strengths. The damage threshold ($m = 0$) can be established from acoustic emission measurements or from field observations of rock mass deformation monitoring /23/, or from borehole fracture surveys /32/. While Martin *et al.* /66/ showed that the $m=0$ was valid stability criterion for single openings, Diederichs /32/ showed that the same approach was also valid for multiple interacting openings.

2.4 Summary

Because spalling occurs in brittle rock when the tunnel boundary stresses exceed the damage initiation threshold, failure can be predicted using a bi-linear failure envelope cut-off as shown schematically in Figure 11. In terms of the Hoek-Brown failure criterion, the first portion of the brittle strength envelope is modelled by using the so-called brittle strength parameters: $m = 0$, $s = 0.11$ to 0.25. Substituting these values into the Hoek-Brown equation leads to the principal stress equation:

$$(\sigma_1 - \sigma_3) = K\sigma_c \qquad (6)$$

where K is a function of the rock mass and for many crystalline rock masses $K = 1/3$. This yield criterion is appropriate for defining damage around the underground openings. The initiation of damage is fundamentally a cohesion loss process and as shown by Martin *et al.* /66/ there is a good correlation between damage initiation in laboratory samples and damage initiation back-calculated from field studies. Hence, quantifying damage initiation of laboratory samples is a necessary first step when evaluating the potential for spalling around underground openings.

3 Laboratory strength of Äspö rocks

Over the past ten years laboratory tests have been carried out in conjunction with SKB's research at Äspö Hard Rock Laboratory. The two common rock types from Äspö that have been tested are the Äspö diorite and the Småland (Ävrö) granite. A general summary of the laboratory test results is given in Stille /101/.

The Äspö diorite and the Småland (Ävrö) granite are both varieties of the Småland granite which belongs to the 1700-1800 million years old Trans-Scandinavian Granite-Porphyry belt. The rocks making up the Äspö diorite group are the most common in the Äspö area. They are grey to reddish-grey and medium-grained with large crystals of potassium feldspar, more or less scattered through the rock. Granodiorites and quartz monzonites are the most common rocks in this group but it also to some extent contains tonalities and quartz diorites. The age of this group has been determined 1803 ± 3 million years. The Småland (Ävrö) granites are somewhat brighter and more reddish than the Äspö diorite. In many places the granite can be seen to cut through the diorite, hence implying that the granite is the younger of the two. Although the age difference between the two is most likely relatively small. A general summary of the Äspö geology is given in Rhén *et al.* /92/.

3.1 Laboratory testing of intact rock

Testing procedures of all hard rocks should follow the ISRM Suggested Methods of Testing or other such suitable standards. These procedures for the triaxial compression test usually include recording the axial (ε_{ax}) and lateral (ε_{lat}) strains in a sample as it is loaded with or without a fixed confining stress. Cook /27/ proved that the volumetric strain of a sample measured by surface strain gauges was a pervasive volumetric property of the rock and not a superficial phenomenon. Hence by plotting the axial, lateral and the calculated volumetric strains versus the applied axial stress the path of a rock sample to failure can be followed. An example of axial, lateral and volumetric strain versus axial stress curves for typical granite in uniaxial compression is given in Figure 12. Note the relatively linear axial-stress and axial-strain curves, indicating essentially an elastic response.

From Section 2, it is apparent that damage initiation is a key parameter that should be recorded in all laboratory tests. Martin and Chandler /62/ pointed out that damage initiation (σ_{ci}) and crack-coalescence[3] were true rock properties while peak strength was a function of the geometry of the sample, the loading rate and the testing environment. Figure 12 illustrates the various methods that can be used to capture the crack (damage) initiation point. These various methods, while originally developed for isotropic granite, were also used by Hakala and Heikkila /38/ to establish the stress-strain behaviour of Olkiluoto mica gneiss, an anisotropic rock.

The determination of damage initiation is often difficult, if only one method is relied on. Acoustic emission monitoring should be routinely used in all laboratory tests to verify the

---

[3]In many rocks such as granites the stress magnitude associated with crack-coalescence is equivalent to the long-term strength defined by Bieniawski /14/.

damage initiation values obtained from the stress-strain curves. The following standard strength parameters for intact rock should be determined:

- Tensile strength

- Uniaxial compressive strength

- Triaxial compressive strength with σ_3 values ranging from 0 to the value of the maximum principal stress.

Other parameters that should also be determined are:

- Young's modulus

- Poisson's ratio,

- P-wave velocity,

- Fracture toughness and

- Thermal coefficient of expansion.

All samples tested should be characterized describing their mineral composition and measured grainsize.

In addition to the testing noted above, samples that behave in an anisotropic manner will require specialized testing procedures to determine the degree and type of anisotropy.
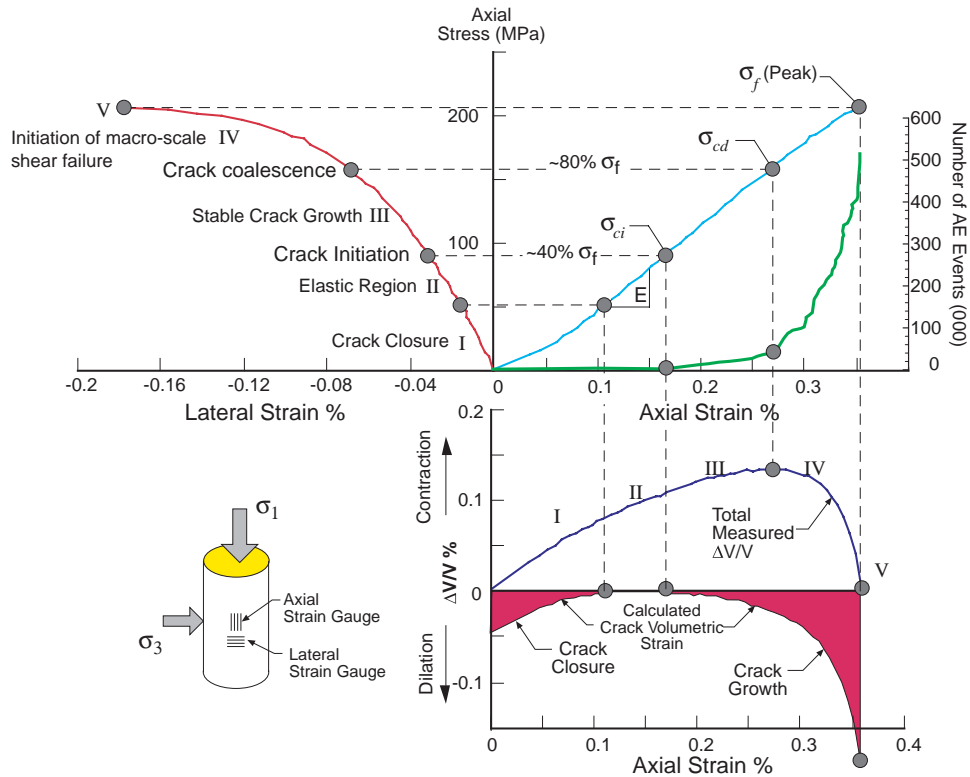

Figure 12: *Typical stress versus strain plot for hard rocks. Both the strain and the acoustic emissions are used to determine damage initiation (σ_{ci}) and crack-coalescence σ_{cd} .*

3.2 Sample disturbance of intact rock

At first glance, it would appear that obtaining samples of hard rocks for laboratory testing would be a straightforward task. For deep tunnelling excavations it is routing to core samples at depths greater than 500 m and in the mining and petroleum industry samples often come from depths of several kilometres. It is generally recognized, in the petroleum industry, that softer rocks, i.e., shales, siltstones, etc., are susceptible to sample disturbance and that this process affects their laboratory properties /94/.

The process of drilling a core sample from a stressed rock mass induces a stress concentration at the sampling point. When this stress concentration is sufficient grain-scale microcracking occurs and the accumulation and growth of these microcracks ultimately leads to core discing. Martin and Stimpson /71/ showed that the accumulation of these microcracks is progressive and a function of the stress environment, i.e., increasing depth. They also showed that the accumulation of these microcracks:

- reduces the uniaxial compressive strength,

- decreases the Young's modulus,

- increases Poisson's ratio,

- increases the porosity and permeability, and

- reduces the P-wave velocity.

Of the laboratory properties examined by Martin and Stimpson /71/, the P-wave velocity showed the greatest sensitivity to sample disturbance. Figure 13 shows the comparison of
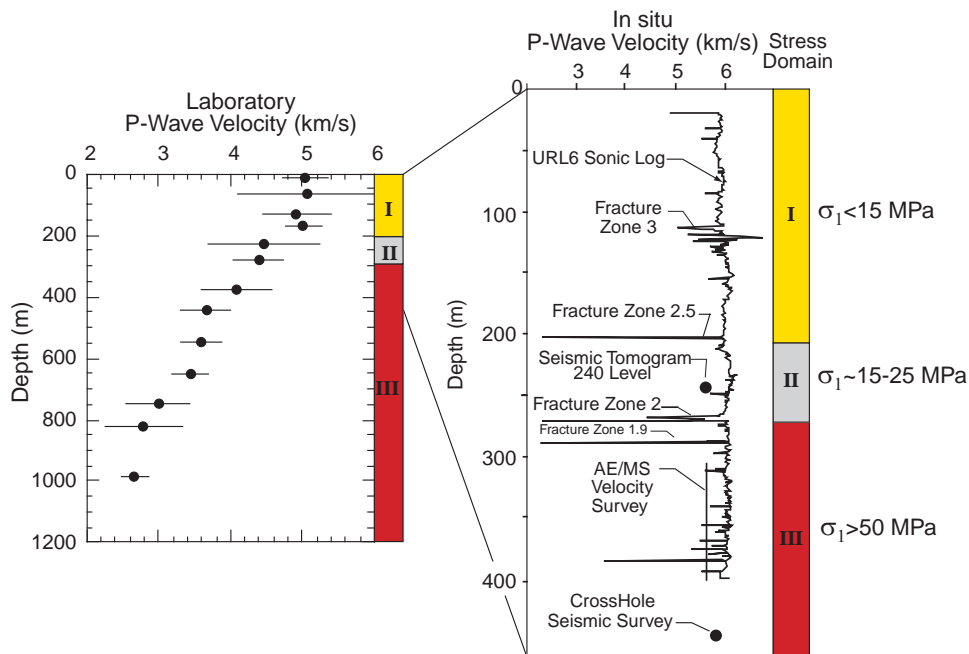

Figure 13: *Comparison of the variation in P-wave velocity in laboratory samples and in-situ, modified from Martin and Stimpson /71/.*

the P-wave velocity measured on laboratory samples and the P-wave velocity recorded from in-situ seismic surveys. Martin and Stimpson observed a reduction in P-wave velocity of approximately 50% for granite samples taken at 1000-m depth compared to those taken at shallow depths.

Martin and Stimpson /71/ suggested that sample disturbance started to affect the laboratory properties of Lac du Bonnet granite when the ratio of far-field maximum stress to the uniaxial compressive strength was greater than 0.1. When this ratio reached approximately 0.3, the uniaxial compressive strength and tensile strength of Lac du Bonnet granite were reduced by nearly 30 and 60% , respectively. It is important to recognize this phenomenon and take it into account when using design criterion that rely on properties that can be affected by sample disturbance.

3.3 Äspö laboratory properties

The Äspö rock strength database consists of 83 samples from 24 different bore holes at Äspö (and nearby Laxemar). The rock types at Äspö and Laxemar are granite, diorite and gneiss.

The values below 400 meters all comes from either the ZEDEX tunnels (depth approximately 415 m) or from the Prototype Repository access tunnel (depth approximately 450 m). The uniaxial strength of the samples from the ZEDEX area appears lower then the uniaxial strength of the samples from the access tunnel (Figure 14).

Limited testing has been carried out to determine the triaxial strength of Äspö rocks (Figure 15, see Appendix A).
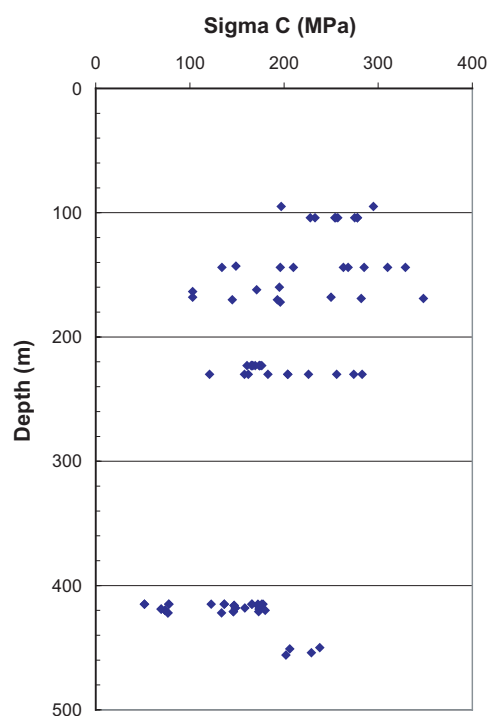

Figure 14: *Results from uniaxial testing of cores from Äspö.*

22
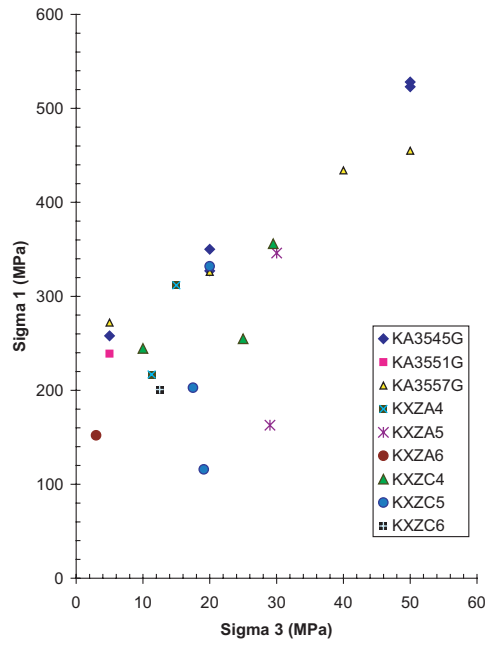
Figure 15: *Results from triaxial testing of cores from Äspö.*

Figure 16 shows the relationship between Young modulus and the uniaxial compressive strength for the Äspö rocks. The classification shown in Figure 16 is based on the work of Deere /30/ and indicates that the Äspö rocks display characteristics of similar hard rocks.
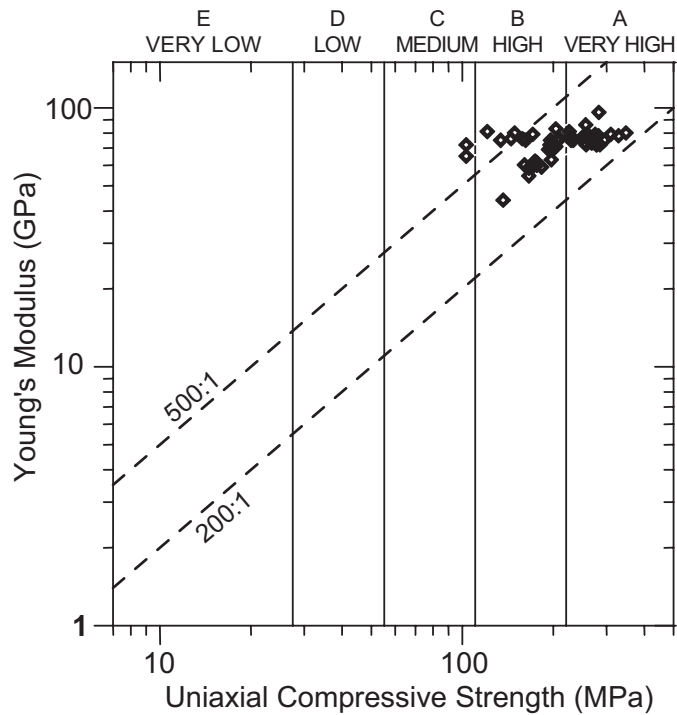

Figure 16: *Relationship between Young's modulus and Unixial compressive strength using the classification of Deere /30/.*

4 In-situ stress

The results from triaxial stress measurements are usually reported in terms of the principal stresses σ_1, σ_2 and σ_3 and their associated trend and plunge. However, in Sweden and Canada the major (σ_1) and intermediate (σ_2) principal stresses tend to dip between zero and about $10°$ and the minimum principal (σ_3) stress tends to be approximately vertical. Consequently, the maximum (σ_H) and minimum (σ_h) horizontal stress and the vertical (σ_v) stress are used synonymously with σ_1, σ_2 and σ_3, respectively. This notation is also used in this report.

4.1 Vertical stress

The gravitional vertical stress at a depth D is the product of the depth and the unit weight (γ) of the overlying rock mass. The unit weight of intact rock varies, in general, between 25 and 30 kN/m^3 for most common rocks such as granite, volcanics, metasediments, limestone, etc. Thus the vertical gravitional stress (σ_v) is estimated from the simple relationship:

$$\sigma_v = \gamma D \tag{7}$$

and should increase linearly with depth (D) with a gradient between 0.025 and 0.030 MPa/m. Measurements of vertical stress at various mining and civil engineering sites supports Equation 7 (see Table 1). Because the minimum principal stress is usually subvertical the minimum principal stress gradient must be less than the vertical stress gradient. However, the close agreement between the two gradients suggests that in general the minimum principal stress is very close to vertical. Johansson and Hakala /52/ also used this assumption for evaluating the critical depth for a KBS-3 type repository.

While the vertical stress tends to be on average equal to the weight of the overburden, the vertical stress can vary significantly from this trend. For example Martin and Chandler /61/

Table 1: Summary of measured vertical stress gradients in various rock types.

Vertical Stress Gradient (MPa/m)	Location (rock type)	Depth (m)	Reference
0.0249	Elliot Lake (Quartzites)	900	/40/
0.0266 ± 0.0028	World data	0-2400	/42/
0.0270	World data	0-3000	/19/
0.0265	World data	100-3000	/75/
0.026 ± 0.0324	Canadian Shield	0-2200	/43/
0.0266 ± 0.008	Canadian Shield	0-2200	/8/
0.027	URL, Granite	0-440	/59/
0.0285	Canadian Shield	0-2300	/44/
0.0260	Canadian Shield	0-2200	/9/
0.0264	Äspö HRL, Diorite	150-420	/5/
0.0249 ± 0.00025	Sellafield, UK (Sandstones/Volcanics)	140-1830	/13/

showed that the vertical stress normalized to the weight of the overburden, around large-scale faults, ranged from 1 to 3 (Figure 17). They showed that this variation was caused by large-scale asperities along the faults, and that these asperities resulted in heterogeneous normal stresses acting on the faults. These stress perturbations influenced the vertical stress approximately 150 m away the fault. Hence, while the vertical stress can be estimated by the weight of the overlying rocks, within the depth range of a nuclear waste repository, significant deviation from this mean should be anticipated. Experience shows that these deviations are greatest close to the ground surface.

4.2 Horizontal Stresses

The horizontal stresses acting on an element of rock at a depth D below the surface are much more difficult to estimate than the vertical stresses. Normally, the ratio of the average horizontal stress to the vertical stress is denoted k such that:

$$k = \frac{\sigma_1}{\sigma_3} \tag{8}$$

Measurements of horizontal stresses at sites around the world show that the ratio k tends to be high at shallow depth and that it decreases at depth /45/. The ratio of the horizontal stresses σ_1/σ_2 shows a similar trend and at AECL's URL the ratio below 500 m tended towards unity suggesting that in the horizontal plane the deviatoric stresses are very small
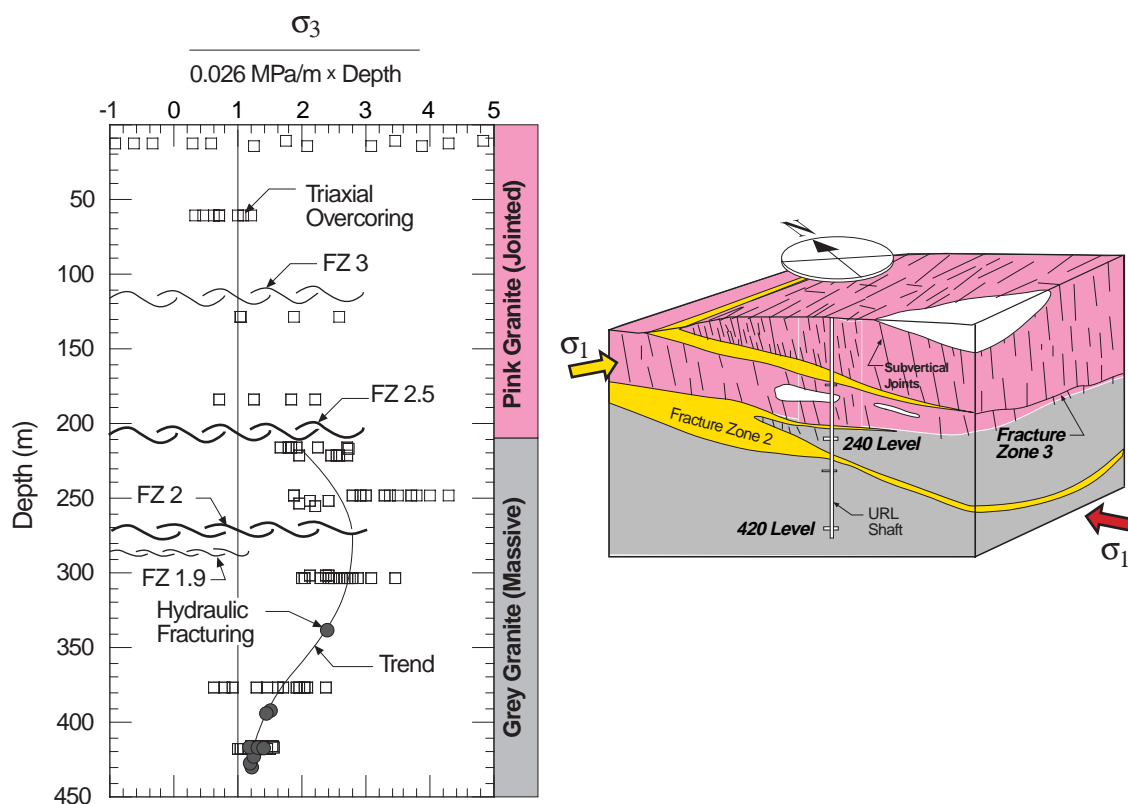

Figure 17: *The variation in vertical stress with depth measured at AECL's URL, modified from /61/.*

25

(Figure 18). This would imply that below 500 m aligning tunnels relative to the maximum stress direction may not be significant. However, as shown by Martin *et al.* /69/ at the 420 Level of AECL's URL tunnels aligned parallel to the maximum horizontal stress showed no evidence of failure while tunnels aligned parallel to minimum horizontal stress showed significant spalling.

4.3   Stresses in the Canadian Shield

There are no sites in the Canadian Shield where detailed in-situ stresses have been measured from ground surface to great depths. However, CANMET /45; 9/ compiled in-situ stress measurements from various mines in the Canadian Shield to provide a composite distribution of stresses to depths of 2200 (Figure 19). These measurements were carried out in a variety of rock types and geological environments. In addition to the CANMET 1990 database, an extensive in-situ stress characterization program was carried out at AECL's Underground Research Laboratory (URL) located on the western edge of the Canadian Shield in southeastern Manitoba. This program (130 measurements) characterized the in-situ stress distribution from a depth of 20 m to 950 m and showed that stress magnitudes and orientations are significantly affected by geological structures such as joints and faults, see Martin and Chandler /61/.

Experience has shown that predicting in-situ stress magnitudes from a stress database is fraught with difficulties /63/. For example the maximum stress magnitude at a depth of 2500 m in the Canadian Shield can range from 50 to > 100 MPa, depending on the method of prediction (Figure 20). While the linear best fit line is normally used to project the stress magnitudes at depth, there are other choices, as indicated by the curved lines in Figure 20. Hence, projecting stress magnitudes at depth is not straightforward.

The trend of the horizontal stress in the Canadian Shield tends to align Northeast-Southwest. In the deep mines of Sudbury Basin, Ontario, this trend is also observed and this trend was also found at AECL's URL /59/. However, at the URL the trend of the maximum horizontal
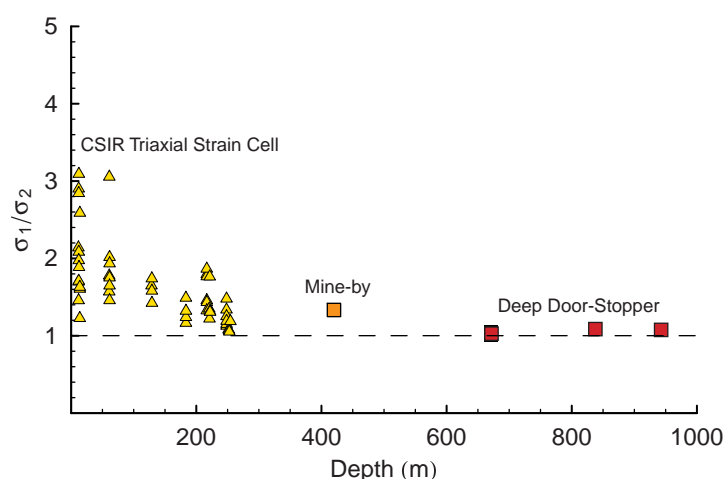

Figure 18: *The ratio of the horizontal stresses measured at AECL's Underground Research Laboratory.*
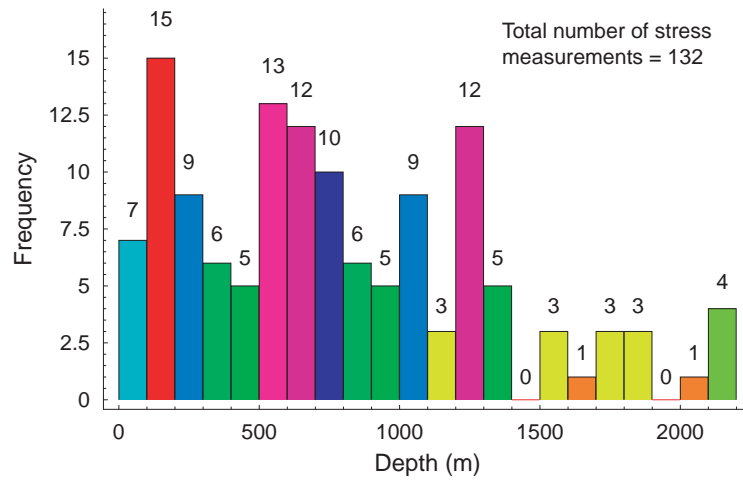
***Figure 19:** The distribution of stress measurements with depth in the Canadian Shield.*
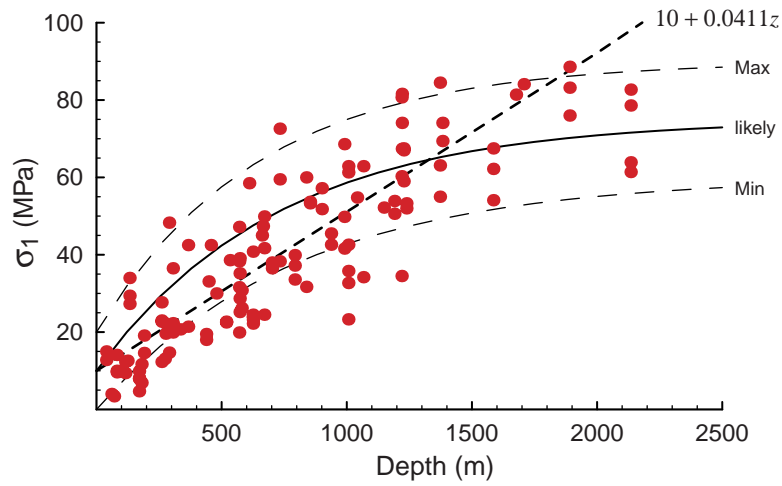
***Figure 20:** Maximum stress distribution with depth in the Canadian Shield. The linear best-fit line is normally used to project stress magnitudes with depth.*

stress rotated 90 degrees below a major thrust fault (see Figure 17). Hence, it is not unusual to have both the trend and magnitude of the in-situ stresses vary over a given site.

4.4   General trends from the Fennoscandian Shield

Stephansson /98/ provided an overview of general stress trends in the Fennoscandian Shield. This work was augmented with recent data from the Swedish and Finnish nuclear waste management programs. These databases include results from both overcoring and hydrofracturing measurements.

4.4.1   Swedish Data

The Sweden database contains 46 bore holes with 418 individual measurements. These stress measurements in Sweden have been carried out in gneiss, granite and diorite.

Figure 21 shows the Sigma 1 and Sigma 2 magnitudes with depth. Like Canada, Sigma 1 and Sigma 2 tend to be aligned in a horizontal plane. Figure 21 also shows the vertical stress (Sigma 3) plotted against depth based on 179 measurement values from 29 different bore holes.

4.4.2   Finnish Data

The stress database from Finland is based on 136 measurements from 15 boreholes. The measurements have been performed by Swedish State Power Board for Posiva Oy in gneissic
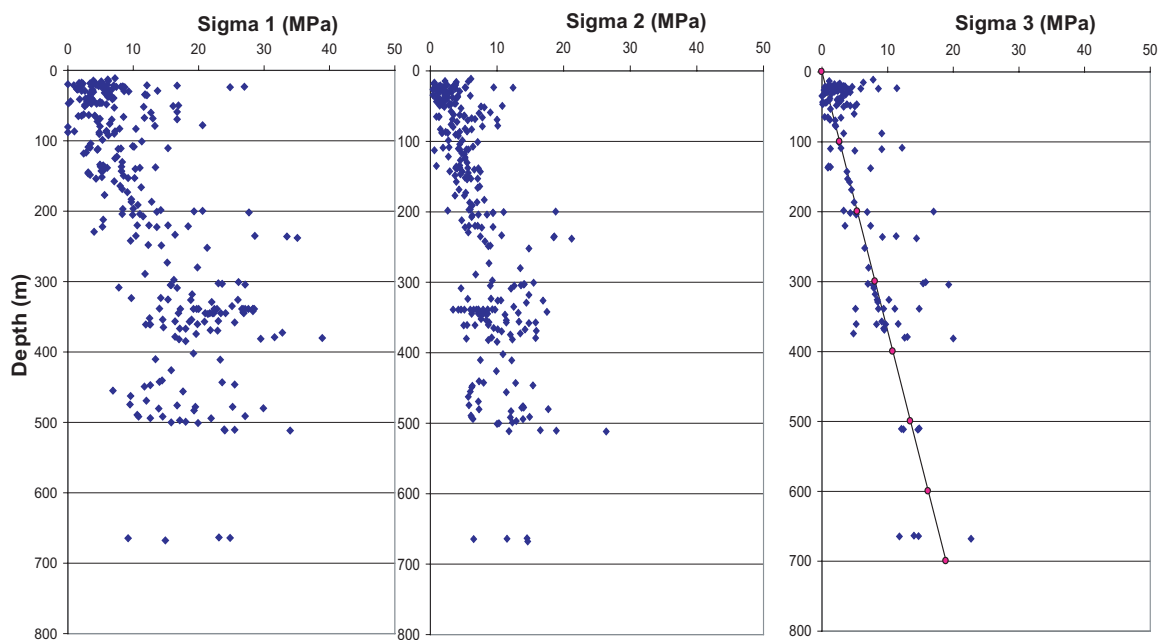

Figure 21: Summary of the in-situ stresses versus depth for Sweden. The linear function for Sigma 3 assumes a stress gradient of 0.027 MPa/m.

and granitoidic rock mass at the investigation sites: Kivetty, Romuvaara and Olkiluoto /56/ and at the Posiva Oy test site at Hästholmen /55/. Their results are summarised below in Figure 22 and are in general agreement with the data presented in Figure 21.

4.5 Examples of stress variability in Sweden

4.5.1 Äspö Hard Rock Laboratory

The Äspö Hard Rock Laboratory (HRL) is located on the Swedish east coast, about 350 km south of Stockholm. Site investigations started in 1986, and the excavations started in 1990. The construction phase was completed in 1995. The geological, hydrogeological and geotechnical site conditions are summarized by Rehn et.al (1997).

The stress measurements at Äspö and the nearby Laxemar area have been performed in gneiss, granite and diorite. Nineteen boreholes have been used to conduct 157 measurements and these results are included in Figure 21. Four deep boreholes have been used for stress measurements at Äspö HRL and these borehole all penetrate fractured zones at depths between 470 - 600m. At these depths there is a significant increase in stress magnitude in all boreholes. An example from one of the boreholes is given in Figure 23. At present there is no clear explanation for this rapid increase in stress magnitude. A possible explanation may be linked to an increase in fracture frequency between 470 - 600 m depth. However,
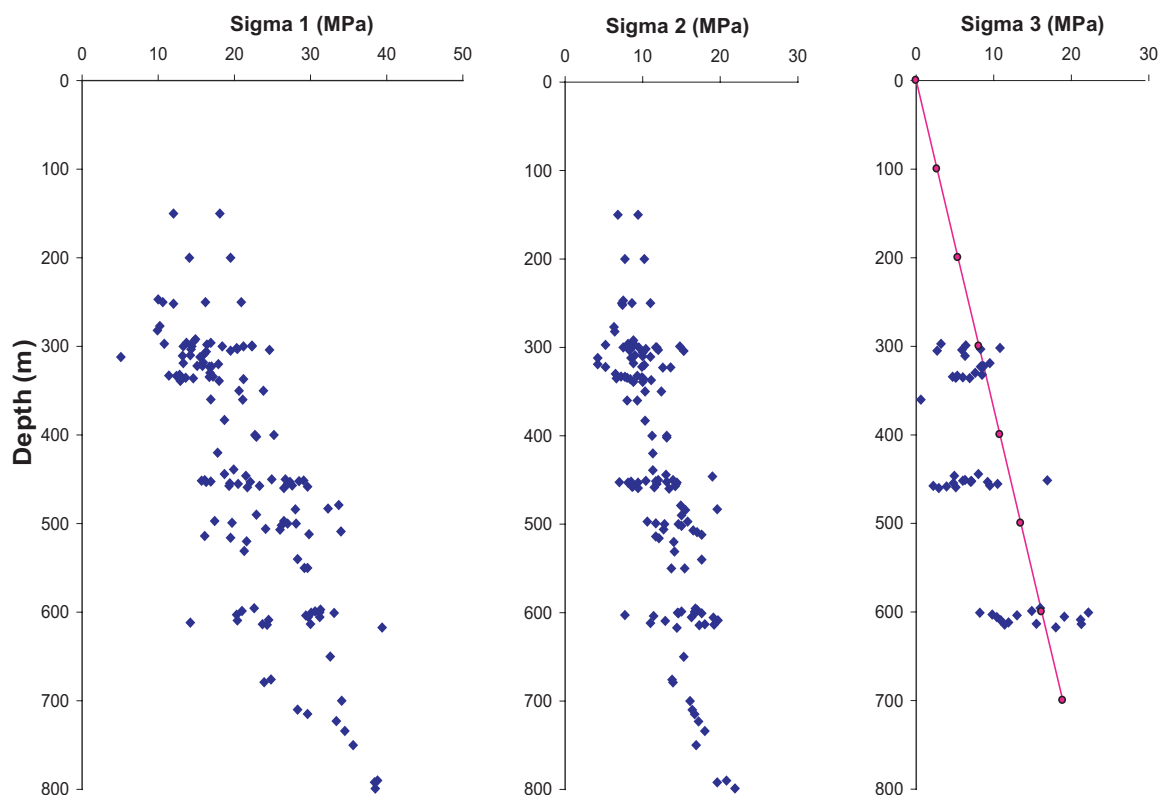

Figure 22: *Summary of the in-situ stresses versus depth for Finland. The linear function for Sigma 3 assumes a stress gradient of 0.027 MPa/m.*

the relatively higher fracture frequency is only observed in some of the boreholes usually over distances of approximately 100 m. Due to the relatively large distance between some of the stress-measurement boreholes it is likely that more than one geological structure is causing the stress magnitude increase. One possible hypothesis is that the upper geological domain with the lower stress magnitudes is more fractured due to fracturing associated with isostatic rebound. However, at this time this is merely an hypothesis and this topic requires further study.

4.5.2 The Forsmark area

Forsmark is located at the East Coast of Sweden, about 130 km north of Stockholm. At this site three of the nuclear power units in Sweden are located, as well as the Final Repository for Low and Intermediate Reactor Waste (SFR). All three power units are founded on rock, and the cooling water is discharged through two submarine tunnels with a length of 2300 and 2500 m. The SFR facility is located under the sea about 1 km from the harbor of Forsmark.

Site investigations started in 1971 and were ongoing to the end of the construction of the SFR in 1986. Carlsson and Christiansson /20/ summarize the geological and geotechnical results from those investigations. The former Swedish State Power Board (SSPB) also used the site for testing of a modified version of the Leeman triaxial strain cell. The SSPB cell was
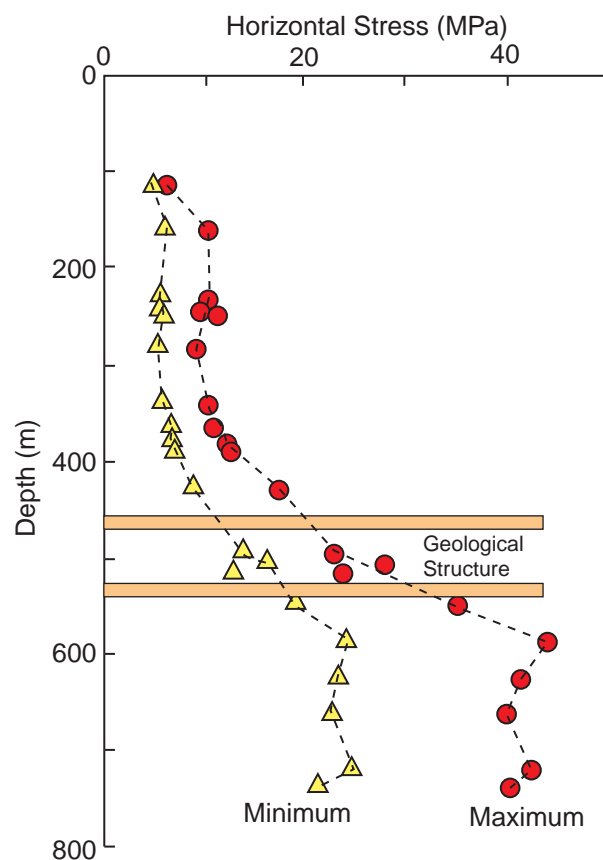

Figure 23: *Horizontal stress (σ_1 and σ_2) versus depth measured in borehole KAS02. Zones of geological structure (mylonites) are also shown, data from Lundholm /58/.*

30

designed for three dimensional stress measurements by overcoring using 100-mm-diameter boreholes. The overcoring cell was successfully tested down to 500-m depth Carlsson and Olsson /21/. The 500-m deep borehole was later used for hydraulic fracturing stress measurements by Stephansson and Ångman /99/.

During testing of the SSPB stress measurement cell in the boreholes DBT-1 and DBT-3 just north of unit 3 a sub-horizontal fracture zone penetrated was at 320 m depth in the deeper borehole /21/. The results from these stress measurements and the location of the fracture zone are shown in Figure 24.

A significant increase in stress magnitude was measured beneath the sub-horizontal fracture zone. The first attempts to measure stresses just below the fracture zone failed due to discing of the cylindrical core during overcoring (ring discing). This indicates a significant anisotropy in the stress magnitude caused by the sub-horizontal fracture zone. The orientation of the maximum horizontal stress was sub-parallel to the NW - SE trending Singö fault zone both above and below the sub-horizontal fracture zone.

4.6 Excavation-induced stresses

For stability assessment, it is the maximum induced stress near an excavation wall that determines whether failure occurs. The excavation-induced stresses, of course, are directly related to the in-situ state of stress but the geometry of the opening and excavations within the zone of influence of adjacent openings often have a more dominant effect on the maximum stress concentration at the excavation wall. This excavation-induced stress increase is often
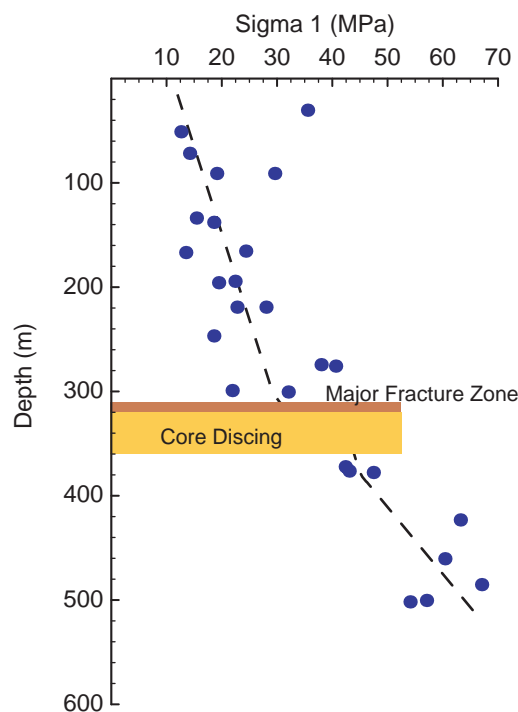

Figure 24: *Maximum principal stress versus depth for SFR Facility, Forsmark, after Christiansson and Martin /24/.*

referred to as stress change.

Stress change will play a significant role where multiple openings are within the zone of influence of each other. The effect of this interaction can be illustrated with the concept of the extraction ratio (r), which is commonly used in the mining industry. Extraction ratio is defined as the area excavated divided by the total area. While extraction ratio is commonly used in mines with planar horizontal ore bodies it can be adapted for any orientation. According to Brady and Brown /17/ the stress concentration (SC) resulting from this extraction is given as:

$$SC = \sigma \frac{1}{1-r} \tag{9}$$

For example, consider the section view of the emplacement tunnels to determine the influence of one emplacement tunnel on another and the additional stress concentration the pillar, i.e., the rock mass, between these rooms will be subjected to. Figure 25 shows the stress concentration factor for the borehole emplacement and room emplacement designs proposed by AECL. The same concept can be applied to the pillars, rock mass, between the waste emplacement boreholes to determine an estimate of the interaction of multiple openings. In this case a plan view would be used to evaluate the stress concentration.

Underground mining operations must operate at very high extraction ratios to remain economically viable. The effect of these high extraction ratios is shown in Figure 25. Mining experience in hard rocks suggests that once extraction ratios exceed 0.5, rock burst conditions should be anticipated. Obviously this depends on the depth of the mine as the far-field stress magnitudes at 1000 m depth will be greater than the far-field stress conditions at 500 m depth. Nonetheless, the distance between emplacement holes and rooms need to be large if there is to be negligible stress increases in the pillars, i.e., rock mass, between
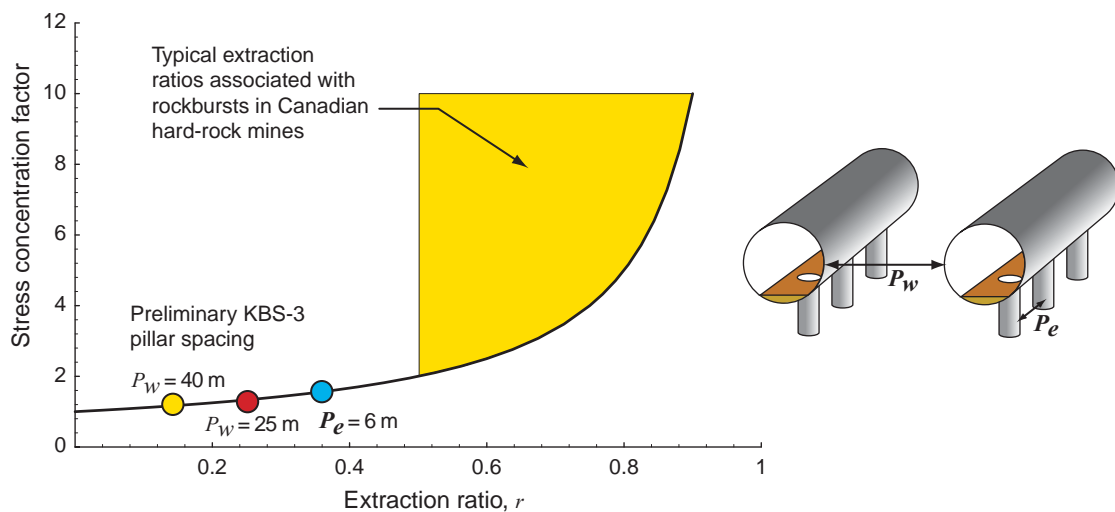

Figure 25: *Illustration of the stress concentration factor as a function of extraction ratio. Also shown is the extraction ratio for the KBS-3 concept with the spacing between 5-m-diameter tunnels at 25 m ($r = 0.014$) and 40 m ($r = 0.25$), and the extraction ratio for the spacing between the emplacement boreholes.*

32

these openings. In most situations, the stress concentration factor can only be determined by three-dimensional analyses because the stress concentration from the deposition tunnel interacts with the stress concentration from the emplacement borehole. The extraction ratio mentioned previously can only be used as a first pass indicator.

At low extraction ratios the stress variability will be more significant than the stress concentrations caused by multiple openings (Figure 26). As discussed in Section 4, stress variability must be anticipated at a nuclear waste repository

4.7 Measuring in-situ stress for a nuclear waste repository

The design of an underground excavation requires in-situ stress as an input parameter, hence here is little debate about the need for stress measurements. The more challenging question is: What stress measurement techniques are best suited for deep excavations in hard rocks?

AECL's URL is often described as an excellent example of a site where the in-situ stress state is known with confidence Amadei and Stephansson /3/. While this is true, the in-situ stress state at the URL was not determined using only one of the methods listed in Table 2. In fact, most of the traditional indirect measurements failed below 300 m depth to give consistent results and in most cases gave erroneous results /59/. Combining all the results from the various techniques mentioned in Table 2 enabled the development of a valid stress tensor below 300 m depth. One of the findings from this combination of methods is that large-scale methods using back-analysis techniques give consistently more reliable results than 'small-scale' traditional methods.

Wiles and Kaiser /106/ showed that even under very good rock mass conditions, such as at AECL's URL, ten overcore tests were needed to provide statistically significant results and that with less than ten measurements, the results were very erratic and with less than five measurements little confidence can be placed on the mean stress. Figure 27 from
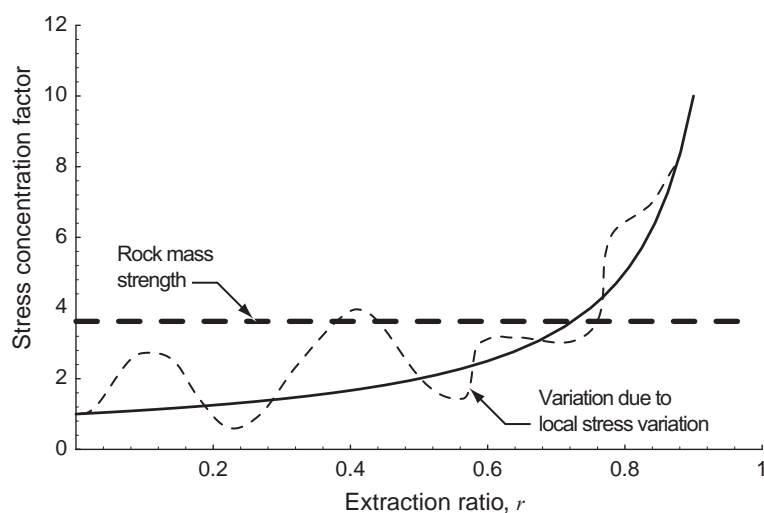

Figure 26: Illustration of the stress variation as a function of extraction ratio.

Table 2: *Stress measurement techniques tried at AECL's URL summarized from Martin /59/ and* Martin *et al. /70/*

Method	Technique	
Indirect	Triaxial Strain Cells	Modified CSIR
		CSIRO
		Swedish State Power Board
		Sherbrooke Cuis Cell
	Biaxial Strain Cells	CSIR Door Stopper
		Modified Door Stopper
		USBM Gauge
		Bock Slotter
	Hydraulic Fracturing	Maximum Stress
Direct	Hydraulic Fracturing	Minimum Stress
Large-scale back-analysis	Convergence	
	Under-excavation	
	Mine-by Experiement	
	Depth of failure	

Martin *et al.* /68/ showed that a single large-scale stress measurement technique gave the same results as the mean of the ten overcore results referred to by Wiles and Kaiser /107/. Martin *et al.* /68/ attributed the variability in overcore results to the systematic errors in the measurement technique and not the variability in stress. Hence, stress measurement techniques must be designed to reduce this variability.
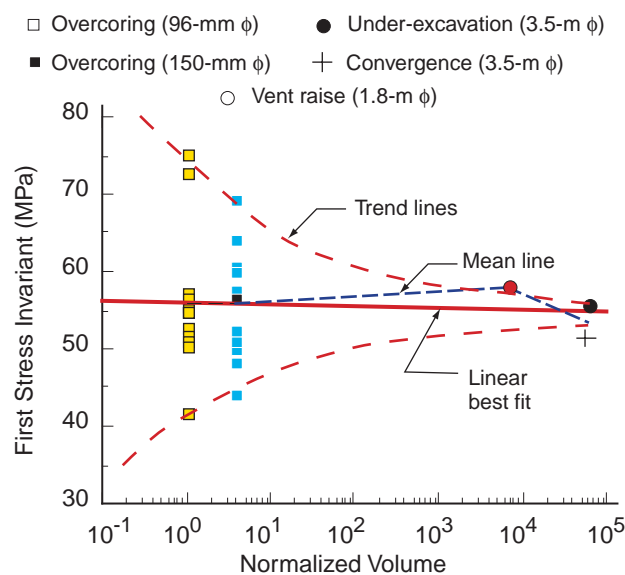

Figure 27: *Effects of scale on stress variability, data from Martin* et al. */68/. This data supports the notion of a representative elemental volume for in-situ stress suggested by Hyett* et al. */51/.

34

4.7.1 Lessons from AECL's URL

The findings from the in-situ stress characterization program that was carried out at the URL from 1980 through to 1990 can be summarized as follows:

1. Traditional strain-relief methods are suitable for shallow depths, i.e, where the ratio of the far-field maximum stress to the uniaxial laboratory strength is less than $\sigma_1/\sigma_c < 0.15$.

2. Where the ratio of $\sigma_1/\sigma_c > 0.15$ the rock mass response will be non-linear and, hence, any strain-relief method that records the non-linear rock mass response and requires the interpretation of these non-linear strains will give erroneous results if interpreted using linear elastic theory. The severity of the error will depend on the magnitude of the ratio of σ_1/σ_c above 0.15. The URL experience indicates that when $\sigma_1/\sigma_c > 0.2$ the results are extremely difficult to interpret and when $\sigma_1/\sigma_c > 0.3$ the results are basically meaningless. In the Canadian Shield these limits occur at depths of approximately 1000 m and 1500 m, respectively. Wiles and Kaiser /107/ showed how the under-excavation technique could be used to overcome these limitations.

3. Where the horizontal stress magnitude is the maximum stress, and the vertical stress is the minimum stress hydraulic fracturing produces sub-horizontal fractures in vertical boreholes and these are difficult if not impossible to interpret. It should also be noted that hydraulic fracturing only provides the minimum stress, attempts to provide the maximum stress should be treated with caution. In addition the pressures required to fracture the rock at depths greater than 1000 m are beyond the capabilities of most hydraulic fracturing equipment, used in conventional exploratory boreholes.

4. Large scale observations and back-analysis of failures similar to those observed in borehole breakouts and circular tunnels, using the depth and extent of failure can reduce the variability that plagues small-scale measurements such as overcoring and provide consistent stress orientations and magnitudes.

4.7.2 Lessons from the Äspö HRL

In-situ stress measurements were carried out from the surface prior to excavation using overcoring by the SSPB Leeman cell and hydraulic fracturing. During excavation overcoring was done using the CSIRO cell. Overcoring has also been carried out for various experiments (ZEDEX and Prototype Repository), using both the CSIRO and the SSPB Leeman cells. Hydraulic fracturing has been carried out in the nearby Laxemar area. Recently, comprehensive testing of the SSPB Leeman triaxial cell and the new AECL Biaxial strain cell has been carried out.

The interpreted stress magnitude results of hydraulic fracturing are normally lower than the results of overcoring. There is however a reasonable agreement in orientation of the horizontal stresses when comparing results from overcoring and hydraulic fracturing.

The results from overcoring at the experimental level of Äspö (410 to 450 m depth) have been subject to detailed studies. It was found that:

1. There is a small anisotropy caused by sample disturbance in the range of 2 to 6%

difference in the P-wave velocity in orthogonal directions. This is caused mainly by local mineralogical variations. The directional differences will not have a significant influence on the interpretation of the overcoring results.

2. The ratio $\sigma_1/\sigma_c \approx 0.15$. Hence the rock mass response is close to or just above the limit where the measured response is linear and elastic.

3. The scattering in overcoring results is partly due to poor quality control during testing and data interpretation /77/.

4. The results of the minor and intermediate stress magnitude from overcore tests varies depending on the orientation (horizontal or vertical) of the borehole.

Hydraulic fracturing in vertical boreholes below a depth of 800-900 m produced non-vertical fractures. At larger depth in the Laxemar borehole it was difficult to identify the induced fractures by the use of impression packers due to the very good quality of the rock mass and the tight induced fractures. Recently completed drilling of a test hole at Oskarshamn (25 km south of Äspö HRL) encounted core discing at a depth of 865 m in similar rock types as at the Äspö HRL. These results indicate, that below approximate 800 m depth at the Äspö HRL, it is difficult to achieve reliable stress measurement results.

4.8 Recommendations for a site stress characterization program

The experiences from various sites in Sweden and Canada presented earlier in this Section can be summarized as follows:

- The limitations of any method used for in-situ stress measurements must be well documented and understood.

- The mechanical behaviour of the rock for the actual stress situation during in-situ stress measurements must be understood.

- The dominant tectonic pattern may have a significant influence on the stress orientations.

- Larger geological structures may have a significant influence on the local stress field and shall, if possible, be avoided if stress measurements are carried out for characterization of the design stress field for the repository.

- Stress ratios may be affected by geological structures.

- A design stress ratio with depth based on linear regression of measurement data may be erratic if sub-horizontal geological structures causes different stress domains.

A site stress-characterization program must therefore adhere to the following guidelines:

- Only well documented and proven methods for in-situ stress measurements shall be used.

- More than one stress measurement method should be used.

- The site stress and strength conditions are not beyond the assumptions used to interpret

36

the data. For most methods this implies that the rock mass response must be linear elastic.

- A mechanical testing program is required in parallel to the in-situ measurements to ensure that the mechanical properties of the rock are understood.

- The geometry of the larger geological structures must be known when planning for in-situ stress measurements.

- The regional orientation of in-situ stresses is most likely best achieved if measurements are carried out in the central portion of the larger tectonic blocks. The possible local influence on stress orientations by geological structures may however need to be studied separately.

- If sub-horizontal fracture zones are identified at the potential repository depth, the occurrence of various stress domains above and below such structures must be investigated.

- A decreasing fracture frequency with depth, may influence the state of stress.

- Indicators of stress orientations and stress magnitude such as borehole breakouts and core discing shall be recorded.

In summary the overall objective of the site stress-characterization program is to quantify the in-situ stress magnitudes and orientations such that repository design proceed. The actual number of stress measurements required for this task will depend on geological complexity of the site. Experience from AECL's URL showed that in the early stages prior to construction of the facility the hydraulic fracturing results from the deep borehole showed that the stress magnitudes below 300 m were probably high. Those initial finding proved to be true, but it took over 50 additional stress measurements to quantify the magnitudes and orientations. Similar experience exists at Äspö HRL.

5 Stability of excavations

The possible depth of repository between 400 and 700 m indicates that the excavations between the ground surface and the repository depth will encounter a range of stability issues. In this section some of the methods used to address these stability issues are discussed.

5.1 Empirical Methods

Empirical methods are commonly used in the early stages of a project for preliminary design purposes to establish the quality of the rock mass and to assess the stability and possible range of support requirements of underground openings. Two commonly used empirical methods for tunnelling are the *RMR* system developed by Bieniawski /15/ and the *Q* system developed by Barton and Grimstad /10/. These techniques involve the quantitative and qualitative assessment of key rock mass properties and characteristics (Figure 28), the assignment of an index value to each and an algebraic relationship resulting in a rock mass quality value within a numerical range representative of the best to the worst rock mass quality. This rock mass classification result can be used in calibrated (empirical) design charts to establish critical spans for excavations, stand-up times for unsupported openings and support requirements (e.g. Figure 29).

The *Q* system was first developed and applied to engineering problems by Barton *et al.* /12/. The quality terms associated with each range interval are illustrated in Figure 29 (top and bottom axes). The *Q* value itself is calculated as:

$$Q = \frac{RQD}{Jn} \times \frac{Jr}{Ja} \times \frac{Jw}{SRF} \tag{10}$$
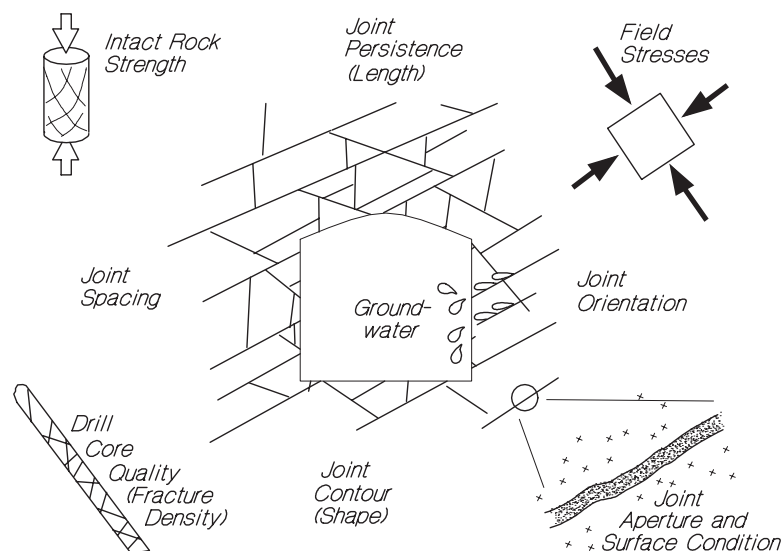
Figure 28: Elements of rock mass classification systems, after Hutchinson and Diederichs /50/.

where

RQD	= Rock Quality Designation - rock core index
Jn	= Joint Set Number (number of unique joint sets)
Jr	= Joint Roughness Number (based on large and small scale roughness)
Ja	= Joint Alteration Number (joint surface condition)
Jw	= Joint Water Reduction Number (effect of water and water pressure)
SRF	= Stress Reduction Factor (accounts for high stress and low confinement)

Empirical correlations have also been established between rock mass classification systems and the deformation modulus (E_D) of the rock mass (Figure 30). Many of these correlations have been established from large scale plate load tests at dam sites and back analysis of measured tunnel deformations. The proposed relationships in Figure 30 provides good agreement with the measured deformation modulus reported for the ZEDEX Experiment /79/ and the Mine-by Test Tunnel /91/.

While the empirical design methods are useful for assessing general support requirements for the repository, many situations will exist where the potential for structurally controlled instability must be assessed on an individual bases, such as major intersections. In such cases numerical tools that include fracture geometry, fracture properties and in-situ stress, e.g., *3DEC*, will be required. The characteristics of the fractures, which will be required as input to the numerical tools, can be assessed using the methodology proposed by Barton and Choubey /11/ and employed during the ZEDEX experiment /79/.
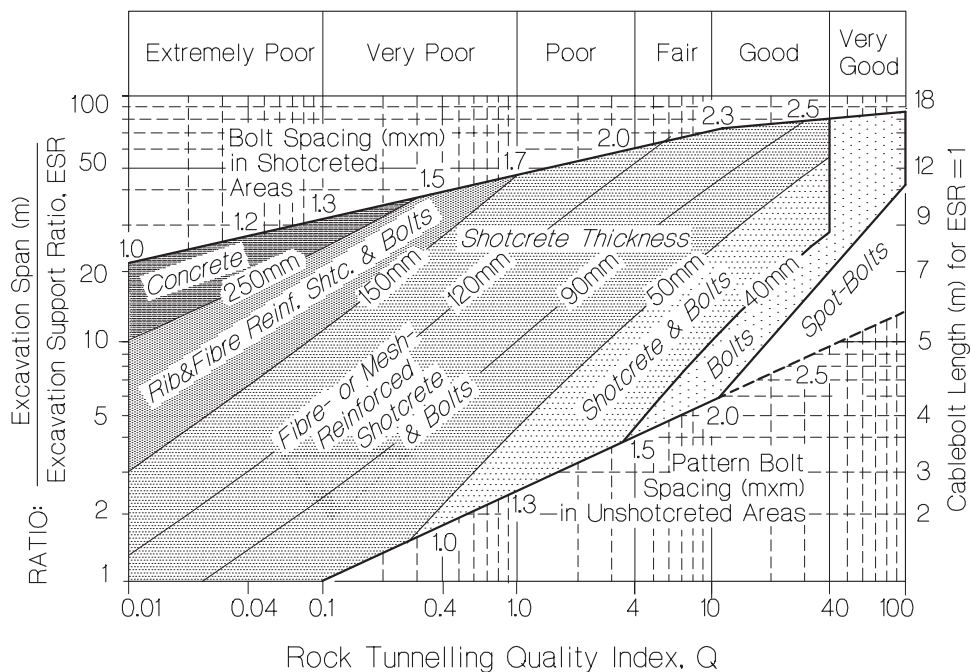

Figure 29: *Support recommendations for underground tunnels based on the Q system (after Barton and Grimstad /10/ and Hutchinson and Diederichs /50/.*

39

5.2 Discrete block/wedge failure and tunnel shape

The stress distribution around an excavation in an elastic rock mass is controlled by the shape of the excavation. For example, openings with corners or small radii of curvature will have high compressive stress concentrations in these locations. Hence, there is a tendency to increase the radius of curvature in the design of underground openings, to avoid overstressing of the rock mass. This is particularly evident in civil engineering where tunnels are frequently circular or horse-shoe shaped. In deep mining, development tunnels often have rectangular shapes with a slightly arched roof to also reduce stress concentrations.

In low-stress environments in the (to approximately 250 m depth) the rock mass response tends to be elastic as the Damage Index is less than 0.4, and hence stability is controlled by the rock mass structure (see Figure 7). Thus the optimum tunnel geometry should reduce the possibility of blocks falling from the roof. Brady and Brown /17/ have shown that sliding along a plane from the roof of a tunnel can be evaluated in two dimensions by:

$$\sigma_{1_f} = \frac{2c + \sigma_3(\sin 2\beta + \tan(1 - \cos 2\beta))}{\sin 2\beta - \tan\phi(1 + \cos 2\beta)} \tag{11}$$

where σ_3 is the minimum principal stress in the plane, c is the cohesive strength, ϕ is the friction angle and β is the angle of the failure plane relative to σ_3. Equation 11 illustrates that the confining stress σ_3 plays a major role in structurally-controlled stability. Hence, optimum tunnel geometry should reduce the region of low σ_3 close to the tunnel roof. Figure 31 show the elastic principal stresses around a typical tunnel with an arched and flat roof. Comparing the arched roof and flat roof in Figure 31, it is immediately evident that a flat roof causes a much bigger region of unloading, i.e., low σ_3, and hence would promote wedge-type failure. Thus in a low stress environment, an arched roof is a better choice in minimizing the potential for structurally controlled failure.
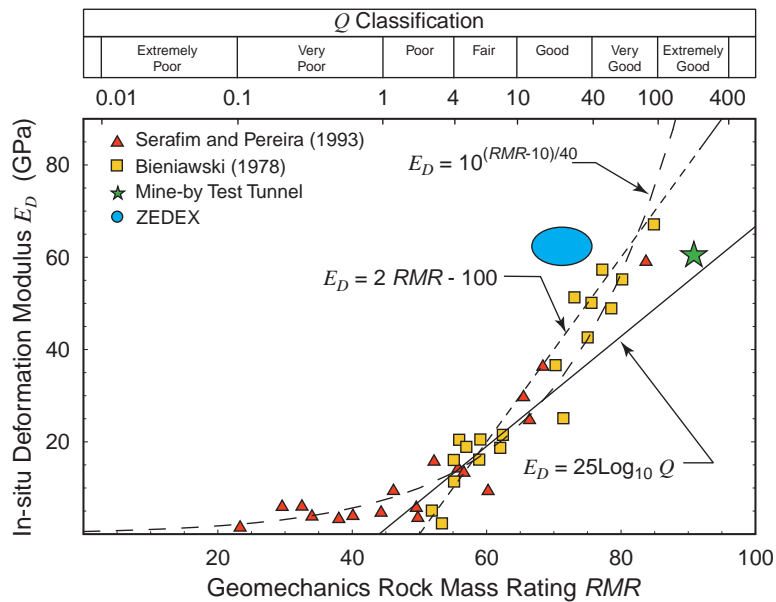
Figure 30: *Relationship between deformation modulus and the rock mass classification systems* RMR *and Q, after Hoek* et al. */48/.*
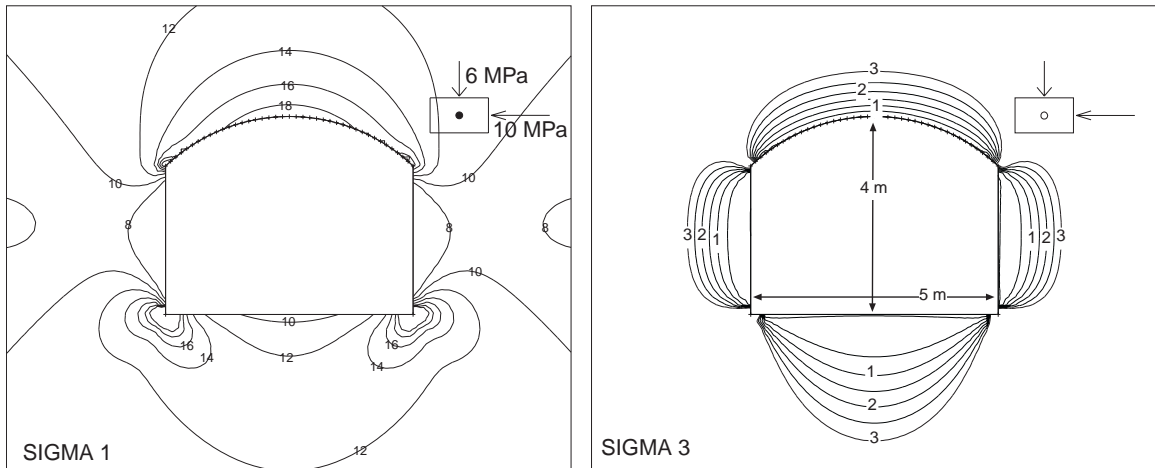
(*a*) Arched roof
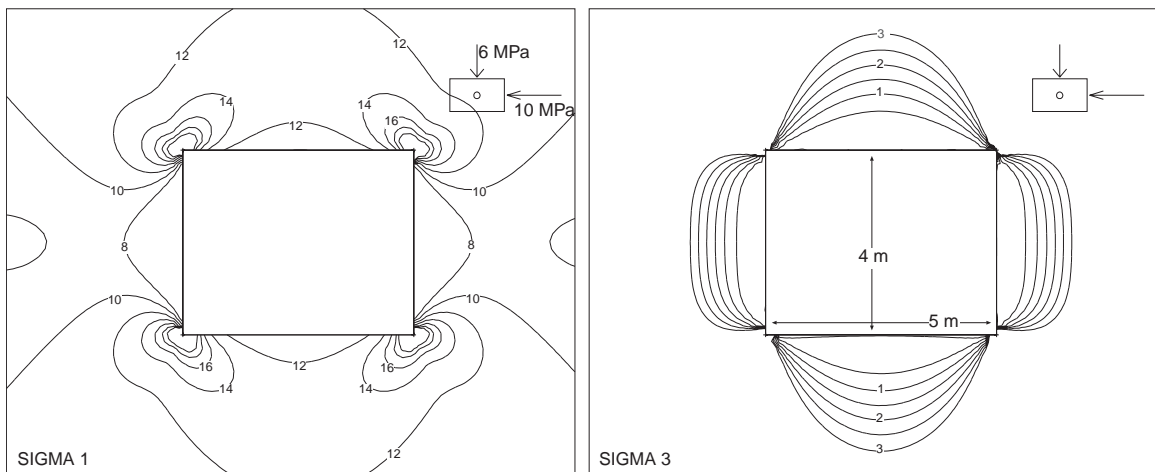
(*b*) Flat roof

Figure 31: *Elastic principal stresses around a tunnel with an arched roof and a flat roof in a rock mass where the far-field in-situ stresses are low relative to the strength of the intact rock. Note that the stress concentrations caused by the sharp corners and large region of low confinement caused by the flat roof compared to the arched roof.*

While two dimensional analysis are adequate to determine the extent of low σ_3 around a single tunnel, three dimensional analysis are required to assess extent of low σ_3 around intersecting tunnels. The three dimensional boundary element program Examine3D was use to determine the distribution of σ_3 around the tunnels on the 420 Level of the Äspö HRL /4/. Figure 32 shows that where tunnel intersections occur, the region of low σ_3 is greater then for the single tunnel. Hence given Equation 11 it is not surprising that the tunnel intersections often required heavier support pressures and longer support elements compared to single tunnels in the same rock mass.

5.3 Depth of fracture/stress reponse

In many situations at the depths of a nuclear waste repository, the discontinuous nature of the geological fractures will not allow discrete wedges to form. For example during the excavation of the ZEDEX 5-m-diameter tunnel no wedges formed in the roof. The geology at the ZEDEX site is predominately Äspö diorite and the overall rock mass quality (Q), using the classification system of Barton *et al.* /12/, ranges from 20 to 26 which can be descriptively referred to as moderately to sparsely jointed and massive. Geological mapping
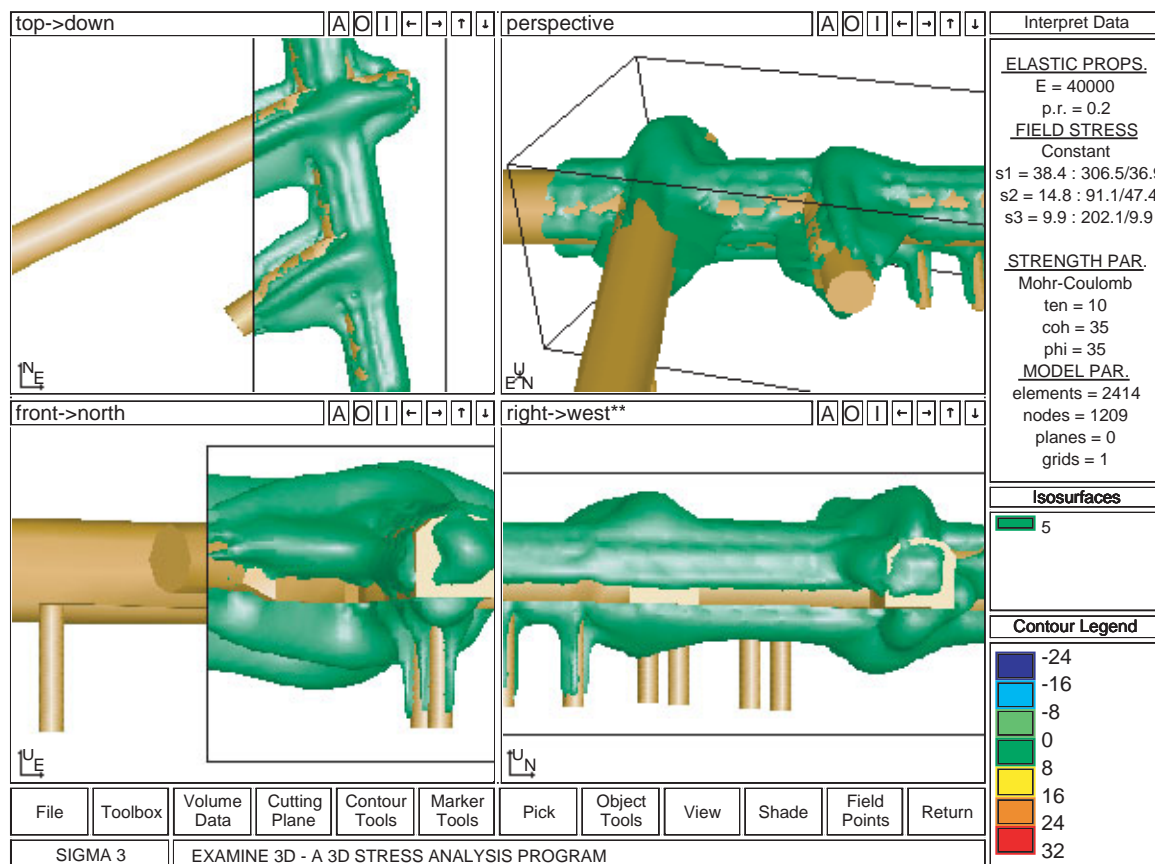

Figure 32: Illustration of the $\sigma_3 = 5$ MPa isosurface formed around intersecting tunnels (the far-field $\sigma_3 = 9.9$ MPa. Note that where the tunnels intersect the loss of confinement (low σ_3) extends further from the tunnel roof. The stresses were calculated using the three dimensional boundary element program Examine3D.

at the site identified two main discontinuous fracture sets with the northwest trending steeply dipping set being considered the dominant water-bearing set (Figure 33). These fractures are mapped as discontinuous en-echelon like fractures. While the fractures are prominent, their discontinuous nature prevents individual block movement. This notion is supported by the relatively small amount (0-1 mm) of convergence measured during excavation. The measured convergence was reasonably estimated by an elastic numerical model suggesting that the rock mass surrounding the tunnel can be treated as a continuum /73/.

While the discontinuous nature of the fractures in the ZEDEX experiment prevented the formation of discrete wedge, microseismic monitoring indicated that adjustment (displacements) along these fractures were occurring some distance from the tunnel boundary into the rock mass. Figure 34 shows the microseismic events around the tunnel and the correlation of the seismic events with the major fracture planes. Martin *et al.* /73/ demonstrated that the regions on those fracture planes where the Factor of Safety (*FOS*) was less than 1 coincided with the regions of microseismic activity (Figure 35).

Martin *et al.* /73/ used the mobilized frictional resistance as the slip criterion to determine the maximum distance that slip would occur from the the ZEDEX tunnel. Assuming friction angles of $\phi = 30°$ and $\phi = 45°$ they found that the maximum radial distance from the tunnel boundary that slip would occur was approximately 2 m and 1 m, respectively. This distance reflects an upper limit for the potential for adjustment along the fracture. It does not imply that there has been measurable slip out to 2 m as microseismic events may also have been generated by the adjustment of asperities to the imposed shear stress. In addition, because of the localized distribution of the shear stresses the potential for slip occurs at very discrete locations around the tunnel, as shown in Figure 35. Hence, the stability of underground openings, in such situations, must be assessed on an individual bases.
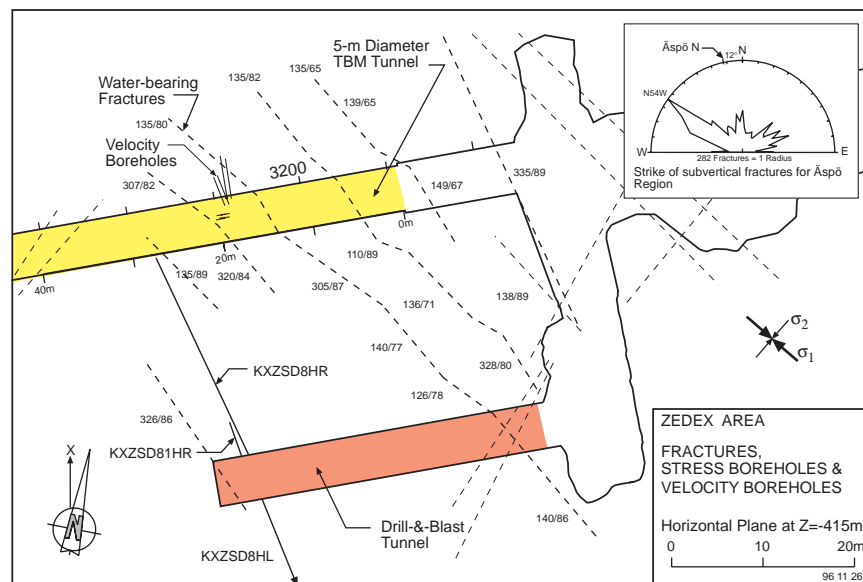
Figure 33: *General arrangement of the ZEDEX Project, including the mapped fractures in the vicinity of the two tunnels and the direction of the maximum principal stress (σ_1), modified from Martin* et al. */73/.*
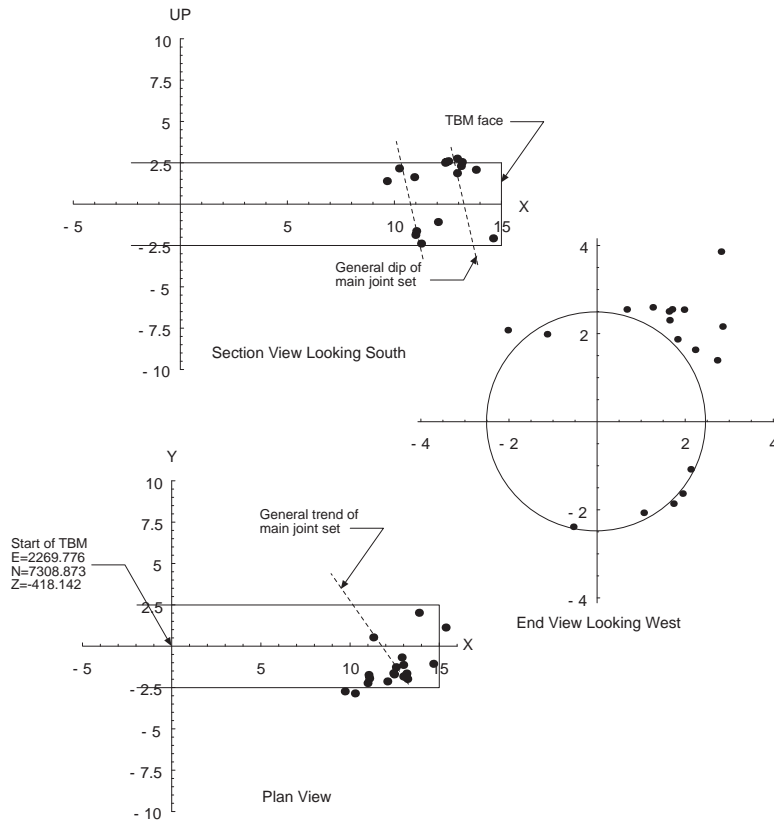
Figure 34: *Acoustic emission events (TBM at 15 m advance) that indicated slip if the frictional strength is* 30° */73/.*
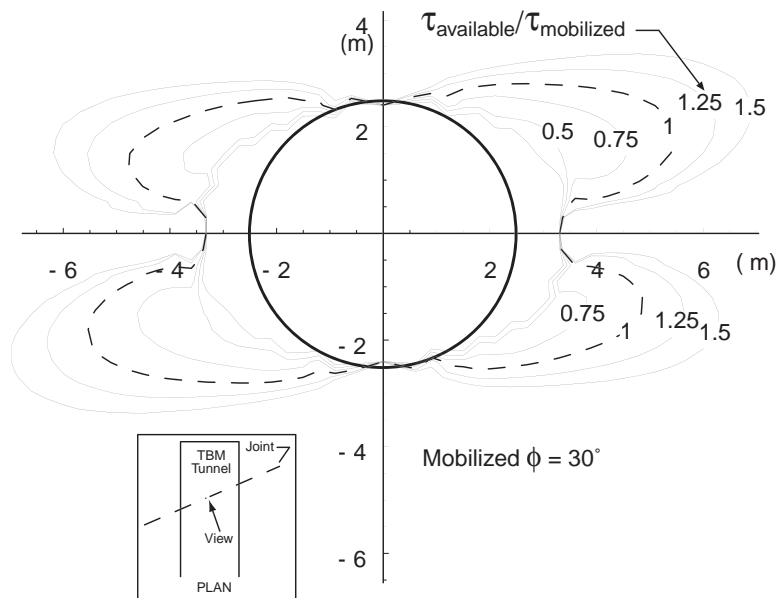
Figure 35: *Mobilized frictional strength on a plane intersected by the TBM tunnel /73/. The plane is aligned with the main fracture set.*

5.4   Depth of stress-induced spalling

In highly stressed ground, failure around a tunnel is initiated by localized spalling when the tangential stresses near an excavation wall reach the rock mass strength. In mining, most tunnels are rectangular in shape with slightly arched backs and stress raisers, at sharp corners of excavations, often initiate this spalling process (Figure 36). This spalling process produces fractures emanating from the stress raisers and will come to equilibrium only when a geometrically more stable excavation shape is formed. This stable excavation shape is usually a v-shaped notch (Figure 36).

Attempts to predict either the maximum depth to which the brittle failure process will propagate, using traditional failure criteria based on frictional strength models, have not met with much success /105; 60; 36; 23; 33/. One approach, which attempts to overcome this deficiency, is to model the failure process progressively by using iterative elastic analyses and conventional failure criteria. The initial zone of failure is removed, and the analysis is then repeated based on the updated tunnel geometry. This incremental excavation sequence is intended to simulate the progressive nature of brittle failure. However, as noted by Martin /60/ this process is not self-stabilizing, and as a result over-predicts the depth of failure by a factor of 2 to 3.

Martin and Chandler /62/ demonstrated in laboratory experiments that in the brittle failure

Figure 36: *Examples of brittle failure (left photo - AECL's Mine-by circular test tunnel at the URL, right photo - rectangular shaped tunnel in a mine. Note the stress-induced fractures in the right photo. These have been removed in the Mine-by tunnel to show the v-shaped notch.*

process peak cohesion and friction are not mobilized together and that most of the cohesion is lost before peak friction is mobilized. They postulated that around underground openings the brittle-failure process is dominated by a loss of the intrinsic cohesion of the rock mass such that the frictional strength component could be ignored. This eventually lead to the development of brittle parameters for the Hoek-Brown failure criteria (see Section 2.3). The applicability of this approach as a general criterion for estimating the depth of brittle failure is illustrated here for tunnels and in the following section for pillars. Vasak and Kaiser /104/ demonstrated that the approach is also applicable for assessing the depth of spalling under dynamic loading conditions, such as rockbursts.

Martin *et al.* /66/ established an empirical relationship between the depth of failure and the stress magnitude. They analysed case studies where the depth of failure (d_f), from excavations around the world failing in a progressive, non-violent manner, were carefully recorded. Their studies showed that the depth of failure normalized to the tunnel radius a is linearly proportional to the stress level σ_{max}/σ_c, calculated as the ratio of maximum tangential stress at the wall of a circular opening to the laboratory uniaxial compressive strength σ_c:

$$\frac{d_f}{a} = 1.25\frac{\sigma_{max}}{\sigma_c} - 0.5 \pm 0.1 \tag{12}$$

From Equation 12, if $\sigma_{max}/\sigma_c \approx 1/3$ then $d_f = 0$. Figure 37 presents the data used to derive the linear best fit represented by Equation 12. Martin *et al.* /66/ demonstrated using Phase2[4] that this empirical relationship (Equation 12) could be predicted utilizing the proposed brittle Hoek-Brown parameters ($m = 0$; $s = 0.11$) in elastic numerical models (Figure 37).

---

[4]Available from Rocscience Inc., 31 Balsam Ave., Toronto, Ontario, Canada M4E 3B5, http://www.rocscience.com
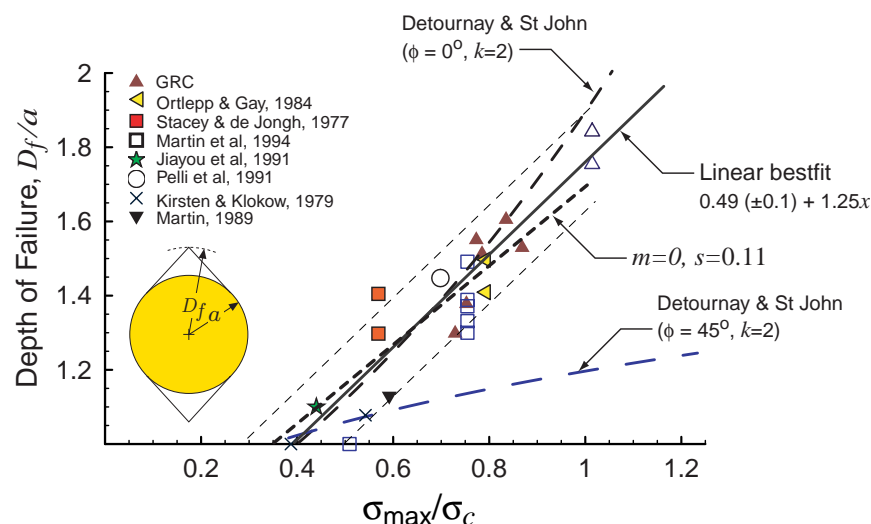

Figure 37: *Depth of failure data compared to predictions utilizing brittle rock parameters (m or $\phi = 0$).*

Utilizing equivalent brittle parameters ($\phi = 0$), this interdependence can also be predicted for circular tunnels in deviatoric stress fields with the closed-form solutions presented by Detournay and St. John /31/. Figure 37 illustrates for $k = 2$ the maximum depth of failure using this approach. However, if conventional parameters with a friction angle of 45° were applied, the Detournay and St. John approach significantly under-predicts the depth of failure (Figure 37). Additional analyses showed that this approach is essentially insensitive to the stress ratio.

The yield criterion given in Equation 6 and used to develop the depth of failure given in Equation 12 can also be used to assess the potential for brittle failure around tunnels. A three dimensional elastic analysis was carried out for the 420 Level excavations at the Äspö HRL. Figure 38 shows the constant deviatoric stress isosurface for $\sigma_1 - \sigma_3 = 75$ MPa. Note that the criterion is only exceeded locally and only on tunnels with a particular orientation. If the rock mass displayed spalling at this depth and stress level, Figure 38 could be used to assess which tunnels would be subjected to stress-induced spalling.

5.4.1 Modelling brittle failure

Hoek in his keynote address at the U.S. Rock Mechanics Symposium (Vail, 1999) noted that quantifying the post-peak response of rock masses was the biggest challenge facing the rock mechanics community. In 1991, a circular test tunnel was excavated, without blasting, in
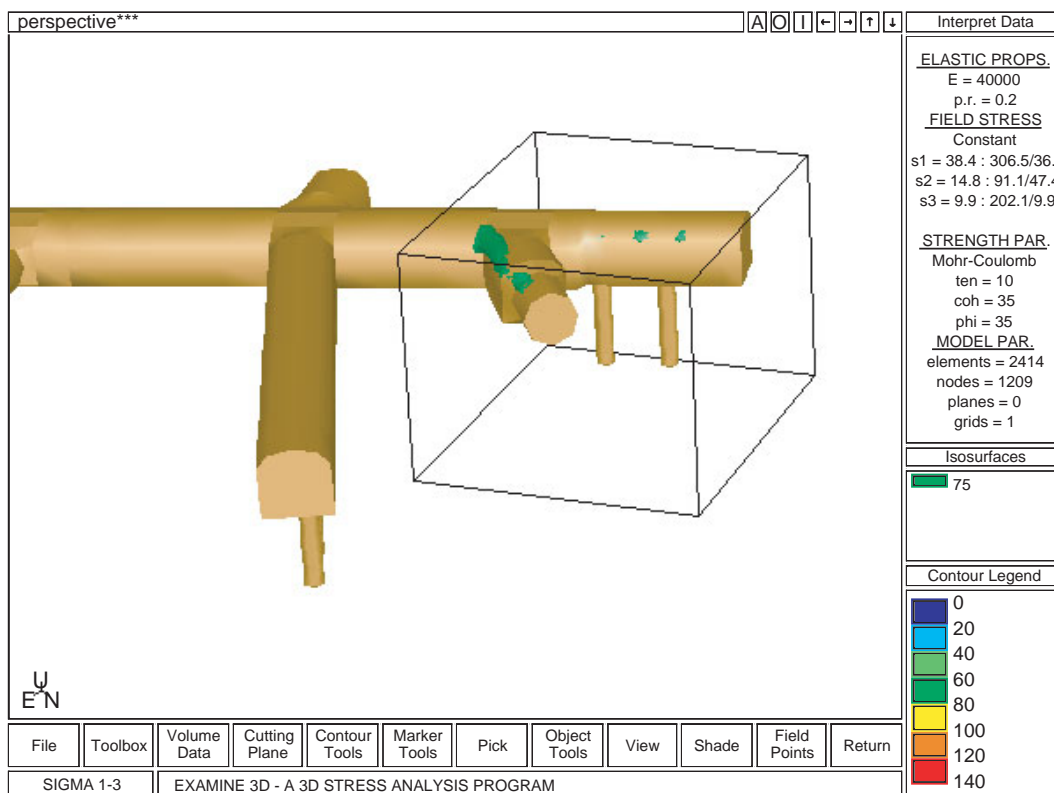
Figure 38: *Example of the constant deviatoric stress isosurface for $\sigma_1 - \sigma_3 = 75$ MPa using the three dimensional boundary element program Examine3D. Note that the criterion is only exceeded locally and only on tunnels with a particular orientation /4/.*

massive homogeneous isotropic linear elastic granite at AECL's Underground Research Lab as part of the Mine-by Experiment. Modelling of this simple geometry and rock mass was carried out using the Hoek-Brown failure criterion and the constitutive models suggested by Hoek and Brown /47/. The results from these models using the finite element program Phase[2] are summarized in Figure 39 and compared to the observed failure. None of the suggested modelling approaches predicted a failure zone that matched the shape of the observed v-shape notch. This is in keeping with the conclusions made by Read /89/ that traditional modelling approaches significantly underestimated the depth of brittle failure and overestimated the circumferential extent.

Since 1996 AECL has been using *PFC* to assess if this modelling approach would provide
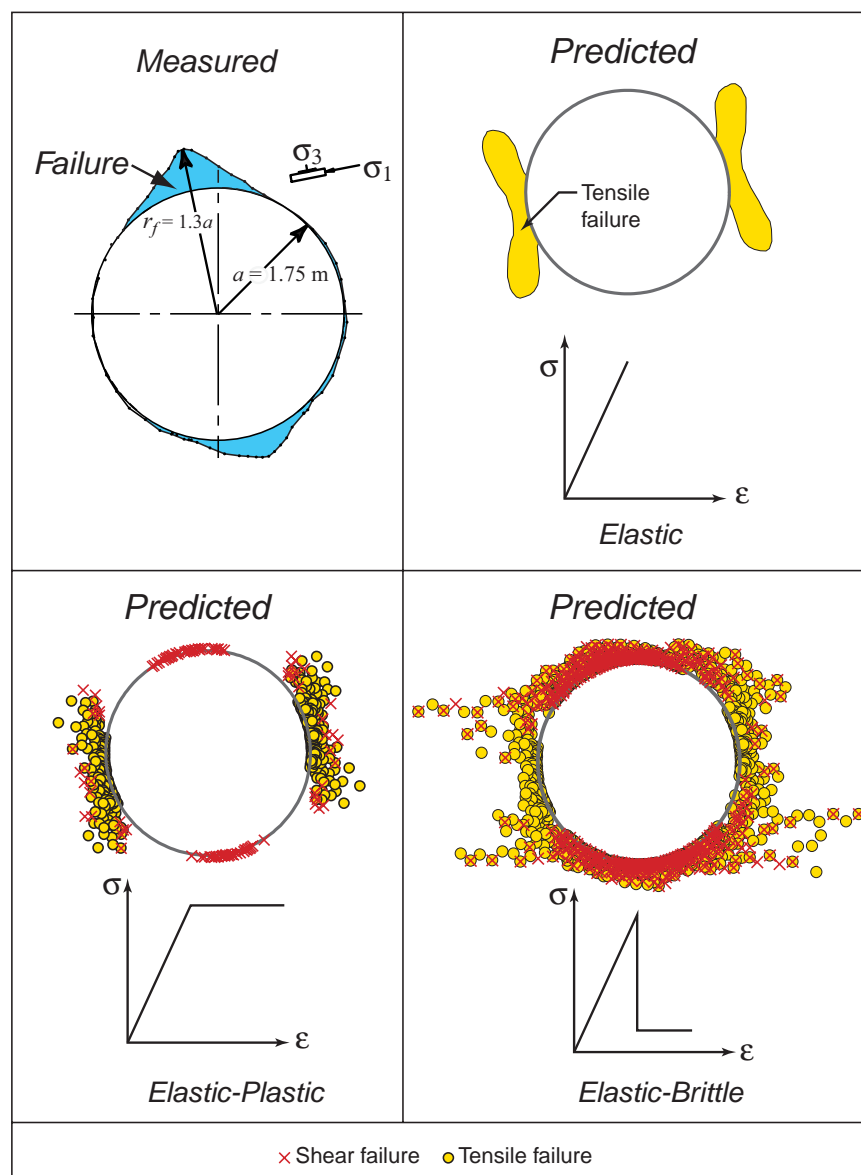
Figure 39: *Measured failure around the Mine-by test tunnel based on measurements and observations /91/ compared to the predicted failure using various constitutive models in the finite element program* Phase2.

better agreement between model predictions and observations /85/. Brittle failure results from the growth and accumulation of tensile cracks, and around underground openings this progressive failure process occurs in the form of spalling or slabbing. This transition from a continuum to a discontinuum failure process is extremely difficult to capture in numerical models despite the advances in discontinuum modelling such as *PFC*. As noted by Potyondy *et al.* /87/ *PFC* simulates the mechanical behaviour of rock by representing it as a bonded assembly of circular or spherical particles where the deformations result from accumulating damage, i.e., breakage of bonds. While the progress with *PFC* is encouraging, extensive calibration work needs to be carried out to simulate different rock types and that our current understanding of this calibration process is still incomplete /86/.

An alternative to the discontinuum modelling approach, is to capture in continuum models the fundamentals of brittle failure. Conventional continuum modelling approaches to this class of problems assume that the mobilization of the cohesion and frictional strength components is instantaneous. This approach overlooks a fundamental observation of brittle failure, that the formation of tensile cracks is the first step in the failure process. The brittle cohesion-friction model introduced by Hajiabdolmajid *et al.* /37/ and shown in Figure 40 implicitly captures this phenomena by making cohesion weakening and friction hardening a function of plastic strain.

The utilization of a continuum-modelling tool to model a discontinuum process will certainly not capture all the subtleties of brittle failure. However, many of these subtleties have little engineering significance. In practice, what is of paramount importance to the designer is
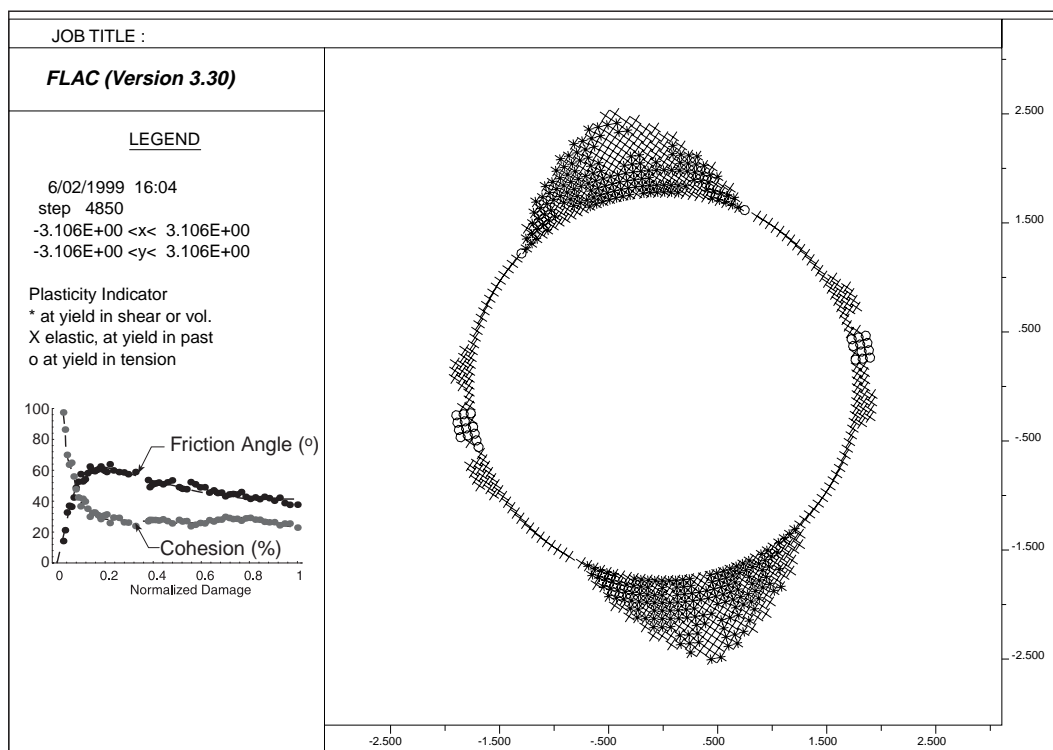

Figure 40: Prediction of failure using the brittle cohesion-friction model for AECL's Mine-by test tunnel /37/.

49

the maximum extent of brittle fracturing since this has a direct relationship to the support requirements.

The brittle cohesion-friction model was implemented in *FLAC* using its internal *FISH* language. The brittle cohesion-friction model captured both the shape and extent of the V-shaped notch that formed around AECL's Mine-by test tunnel constructed in Lac du Bonnet granite. The strain limits used by Hajiabdolmajid *et al.* /37/ were determined from special damage-controlled laboratory tests /62/. Different rocks are expected to have different strain limits for cohesion weakening and frictional hardening. Hence there is a need to conduct additional laboratory test to establish the strain limits for the brittle cohesion-friction model in different rocks.

5.4.2 Brittle failure and tunnel shapes

The theory of elasticity would suggest that the optimum shape of a tunnel is an ellipse with the major axis parallel to the direction of maximum in-plane stress, with the ratio of major ($2a$) to the minor ($2b$) axis of the ellipse being equal to the ratio of the maximum (σ_1) to minimum (σ_3) stresses in the plane of the excavation (Figure 41). This optimum shape produces uniform tangential stresses on the boundary of the excavation with the tangential stress equal to $\sigma_1 + \sigma_3$. Fairhurst /34/ pointed out however, that while the tangential stress is constant on the boundary it is not constant for the regions behind the boundary of the tunnel and should failure occur the inelastic region that develops for an elliptical shaped tunnel, is much larger than if the tunnel geometry were circular or an ellipse oriented parallel to the minimum stress axis (Figure 41).

Read and Chandler /90/ carried out an extensive study to evaluate the effect of tunnel shape on stability by excavating a series of ovaloids and circular openings at the Underground Research Laboratory, Manitoba. Because of the extreme in-situ stress ratio $\sigma_1/\sigma_3 \sim 6$, it was not practical to excavate an ellipse of the optimum shape (e.g., 18 m by 3 m in dimension). As a compromise, they excavated an ovaloid 6.6 m wide and 3 m high in a very competent rock mass. Figure 42 shows the observed shape of the failed region that formed shortly after excavation, which supports the notion that failure would be extensive. In fact the extent of
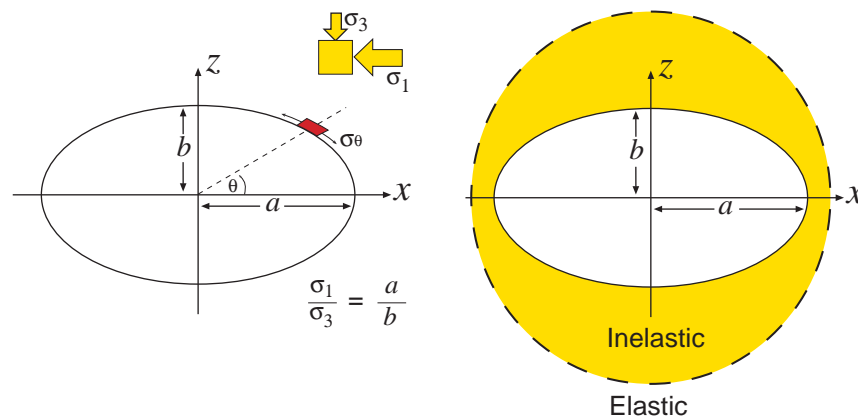

Figure 41: Illustration of the stress distribution and the potential inelastic zone for an elliptical tunnel, modified from /34/.

failure, encompassed nearly the entire roof of the excavation. Elastic analysis of the ovaloid with the Hoek-Brown brittle parameters provided a good estimate of the extent of failure, and showed that slabs would form over the entire width of the roof (Figure 42).

It is not practical to excavate elliptical shaped openings or to ensure that brittle slabbing will not occur. In mining, when brittle failure is anticipated, flat rather than arched roofs are employed to control the extent of failure /66/. While this is counter intuitive, Martin *et al.* /66/ showed that the Hoek-Brown brittle parameters indicated that an excavation with a flat roof is in fact more stable than a tunnel with an arched roof when the failure mode is stress-induced spalling. These findings are in keeping with the practical experience from Canadian hard rock mines.

The previous examples illustrated that the shape of the tunnel can be used to control when brittle failure initiates for any given stress state. However in some situations, such as during the excavation of large caverns or openings in a repository environment, the final stress state will change significantly from the original stress state as sequential excavations are used to obtain the final geometry. From a support perspective it is important to know the effect of changing tunnel shape on the depth of brittle failure for various stress states.

A series of elastic analyses was carried out to investigate the depth of brittle failure for various shaped openings in a good quality rock mass. The analyses used a vertical stress gradient equal to the weight of the overburden and a horizontal stress of twice the vertical stress. This is consistent with general stress trends for the Fennoscandian Shield /98/. In the analyses, the excavation shapes had a constant span S of 5 m and a height H of 5 m such that the span to height ratio was one ($S : H = 1$).

STRENGTH FACTOR   Contour Interval = 1.00e-001
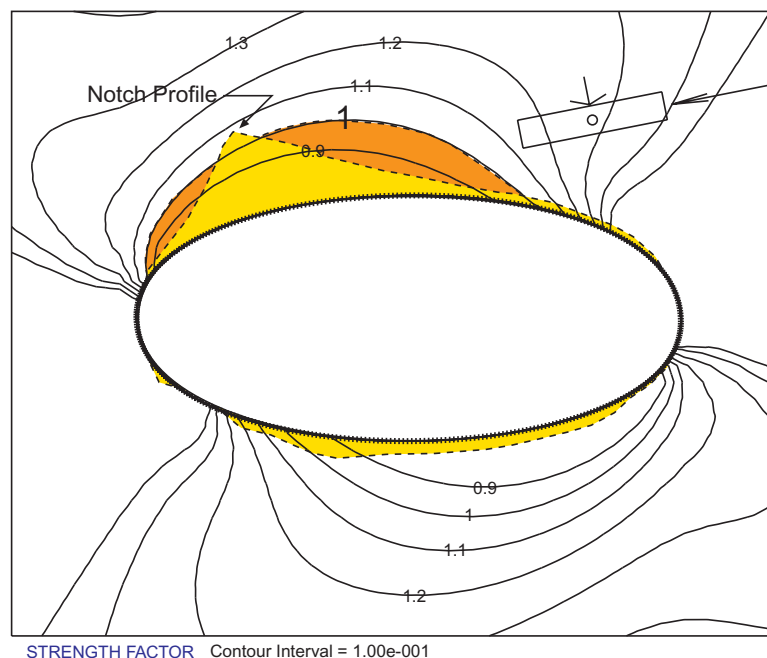
Figure 42: Observed failure around a near elliptical shaped opening compared to the that predicted suing the Hoek-Brown brittle parameters ($m = 0$, $s = 0.11\sigma_c$).

51

Figure 43 shows the results from these analyses in dimensionless form where the depth of brittle failure, measured vertically from the mid-span of the tunnel, is normalized to the span of the opening. The vertical depth of the excavation is expressed as the ratio of the far-field maximum stress to the unconfined compressive strength, e.g., a depth of 1000 m is expressed as $(1000 \times 0.027 \times 2)/240 = 0.225)$. The results show that brittle failure around the circular tunnel initiates at a depth of approximately 600 m ($\sigma_1/\sigma_c \sim 0.12$) and that the increase in the depth of brittle failure is approximately linear as the far-field stress magnitude increases. However, the tunnel with flat-roof showed that brittle failure did not initiate until the depth exceeded 1000 m. Hence at the proposed depth of a repository the tunnel geometry may be used to control the initiation and depth of brittle failure especially if siting will be done at approximately 600 m depth or deeper (Figure 43).

5.4.3   Tunnel orientation and brittle failure

A nuclear waste repository will have underground openings at various depths and oriented in different directions. Section 4 showed that the stress magnitudes in the Fennoscandian Shield vary with depth and hence there is the opportunity to optimize the relationship between stresses on the boundary of the underground openings, depth and orientation. Figure 44 provides an example of this optimization using the stress magnitudes from Figure 21 and the Damage Index. Three orientations are used in Figure 44, (1) a vertical shaft; (2) a horizontal tunnel oriented parallel to σ_2; and, (3) a horizontal tunnel oriented parallel to σ_1. Using a $D_i = 0.4$, based on Figure 7, Figure 44 indicated that stress-induced failure should be anticipated in vertical shafts and in horizontal tunnels oriented parallel to σ_2 below a depth of approximately 300 m. However, horizontal tunnels oriented parallel to σ_1 should not be subjected to stress induced spalling.

Similar relationships between tunnel orientations and the in-situ stress state can be observed
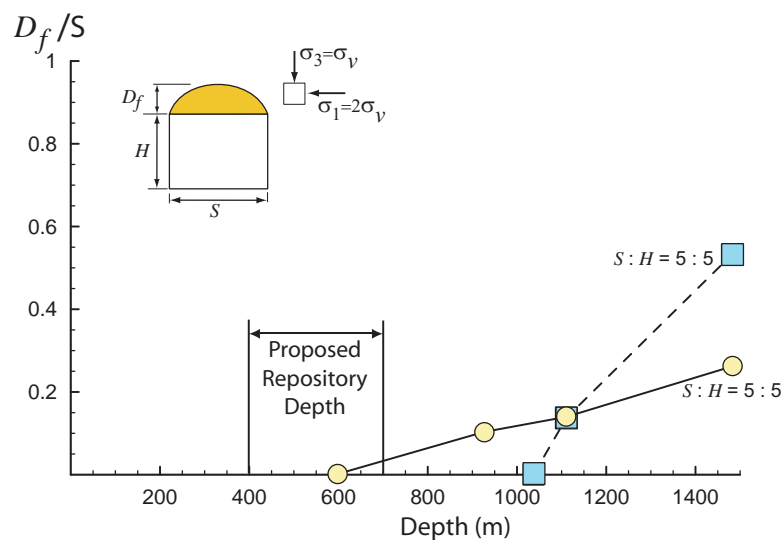
Figure 43: Depth of brittle failure in the roof of circular (represented by circles) and square shaped tunnels (represented by squares) normalized to the span of the opening versus the depth of the tunnel below the ground surface.
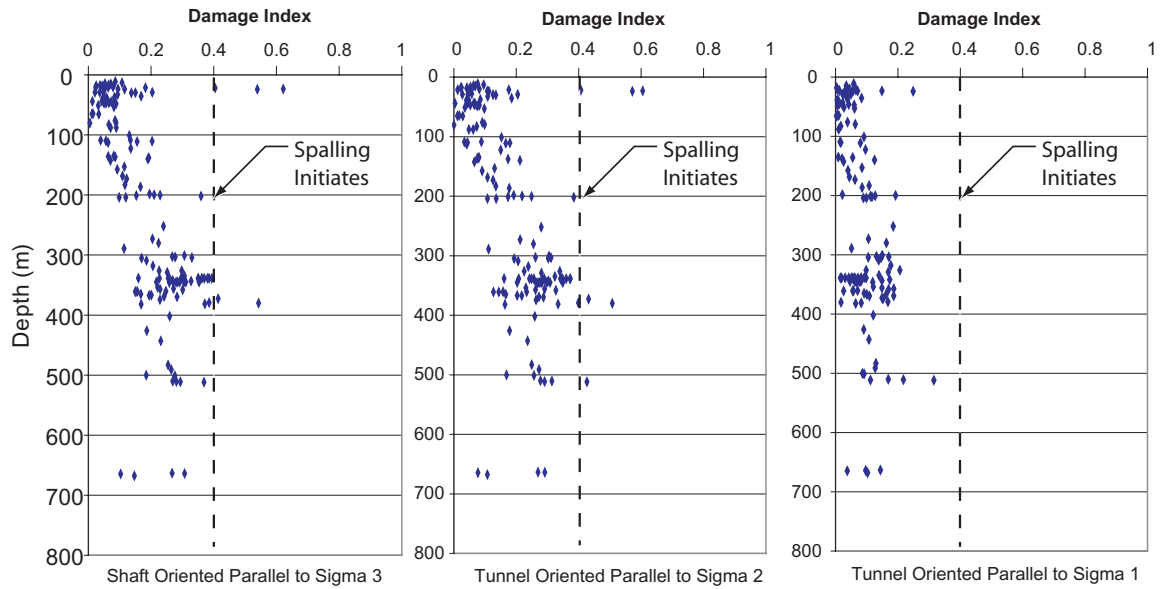
Figure 44: *Relationship between damage and opening orientation and depth for the stress magnitudes given in Figure 21. Note that the vertical dashed line for a Damage Index of 0.4 indicates the onset of spalling.*
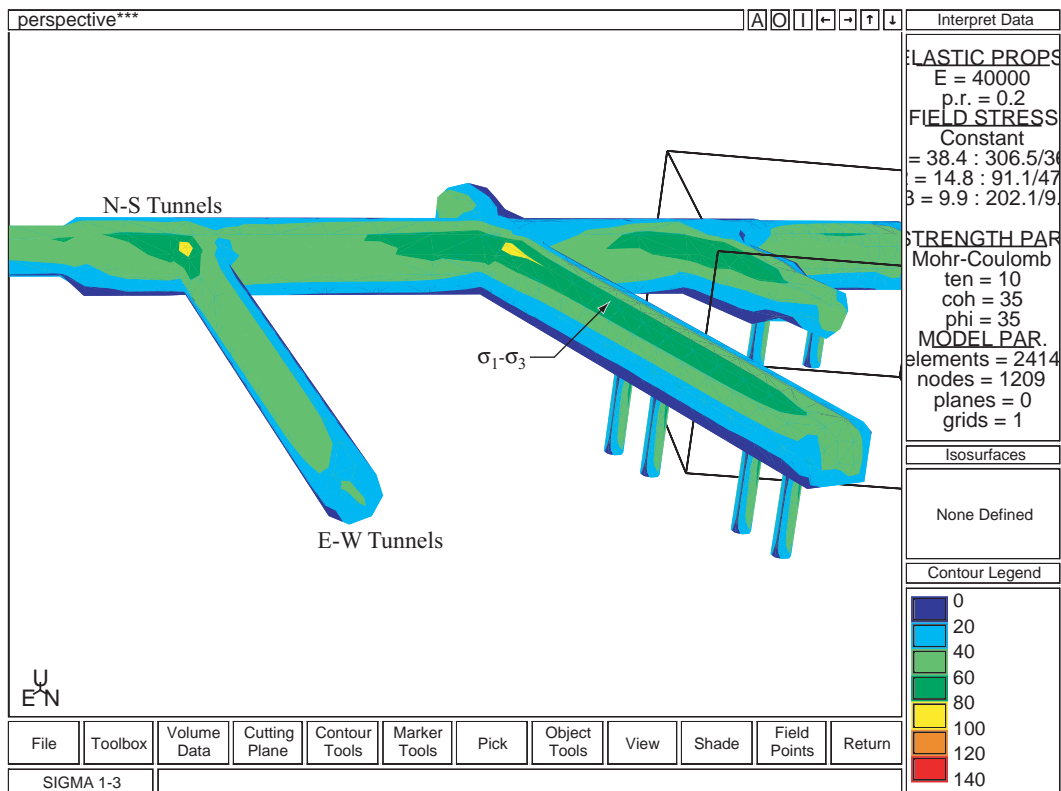
Figure 45: *Illustration of the relationship between tunnel orientation and maximum deviatoric stress. The maximum deviatoric stress occurs around the E-W tunnels. The orientation of the E-W tunnels is approximately the same as the orientation of the drill-and-blast tunnel in Figure 33.*

using three dimensional numerical analysis. Figure 45 shows the calculated elastic surface contours of the deviatoric stress ($\sigma_1 - \sigma_3$) on the tunnels at the 420 Level of the Äspö HRL. The tunnel with the 4 boreholes in the floor, is at the same orientation as the Drill-and-blast tunnel in Figure 33, approximately East-West. Note that the maximum deviatoric stress is more extensive around the tunnels oriented E-W. The deviatoric stress around the tunnels oriented N-S is greatest near the intersection with the E-W tunnels and decreases significantly as the tunnels approaches plane-strain conditions.

The results discussed above illustrate the importance of choosing the appropriate depth for the repository as well the appropriate orientation for the critical tunnels in the repository. When the tunnels are not aligned with the principal stress directions, three dimensional analysis will be required to assess the impact of tunnel orientation on stress magnitudes.

5.5 Summary

No one failure criterion can be used to assess the performance of an underground opening. When choosing a criterion the designer must first consider the mode of failure. For structurally controlled failure such as gravity driven wedges, empirical support charts may be adequate. In special situations numerical tools such as *UDEC* or *3DEC* may be required. For estimating the depth of stress-induced brittle failure, the Hoek-Brown brittle parameters were found to be adequate.

6 Stability of pillars

Pillars can be defined as the in-situ rock mass between two or more underground openings. Hence, the construction of an underground nuclear waste repository will create pillars of variable geometries. The two most frequently encountered pillars, for repositories that utilize the borehole emplacement disposal method, will be: (1) the deposition tunnel pillar; and (2) the emplacement borehole pillar (Figure 46). These pillars will be subjected to various stresses over the life of a repository: 1) static stresses resulting from in-situ stresses, modified by the excavations required for construction of the repository; 2) thermal stresses generated by the heat from the nuclear waste; 3) dynamic stresses associated with seismic events; and 4) glacially-induced stresses.

In keeping with the safety requirements and performance of a nuclear waste repository, these induced pillars stresses should not reach the rock mass pillar strength. The designers of these pillars need a thorough understanding of the rock mass failure process. Such an understanding is necessary to develop a comprehensive failure criterion for pillars to ensure that the pillar performance is in accordance with the safety requirements. This section reviewers the current approaches used to design pillars in hard rocks.

6.1 Pillar failure observations

Using detailed mapping and observations Pritchard and Hedley /88/ compiled the progressive nature of hard-rock pillar failure that was observed in the hard rock room-and-pillar mines near Elliot Lake Canada (Figure 47). These pillars were located at a depth of approximately 500 to 700 m and failure did not commence until the mining extraction ratio exceeded approximately 70%. Their observations clearly showed the initiation of spalling on the boundary of the pillar and the gradual loss of the pillar's load carrying capacity as the pillar developed an hourglass geometry (Figure 47). They suggested that the peak strength of the pillar was reached by Stage II in Figure 47 when axial splitting, i.e., extension fracturing, of the pillar was observed.

Pritchard and Hedley /88/ noted that in the early (pre-peak strength) stages of pillar failure stress-induced spalling on the boundary of the pillar dominated the failure process while in the latter stages (post-peak strength), after spalling had created the typical hour-glass shape,
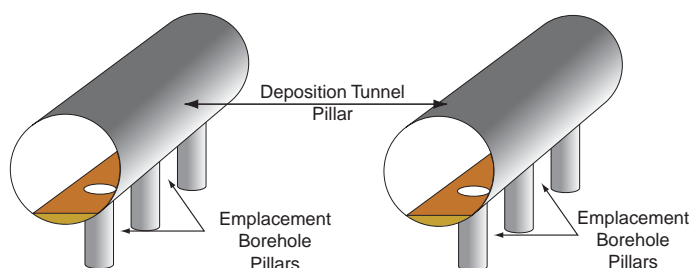

Figure 46: *Illustration of the deposition tunnel pillar and the emplacement borehole pillar in the* KBS3 *concept.*
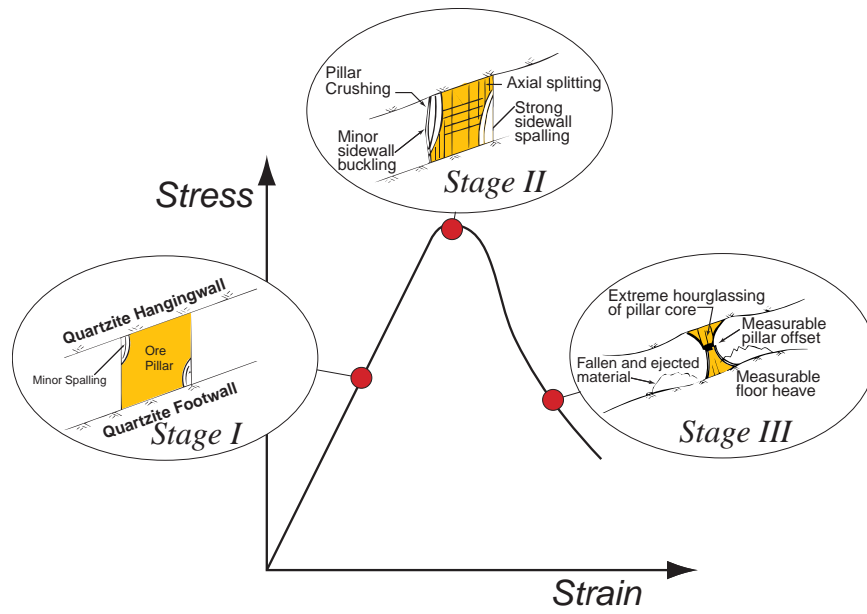
(*a*) Stages in pillar failure
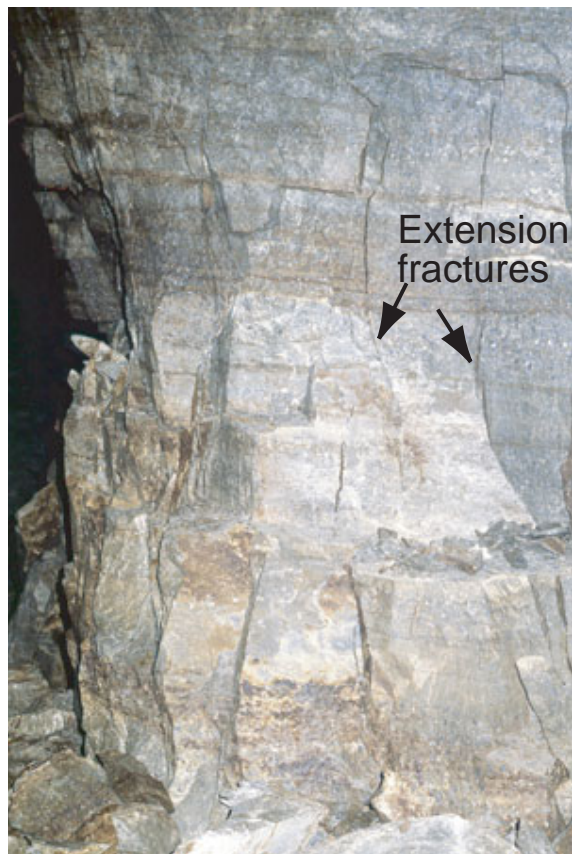
(*b*) Pillar at peak strength, (Photo courtesy of C. Pritchard)

Figure 47: *Observations and illustration of the progressive nature of hard-rock pillar failure, data from /88/.*

slip along structural features such as bedding planes and joints played a more significant role in the failure process. These observations are in keeping with the laboratory findings of Hudson *et al.* /49/ and Martin and Chandler /62/ who demonstrated that the development of the shear failure plane in laboratory samples also occurs after the peak strength is reached.

More recently, findings from experiments carried at SKB's Äspö Hard Rock Laboratory support the observations made by Pritchard and Hedley /88/ and the notion that the early stages of damage to a pillar occurs at the edge of the pillar. Pettitt /84/ used acoustic emission/microseismic monitoring techniques to monitor the performance of the pillar between two emplacement boreholes (Figure 48). During the drilling of the first boreholes only minor isolated AE activity was recorded on the boundary of the borehole. However, during the drilling of the 2nd borehole considerably more AE activity was detected indicating: (1) the stress magnitudes in the pillar were elevated due to the presence of the second borehole; and (2) damage to the pillar was concentrated at the pillar edge.

In a nuclear waste repository the stress concentrations in the pillars separating the emplacement boreholes or the deposition tunnels are a function of the pillar dimensions and the depth of the repository assuming that the far-field stress magnitudes increase with repository depth. Hence these pillars, prior to waste emplacement, may approach the critical stress magnitudes that can induce spalling. Once spalling initiates the capacity of the pillar to resist the loads induced by: thermal stresses generated by the heat from the nuclear waste, dynamic stresses associated with seismic events, and glacially-induced stresses, is unknown at present.
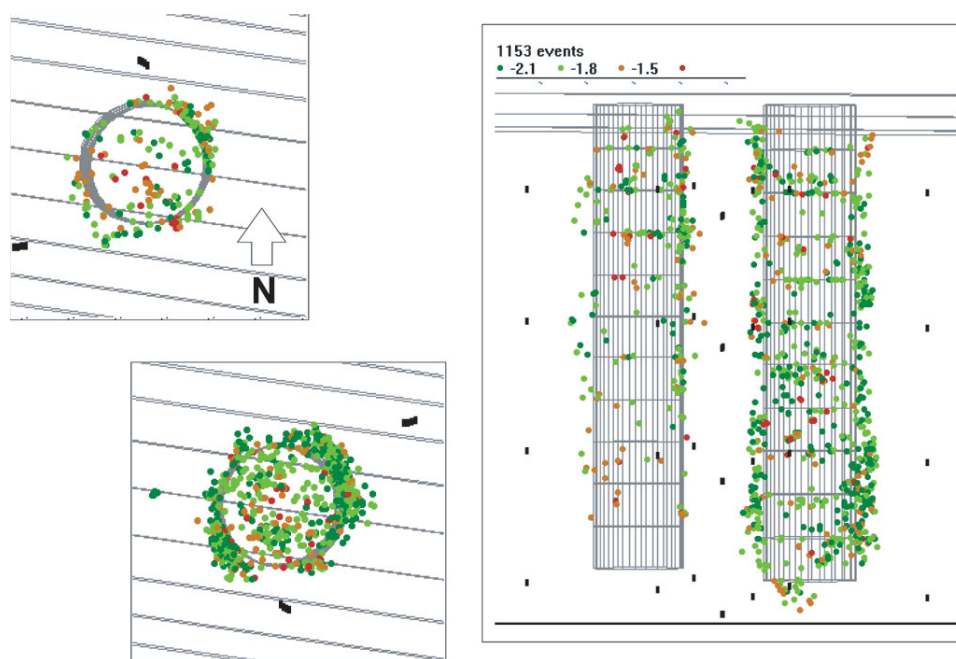

Figure 48: *Acoustic emission (AE) data recorded around two emplacement-scale boreholes, data from /84/. The borehole showing the least number of AE events was drilled first.*

6.2 Empirical pillar strength formulas

Observations of pillar failures in Canadian hard rock mines indicate that the dominant mode of failure is progressive slabbing and spalling. The design of pillars in these rock masses can follow three approaches:

1. attempt to numerically simulate the slabbing process using appropriate constitutive models;

2. select a rock mass strength criterion based on evaluation of rock mass characteristics and calculate the pillar strength to stress ratio at each point using continuum models; and/or

3. use existing empirical pillar stability graphs and pillar formulae.

Despite the advances in estimating rock mass strength using rock mass classification systems, and the advances in our numerically modelling capabilities, pillar design is traditionally carried out using empirical pillar formulas such as:

$$\sigma_p = K_p \frac{W^\alpha}{H^\beta} \tag{13}$$

where σ_p (MPa) is the pillar strength, K_p (MPa) is the strength of a unit volume of rock, and W and H are the pillar width and height in metres, respectively. The notion that the strength of a rock mass is to a large part controlled by the geometry of the specimen, i.e., the width to height ratio, has since been confirmed by extensive laboratory studies, e.g., Hudson *et al.* /49/. Such formulas are developed using a "back-calculation" approach and have successfully been used to design soft and hard rock pillars over the past 4 decades.

One of the earliest investigations into the design of hard-rock pillars was carried out by Hedley and Grant /40/. They analyzed 28 rib pillars (3 crushed, 2 partially failed, and 23 stable) in massive quartzites and conglomerates in the Elliot Lake room and pillar uranium mines. They concluded that Equation 13 could adequately predict these hard rock pillar failures but that the parameters needed to be modified to:

$$\sigma_p = K_p \frac{W^{0.5}}{H^{0.75}} \tag{14}$$

where the units are the same as Equation 13. The value of K_p in Equation 14 was initially set as 179 MPa but later reduced to 133 MPa /41/. Equation 14 was used to design pillars in the Elliot Lake mines until their closure in the late 1990's.

Since 1972 there have been several additional attempts to establish hard rock pillar strength formulas, using the empirical "back calculation" approach. Martin and Maybee /67/ reviewed these published pillar formulas and compared the predicted pillar strength normalized to the uniaxial compressive strength for a pillar height of 5 m (Figure 49). Despite the wide range in uniaxial compressive strength (92 to 250 MPa) all formulas predicted similar pillar strength.

Söder and Krauland /96/ reported on the results from an extensive series of in-situ full-scale tests to determine the strength of pillars in the Laisvall mine, a lead-zinc mine located in northern Sweden. The pillars were located in flat lying quartzitic sandstone with an average

uniaxial compressive strength of 210 MPa and the thickness of the overlying strata varied from 110 to 300 m. Nine pillars were subjected to increasing stress until failure occurred and from these tests Söder and Krauland concluded that the strength of pillar with a $W/H = 1$ was approximately 23 MPa or $1/10\sigma_c$. This is considerably less than that indicated in Figure 49, where the strength of a pillar with a $W/H = 1$ is approximately $1/3\sigma_c$. Swan /102/ summarized the strength of pillars with W/H ratios varying from approximately 0.5 to 1.7 and also concluded that the average pillar strength was approximately $1/3\sigma_c$.

6.3 Pillar strength using Hoek-Brown Brittle Parameters

Martin and Maybee /67/ used Phase2 and the Hoek-Brown brittle parameters ($m = 0$, $s = 0.11$) to evaluate pillar stability over the range of pillar W/H ratios from 0.5 to 3. These analyses were carried out using an in-situ stress ratio $k = 1.5$ and the results are presented as thick solid lines in Figure 50 for both a Factor of Safety (FOS) equal to 1 and a FOS equal to 1.4. A pillar was considered to have failed when the core of the pillar had a $FOS=1$. A similar approach was used to establish when the pillar reached a $FOS=1.4$. The empirical pillar strength formulas of /40/ and /57/ are also shown in Figure 50 as well as the database used by Lunder and Pakalnis /57/.

Figure 50 shows there is only a small difference between the predicted $FOS=1$ line using the Hoek-Brown brittle parameters and the empirical stability lines proposed by Hedley and Grant /40/ and Lunder and Pakalnis /57/ between a pillar W/H of 0.5 and 1.5. However, between a pillar W/H of 1.5 and 2.5 the empirical formulas suggest only a modest increase
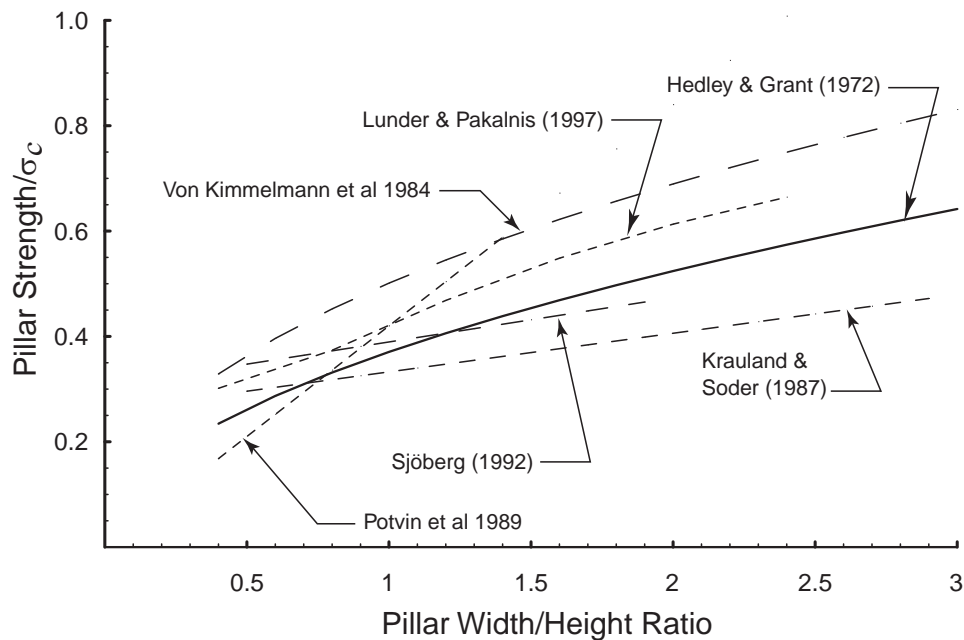

Figure 49: *Comparison of various empirical pillar strength formulas for hard rocks /67/.*

in pillar strength while the predicted brittle stability line suggests a significant increase in pillar strength. This predicted increase in pillar strength is more in keeping with observations as the number of pillar failures decreases significantly once the pillar W/H increases beyond 1.5 (see Figure 50). Also in contrast to the empirical stability lines for pillar $W/H < 0.75$ the predicted pillar strength is essentially constant, reflecting the low confinement for these slender pillars. This is also in keeping with observations except for the special case of pillars subjected to shear loading, which is discussed in the following section.

6.4 Pillars subjected to inclined stresses

Deep geological disposal for nuclear waste in Sweden and Finland utilizes the *KBS3* concept which places the waste in vertical boreholes drilled from the floor of horizontal tunnels (Figure 46). In these countries, like many places around the world, the horizontal stresses exceed the vertical stress. As a result the emplacement borehole pillars and the deposition tunnel pillars will be subjected to different loading conditions and will have different pillar width to height ratios. Figure 51 shows the P_w/P_h ratios are 2.4 and 7 for the emplacement boreholes and deposition tunnels, respectively. Comparing these ratios to Figure 50, reveals that hard rock pillars failure have been observed at P_w/P_h ratios of 2.5. Thus the emplacement borehole pillars have a P_w/P_h ratio that could fail provided the stress magnitudes exceed the pillar strength.

The empirical pillar formulas assume that the load on the pillar is normal to the plane of the pillar. Hedley *et al.* /41/ described pillar failures at Quirke mine that were inclined to the vertical stress. These pillars were stable when oriented along the dip of the orebody but became unstable when aligned along the strike of the orebody. In both situations the pillar W/H ratio was similar. Hedley *et al.* /41/ analyzed the Quirke mine pillars and concluded that the shear stresses caused by the inclination of the pillars to the stress field was the likely reason for the reduced strength. Whether this phenomena contributed to the reduced pillar strength observed by Söder and Krauland /96/ and discussed in Section 6.2 is unknown.

Maybee /74/ carried out a series of elastic analysis using Hoek-Brown brittle parameters
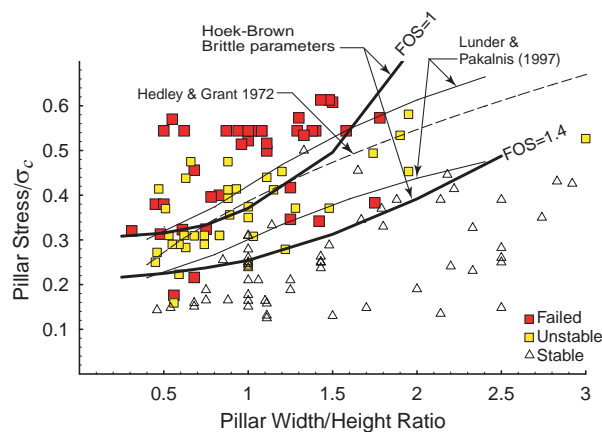
Figure 50: *Comparison of the pillar stability graph and the Phase2 modeling results using the Hoek-Brown brittle parameters. (Data points from /57/).*

to investigate the effect of an inclined far-field stress on pillar strength. The analysis were carried out with a pillar height of 5 m, a horizontal to vertical stress ratio (k) of 1.5 and by varying the inclination of the far-field stress from 0 to 90° in increments of 22.5°. Figure 52 shows that for pillar W/H ratios between 0.25 and 1 pillar strength is essentially unaffected by an inclined far-field stress. However, there is a significant reduction in strength when the pillar W/H ratio exceeds 1.5.

Recently, Christiansson and Martin /24/ highlighted the detailed stress profiles with depth at two sites in Sweden and one in Canada. In all three cases stress magnitudes varied considerably at the potential depth of nuclear waste repositories. Such variable stress conditions may also significantly influence the approaches to pillar design.

6.5 Summary

Pillar design is traditionally carried out by empirical methods. This approach, while practical in an operating mine, may not be suitable for a nuclear waste repository where pillars must withstand: excavation induced stresses; thermal stresses generated by the heat from the nuclear waste; dynamic stresses associated with seismic events; and glacially-induced stresses.

Martin *et al.* /66/ have argued that in hard, brittle rocks, the pre-peak failure process is controlled by progressive loss of cohesion, and the frictional component of strength is
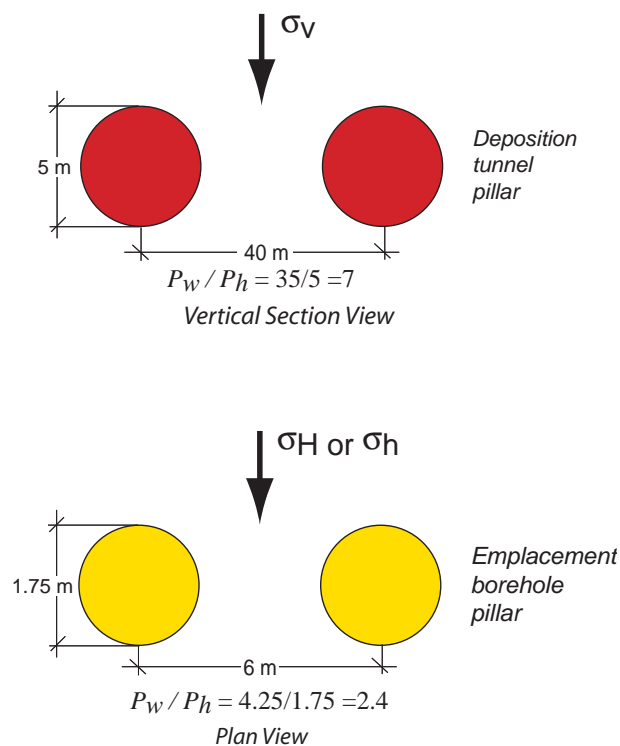
Figure 51: Illustration of the loading on the deposition tunnel pillars and the emplacement borehole pillars in the KBS-3 concept. Pillar dimensions taken from Olsson /80/.

not significantly mobilized until the post-peak region. This process concept was used to produce brittle stability predictions for hard-rock pillars. The results show excellent correspondence with observed performance data. Design curves based on empirical pillar design formulae, and those based on the brittle stability predictions, are generally in close agreement. However, compared to empirical design curves, the brittle stability curves are not in agreement with wide pillars, i.e, W/H ratios greater than about 1.5. These wide pillars are proposed for nuclear waste repositories. While the results from these studies are encouraging, the effects of inclined stresses and thermal loads on pillar strength is also unknown. It would appear from current practice that pillar design can only be verified by examining pillar failures. Hence, experiments should be planned that demonstrate our ability to predict pillar failure under a variety of loading conditions. Such experiments would provide confidence in our ability to predict *a priori* pillar performance.
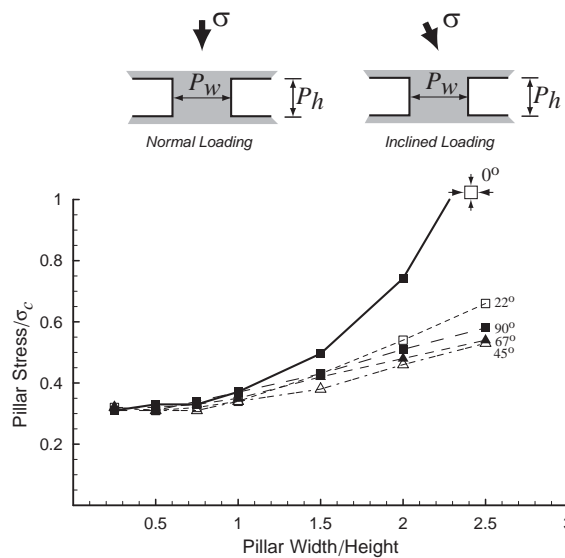
Figure 52: Effect of in-situ stress field rotation on pillar stability using the Hoek-Brown brittle parameters and k = 1.5, data from /74/.

7 Rock bursting

The energy changes that occur when an underground opening is created have been described by Cook /25/ and Salamon /93/. When a hole is created in a stressed rock mass the surface of the excavation moves inwards. As a result there is energy released. If the rock mass behaves in a linear elastic fashion the released energy is of no practical consequence as the excavation is stable. However, if the rock mass around the tunnel is loaded beyond its yield point nonelastic displacements occur and the strain energy released is greater than in the elastic case. When the rock mass is strong and brittle the nonelastic failure process usually involves the rapid release of strain energy which creates seismic waves. These seismic waves are termed mining-induced seismic events.

Mining-induced seismicity is commonly found in deep mines. Like earthquakes these seismic events are quantified using a logarithmic moment-magnitude scale ranging from -6 to 5. However, as noted by Cook *et al.* /28/ many seismic events occur during the excavation of underground openings and do not cause damage in the mining context and therefore are not identified as rockbursts. Based on the work of Hedley /39/, the following definitions have been adopted for this report.

Seismic event: A transient earth motion caused by a sudden release of potential or stored strain energy in the rock mass. As a result, seismic energy is radiated in the form of strain waves. The magnitude of the seismic event is usually determined from the peak amplitude of the strain wave, using a logarithmic scale (e.g., Richter Magnitude).

Rockburst: A seismic event which causes injury to persons, or damage to underground workings. The general and essential feature of rockbursts is their sudden, violent nature.

Consequently, all rockbursts are seismic events but not all seismic events are rockbursts. It should be recognized that there is a gradual change from spalling conditions to rock burst conditions.

The purpose of this section is to provide, based on mining experience, a general classification for rock bursts conditions and an approximate correlation between the size of the seismic event and the amount of damage that may result from that seismic event.

7.1 Types of rockbursts

Ortlepp /82/ has proposed the classification given in Table 3 for the types of rockbursts commonly found in deep South African mines. Also shown in Table 3 is the Richter magnitude of the seismic event, according to the type of rockburst. Hedley /39/ noted that in Ontario mines (Canada) three types of rockbursts were common:

1. strain bursts;

2. pillar bursts; and

3. fault-slip bursts.

Table 3: *Suggested classification of seismic event source and associated event magnitude, after /82/*

Rockburst Type	Possible Source Mechanism	Richter Magnitude M_L
Strain-bursting	Superficial Spalling	-0.2 to 0
Buckling	Outward expulsion of large slabs around an opening	0 to 1.5
Pillar or face crush	Sudden collapse of stope pillar	1.0 to 2.5
Shear rupture	Violent propagation of shear fracture through intact rock	2 to 3.5
Fault-slip	Sudden movement along existing fault	2.5 to 5.0

7.2 Conditions for strain bursting

All rocks will fail if subjected to sufficiently large deviatoric stresses ($\sigma_1 - \sigma_3$), however not all rock failure is described as 'bursting'. This was formally recognized shortly after the pioneering work of Griffith /35/ and the terms 'stable' and 'unstable' fracture growth were introduced to reflect the important difference between gradual and violent failure modes. The most common form of rock bursting around single openings is the strain burst. This form of strain energy release results in the formation of relatively thin slabs of rock adjacent to a tunnel wall. This process was observed during the excavation of the Mine-by Test Tunnel /91/ but was not classed as 'bursting' because of the gradual nature of the spalling process.

Given that all rocks can 'spall' but only some burst additional factors must be evaluated in order to assess the potential for strain bursting around a tunnel. Based on the the findings from the Canadian Rockburst Research Program /53/ and the current understanding of this complex issue, assessment of the potential for strain bursting around a underground opening must consider three factors:

1. the peak strength of the rock mass;

2. the post-peak response of the rock mass; and

3. the stiffness of system containing the underground opening.

7.2.1 Rock mass strength

The strength criterion for a rock mass has been discussed in Section 2.3.2. Using any one of the criteria discussed in Section 2.3.2, an assessment can be made to determine where the rock mass strength has been exceeded around a tunnel. The more challenging step is to determine if the failure process will be violent.

7.2.2 Post-peak response of a rock mass

Once the peak strength of the rock mass has been exceeded, the post-peak response of the rock mass must be considered. The early work of /49/ showed that the post peak response of the rock is dependent on confinement (Figure 53). The stiffness of the post-peak response in Figure 53 is defined as $|\lambda_m|$ and as confining stress increases the post-peak response becomes less brittle, i.e, $|\lambda_m|$ decreases. At sufficiently high confinement the post-peak response would become plastic. Hence at low confinement, the post-peak response is brittle and this phenomena has been observed in weak to hard rocks.

7.2.3 System stiffness

The stiffness of the rock mass containing the tunnel, i.e., the system stiffness, will determine the potential for the violent release of stored strain energy. The system stiffness can be defined as $|\lambda_s|$ and can vary from infinitely soft (horizontal line in Figure 54) to infinitely stiff (vertical line in Figure 54). In reality, the system stiffness lies somewhere between these two extremes.

The system stiffness for a tunnel is difficult to determine as it is a function of orientation, the horizontal to vertical stress ratio, the size of the drift and the shape of the damaged zone around the drift /2/. Nonetheless, the concept of system stiffness is key to the understanding of instability and violent failure processes /54/. Today three dimensional numerical models are used to determine the system stiffness and evaluate burst prone ground.

7.3 Stress magnitude and damage around openings

Damage to underground openings in hard rocks is a function of the in-situ stress magnitudes and the characteristics of the rock mass, i.e., the intact rock strength and the fracture network.
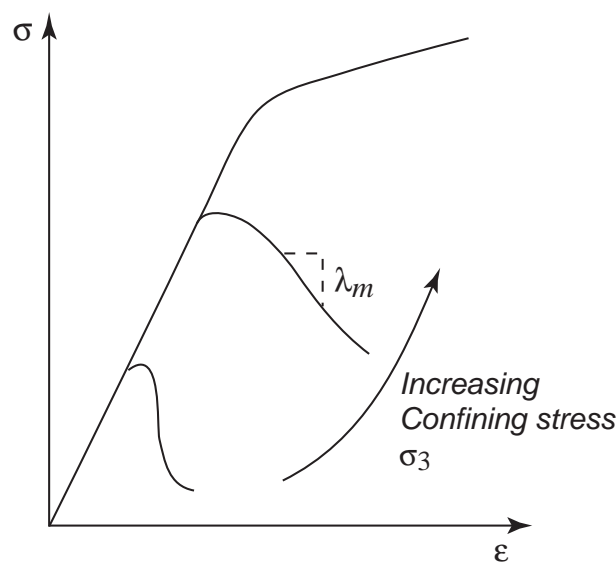

Figure 53: *The effect of confinement on the post-peak response of hard rocks.*

The design of a repository will require knowledge of the the extent of this zone as it within this zone that most of the seismic events will occur (see Olsson *et al.* /79/).

Hoek and Brown /46/ used South African observations from underground mining in massive brittle rocks to quantify this damage for square tunnels. They found that the stability of a square tunnel can be estimated by considering the ratio of σ_1/σ_c, where σ_1 is the maximum far-field stress magnitude and σ_c is the laboratory short-term unconfined compressive strength (Figure 55). This classification was also found to be applicable to the excavations at the URL and the Äspö HRL (Figure 55). When the ratio of $\sigma_1/\sigma_c \leq 0.1$ the rock mass will respond elastically and no excavation-induced damage will occur in the disturbed zone. At a ratio of $\sigma_1/\sigma_c \approx 0.2$, some microseismic events will occur in the disturbed zone close to the excavation wall, as a result of either the removal of the confining stresses or the loading by stress concentrations, thus creating a permanent damage zone near the opening.

At a ratio of $\sigma_1/\sigma_c \approx 0.3$, the rock mass is so severely damaged near the opening that the maximum load-bearing capacity of the rock mass is exceeded. The accumulated strains in the damage zone are excessive and lead to rock mass disintegration, e.g., by slabbing of the excavation walls. The microseismic events associated with this type of damage range in moment magnitude from -6 to -2 and were encountered during the excavation of AECL's Mine-by test tunnel. However, even when slabbing occurs, the shape of the opening eventually will stabilize and the surface instability mechanisms will disappear. The opening will remain stable unless further disturbed, e.g., by a disturbance from a nearby opening or by stress changes caused by thermal gradients.

At ratios of $\sigma_1/\sigma_c > 0.5$, the failure process propagates rapidly, extending the depth of the damaged zone. These conditions are generally found at great depth or in mines where extraction ratios are very high, i.e., greater than 60%. For example, if we assume $\sigma_1 = \sigma_v$ (the vertical stress) and $\sigma_c = 200$ MPa, $\sigma_1/\sigma_c > 0.5$ will occur at depths of ≈ 3.5 km or greater. Consequently, from a stability point of view, severe rock mass damage and associated microseismic events is of concern only at great depth or if two openings are
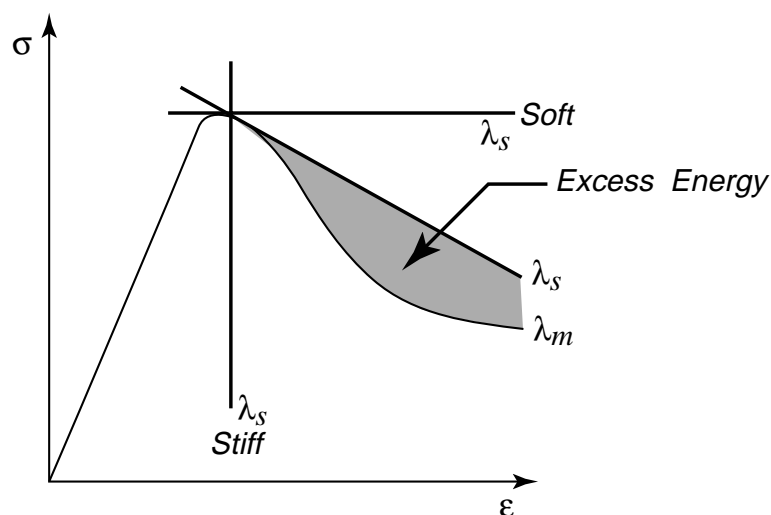
Figure 54: Illustration of the system stiffness and the excess energy that is available when the system stiffness is less then the post-peak response stiffness ($|\lambda_s| < |\lambda_m|$).

σ₁/σ_c < 0.15

Elastic response

0.15 > σ₁/σ_c < 0.3

Minor spalling
Microseismic events with
moment magnitude -6 to -2

0.3 > σ₁/σ_c < 0.4

Minor slabbing and damage
Microseismic events with
moment magnitude -2 to 1

0.4 > σ₁/σ_c < 0.5

Major slabbing and damage
Seismic events with
moment magnitude 1 to 2

σ₁/σ_c > 0.5

Severe damage
Seismic events with
moment magnitude 2 to 4

$D_i = 0.3$
$\sigma_1/\sigma_c = 0.1$

$D_i = 0.6$
$\sigma_1/\sigma_c = 0.2$

$D_i = 0.95$
$\sigma_1/\sigma_c = 0.3$

$D_i = 1.25$
$\sigma_1/\sigma_c = 0.4$

$D_i = 1.6$
$\sigma_1/\sigma_c = 0.5$

Unconfined Compressive Strength σ_c (MPa)

Maximum Far-Field Stress σ_1 (MPa)

🔴 ASPO 420 Level
🟡 420 Level of the URL

Figure 55: Estimate of damage based on the ratio of the far-field maximum stress (σ_1) to the laboratory short term unconfined compressive strength (σ_c), from Andersson et al. /7/.

67

interacting because of their close proximity. Ortlepp /81/ also concluded that a nuclear waste repository constructed with an extraction ratio of 0.25 at the in-situ stress conditions that exist at the 420 Level of AECL's Underground Research laboratory would not experience significant rockbursts. This conclusion is supported by the observations made during the construction of the 420 Level, where only minor microseismic activity was encountered.

7.4 Fault-slip and Underground Damage

7.4.1 Fault-slip Rockbursts

The most violent and damaging type of rockburst is the fault-slip type /82/ (see Table 3). This type of event is common in South African gold mines where tabular mining operations are taking place at depths greater than 3 km. The damage resulting from this type of event in South Africa, is the rapid ejection of rock into an opening. However, in Canada, the damage resulting from seismic events caused by bulk mining operations at depth of about 2 km is falls of ground, i.e., large blocks of rock falling from the roof of the excavation. These falls of ground are induced by seismic shaking and are much less violent than ejection damage experienced in South Africa /53/. In most cases the damage caused by fault-slip rockbursts in Ontario Mines is minimal /39/. Figure 56 shows the relationship between rockburst magnitude, observed damage and distance from the source of the event. For a seismic event to create severe damage the underground opening has to be close to the source of the event. For example, for a seismic event of magnitude 4, the largest ever recorded in Ontario mines, no damage would be experienced by openings that are located 200 m or more from the source of the seismic event.

The area extent of a mining induced fault-slip event was investigated by Ortlepp /83/. The seismic event associated with the formation of the fault had a moment magnitude 3.4, and occurred at a depth of 2080 m in a South African mine. Despite the large moment magnitude of the seismic event, Ortlepp found that the newly formed fault only had a radius
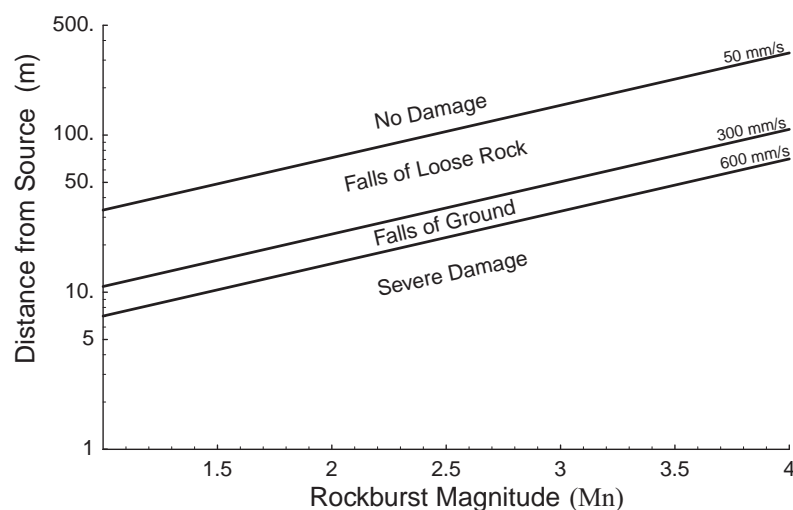

Figure 56: *Damage criteria developed for Canadian hardrock mines, data from /39/. The numbers on the lines in the graph with units of mm/s refer to peak particle velocity.*

of approximately 18 m with offset displacements (slippage) of about 100 mm. Hedley /39/ has also noted that fault-slip events tend to be of small area extent and in most mining situations the slippage occurs when the fault intersects the mine openings.

7.4.2 Natural earthquakes and underground damage

Natural earthquakes are fault-slip events. Therefore it is instructive to evaluate the damage to underground openings caused by these naturally occurring events. A summary of world wide qualitative data regarding the behaviour of underground openings during earthquakes was compiled by Sharma and Judd /95/. The information was compiled from 192 reports of underground behaviour from 85 earthquakes throughout the world. In the course of their study only "94 cases of underground damage were identified while literally thousands of surface structures were damaged". Their main conclusions were

1. Reported damage decreases with increasing depth.

2. Underground facilities constructed in soil can be expected to suffer more damage compared to openings constructed in competent rock.

3. If surface peak ground acceleration values of 0.25 g or less are anticipated in the design, it is unlikely that significant damage would occur to an underground opening at a depth greater than 500 m.

The conclusions from the study carried out by Sharma and Judd /95/ also support the findings discussed in Section 7.4.1, i.e., unless the underground opening is located close to the source of the seismic event it is unlikely to experience significant damage.

7.5 Microseismic monitoring

With the advances in computer technology the monitoring of these stress-induced seismic events is now routine. The monitoring varies from simple source locations to whole-waveform analyses providing some insight into the source mechanisms causing the seismic event. Because of the similarities between mining-induced seismic events and naturally occurring earthquakes the analyses of these seismic events follows the approach used by earthquake seismologists.

It should be noted that seismic events below a magnitude of -1 are seldom recorded in mines because the energy released by these events is so small that it does not cause damage and hence is not classed as a rockburst. These small seismic events, which typically have magnitudes between -6 and -2 are called microseismic events.

Hedley /39/ reported that rockbursts in Canadian mines have been studied since the mid 1930s when they became a problem in the hardrock mines at Kirkland Lake and Sudbury, Ontario. Between 1928 and 1990, almost 4000 rockbursts were reported to the Ontario Ministry of Labour. By 1990 fifteen seismic monitoring systems were in operation at Ontario mines. With the increasing depths of the hardrock mines in the Sudbury basin, rockbursts today are routine and expected, and the potential for their occurrence is incorporated into the mine design. Hence the subject is fairly mature with well established guidelines for

mine design in burst prone ground.

7.6 Methods to control rockbursts

The techniques that are currently used to minimize the effects of mining-induced rockbursts are: mine-layout and sequencing of extraction, and utilization of backfill. Cook /26/ showed that the energy released during mining was a function of the number of mining steps. This practical design tool, which was developed in the 1960s in South Africa, is the Energy Release Rate (*ERR*). The *ERR* is used as an upper bound calculation to determine the potential rockburst intensity. It assumes that no energy is consumed in breaking the rock and all the calculations are based on elastic theory. Thus for any shaped set of openings the *ERR* can be calculated and the proposed mining sequence evaluated. The proposed design depths and layout for a repository will minimize the stress-induced damage and the potential for minor rockbursting. In the areas where opening intersections create complex geometries three-dimensional numerical analyses will be required to assess the stress/strength ratio for each situation and the design principles of *ERR* can be applied.

Current conceptual engineering studies for the design of a nuclear waste repository call for the backfilling of all openings prior to closure. As demonstrated by current mining practice in burst-prone ground, backfilling reduces the occurrence of rockburst significantly /39/. The use of backfill to minimize the number and magnitude of rockbursts can only work if the backfill reduces the total amount of convergence. In a repository most of the convergence will be elastic and will occur during the excavation of a room. However, the thermal loads generated by the used nuclear fuel will also cause the underground openings to converge. Because the rooms will be backfilled before the maximum thermal loads occur, the backfill will be able to reduce the total volumetric closure due to heating the rock mass.

The effect of backfill on tunnel convergence can be evaluated by considering the problem as a ground reaction problem (Figure 57). Consider a plate subjected to a thermal stress σ with a hole with surface tractions equal and opposite to the thermal stress. As the surface tractions are gradually removed, convergence or displacement (u) occurs as shown in Figure 57 by the line p_o to u_o. As the convergence occurs it is resisted by the stiffness of the backfill represented by the line OS in Figure 57. At point S equilibrium is achieved. When equilibrium is achieved the backfill will have been loaded to p_s and the final convergence reduced to u_s. Without the backfill the final convergence would increase to u_o. Such analyses can be carried out to assess the effect of backfill properties and placement sequence. Two of the key problems associated with backfill in this context are:

- quantifying the effect of backfill on rock mass stability, and

- ensuring that the backfill has been placed tight to the rock interface.

In mining, the latter item above is not an issue as most mine backfills are hydraulically placed ensuring adequate contact with the rock.

7.7 Canadian practise

The knowledge base for the design of underground openings against the damage caused by rockbursts has advanced significantly over the last fifty years. For example, in 1992 CANMET published the Rockburst Handbook for Ontario Hardrock Mines /39/ and more recently the Geomechanics Research Centre of Laurentian University published the Rockburst Support Handbook /53/. In addition, the Sudbury Neutrino Project (a major civil engineering installation consisting of a 20-m-diameter, 30-m-high cavern) is located at the 6800 Level (2070 m below surface) of Creighton mine at Sudbury, Ontario. Creighton mine is one of the deepest hard rock mines in Canada and one which experiences seismic events daily. The largest recorded mining-induced seismic event in Canada, magnitude 4, has been recorded at Creighton mine. The Sudbury Neutrino Project has been designed to withstand these large seismic events.

In addition to the hardrock mines in Ontario, rockbursts have been reported in the potash mines of Saskatachewan, the lead and zinc mines of New Brunswick, the gold mines in the Val D'Or area of Quebec and the coal mines in Nova Scotia /39/. Hence rockbursts are not confined to one particular rock type.

7.8 Summary

Excavating large openings at depths in excess of 1 km is routine in Canada's mining industry and mines in Sweden and Finland are approaching 800 to 1000 m depth. In order to make these mining operations safe at these depths the mining industry has developed design guidelines which encompass both theoretical knowledge and practical experience. The experience gained from these deep excavations can be applied to the construction and design of a nuclear waste repository.

The seismic events and associated damage that are caused by these deep mining excavations will not be encountered in a repository constructed between a depth of 400 and 700 m. The major difference between a nuclear waste repository and mining excavations is the
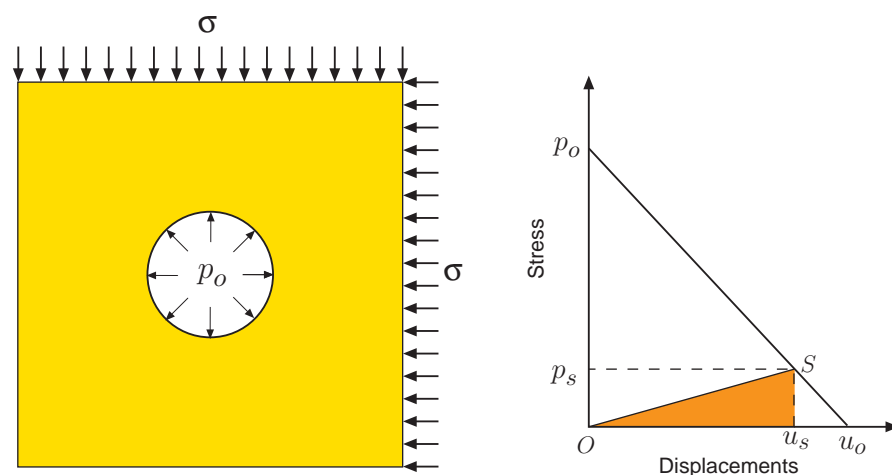
Figure 57: *Illustration of the effect of backfill on total convergence due to thermal loads.*

71

low extraction ratios planned for a repository. With these low extraction ratios the stress concentrations in the rock mass between the rooms containing the waste will not be of sufficient magnitude to exceed the rock mass strength.

The most damaging type of rockburst is the fault-slip type. This type of event is usually found in the deep tabular-mining operations of South Africa. The relatively shallow location of a nuclear waste repository combined with the low extraction ratio will virtually eliminate the risk for this type of rockburst. In order for an underground opening to be significantly damaged by a fault-slip type rockburst, the opening must be located quite close to the source of the seismic event. Given that the site characterization program to be carried out in choosing a repository location will identify the geological faults, the location of the disposal rooms to a fault can be optimized to reduce the rockburst hazard. In addition, backfilling of the repository minimizes the potential for damage resulting from the increase in stress caused by the thermal loading.

8 Conclusions and recommendations

No one criterion or property can be used to assess the performance of an underground opening or the performance of a repository. While there is no unique or single rock mechanics property or condition that would render the performance of a repository unacceptable, certain conditions can be treated as negative factors. For example, a highly fractured rock mass such that the overall rock mass permeability is not acceptable or high in-situ stress magnitudes such that construction of the underground openings will create a safety concern for the construction workers. Outlined below are major rock stability issues that should be addressed during the design of a deep nuclear waste repository.

8.1 Siting requirements

During the site investigations phase, rock mechanics information will be predominately gathered from examination and testing of the rock core. Two major tasks must be accomplished during this period:

1. an assessment of the quality of the rock mass with depth.

2. an assessment of the state of stress with depth.

Empirical methods such as the Q system can be used to assess tunnel support requirements and to establish rock quality domains during the preliminary design phase of the project.

The laboratory testing should be carried out to determine the crack initiation stress, the long-term strength, peak strength and post-peak response in accordance with the information provided in Section 3.1. The determination of these parameters should be determined from stress-strain data, as well as acoustic emission testing techniques, using nationally and/or internationally recognized standards, e.g., the Suggested Methods for Testing of the International Society for Rock Mechanics or ASTM .

The in-situ stress state must be measured with confidence. The number of measurements and the method(s) used will be a function of the geology of the site.

8.2 Rock stability during design and construction

In situations where the stability of a tunnel is controlled by discontinuities, traditional approaches using limit equilibrium analysis or numerical tools such as *3DEC* will be appropriate.

The information provided in this report indicates that stress-induced failure will occur on the boundary of an underground opening when the maximum tangential stresses on the boundary of the opening exceed approximately 0.3 to 0.4 the laboratory uniaxial compressive strength. Hence to assess the potential for spalling, numerical analysis will be required for the various shaped openings planned for the repository. These numerical analysis can be used to optimize the shape of the tunnels, the orientation of the tunnels relative to the far-field

stress state, intersection support, and pillar dimensions.

The support for the tunnels in a repository is expected to range from light support pressure equivalent to standard spot-bolting to local bolts and mesh and fibre-reinforced shotcrete. At major intersections additional support, such as longer bolts and/or thicker shotcrete, may also be required.

8.3   Aspect to consider when choosing construction method

The layout of repository will be similar to a mine using a room-and-pillar mining method. A drill-and-blast excavation method will provide the maximum flexibility for such an excavation technique. In addition, should spalling be encountered, the shape of the tunnels can be changed to control the extent of spalling as illustrated in Section 5.

8.4   Recommendations

The two common modes of failure (structurally controlled and stress-induced spalling) may be analyzed using the approaches outlined in this report. However, it is not clear what approach should be used when the mode of failure is transitional, i.e., structure/stress. Apart from the ZEDEX experiment, very little rock mechanics research has been carried out with the combined in-situ stress magnitudes and well defined structure such as occurs at the 450 Level in Äspö HRL. Because of the likelihood of encountering these transitional conditions at the depth of the proposed repository in Sweden it is recommended that further rock mechanics research be carried out to assess the stress at failure for these transitional conditions. In particular, the strength of the pillars between the emplacement boreholes should be established such that the pillar dimensions can be assessed by means other than empirical formulas developed from mining conditions.

References

[1] AB, S. K., 2000. Integrated account of method, site selection and programme prior to the site investigation phase. SKB Technical Report TR-01-03, Swedish Nuclear Fuel and Waste Management Company, Stockholm, Sweden.

[2] Aglawe, J. P., 1998. *Unstable and Violent Failure Around Underground Openings in Highly Stressed Ground.* Ph.D. thesis, Department of Mining Engineering, Queen's University, Kingston, Canada. In Progress.

[3] Amadei, B. and O. Stephansson, 1997. *Rock Stress and Its Measurement.* Chapman & Hall, London, 1st edn.

[4] Andersson, C. and J. Söderhäll, 2001. Rock mechanical conditions at the äspö HRL. A study of the correlation between geology, tunnel maintenance and tunnel shape. Tech. Rep. SKB R 01-53, Swedish Nuclear Fuel and Waste Management Company, Stockholm.

[5] Andersson, J. and C. Ljunggren, 1997. A geostatistical approach to evaluate differences in results between hydraulic fracturing and overcoring. In *Proc. Int. Symp. on Rock Stress,* Kumamoto (Ed. K. Sugawara and Y. Obara), pp. 223–227. A.A. Balkema, Rotterdam.

[6] Andersson, J., A. Ström, K.-E. Almén and L. O. Ericsson, 2000a. What requirements does the KBS-3 repository make on the host rock? geoscientific suitability indicators and criteria for siting and site evaluation. SKB Technical Report TR-00-12, Swedish Nuclear Fuel and Waste Management Company, Stockholm, Sweden.

[7] Andersson, J., A. Ström, C. Svemar, K.-E. Almén and L. E. Ericsson, 2000b. What requirements does the kbs-3 repository make on the host rock? geoscientific suitability indicators and criteria for siting and site evaluation. Technical Report TR-00-12, Swedish Nuclear Fuel and Waste Management Company, Stockholm, Sweden.

[8] Arjang, B., 1989. Pre-mining stresses at some hard-rock mines in the Canadian Sheild. In *Proc. 30th U.S. Symp. Rock Mech.,* Morgentown, pp. 545–551. A.A. Balkema, Rotterdam.

[9] Arjang, B. and G. Herget, 1997. *In situ* ground stresses in the Canadian hardrock mines: an update. *Int. J. Rock Mech. Min. Sci.*, **34**(3-4):652. Paper No. 015.

[10] Barton, N. and E. Grimstad, 1994. The q-system following twenty years of application in NWT support selection. *Felsbau*, **12**(6):428–436.

[11] Barton, N. R. and V. Choubey, 1977. The shear strength of rock joints in theory and practice. *Rock Mech. and Rock Engin.*, **10**:1–54.

[12] Barton, N. R., R. Lien and J. Lunde, 1974. Engineering classification of rock masses for the design of tunnel support. *Rock Mech. and Rock Engin.*, **6**:189–239.

[13] Batchelor, A. S., K. A. Kwakwa, A. J. Proughten and N. Davies, 1997. Determination

of the in-situ stresses at Sellafield, UK: A case study. In *Proc. Int. Symp. on Rock Stress,* Kumamoto (Ed. K. Sugawara and Y. Obara), pp. 265–276. A.A. Balkema, Rotterdam.

[14] Bieniawski, Z. T., 1967. Mechanism of brittle fracture of rock, Parts I, II and III. *Int. J. Rock Mech. Min. Sci. & Geomech. Abstr.*, **4**(4):395–430.

[15] Bieniawski, Z. T., 1989. *Engineering Rock Mass Classifications*. John Wiley & Sons, New York.

[16] Brace, W. F., B. Paulding and C. Scholz, 1966. Dilatancy in the fracture of crystalline rocks. *J. Geophys. Res.*, **71**:3939–3953.

[17] Brady, B. H. G. and E. T. Brown, 1993. *Rock Mechanics for Underground Mining*. Chapman and Hall, London, 2nd edn.

[18] Brown, E. T., ed., 1981. *Rock Characterization, Testing and Monitoring, ISRM Suggested Methods*. Pergamon Press, Oxford.

[19] Brown, E. T. and E. Hoek, 1978. Trends in relationships between measured and *in situ* stresses and depth. *Int. J. Rock Mech. Min. Sci. & Geomech. Abstr.*, **15**:211–215.

[20] Carlsson, A. and R. Christiansson, 1986. Rock stress and geological structures in the Forsmark area. In *Proc. Int. Symp. on Rock Stressand Rock Stress Measurements,* Stockholm (Ed. O. Stephansson). Centek Publishers, Lulea.

[21] Carlsson, A. and T. Olsson, 1982. Characterization of deep-seated rock masses by means of borehole investigations. Research and Development 5:1, Swedish State Power Board, Stockholm, Sweden.

[22] Castro, L. A. M., M. W. Grabinbsky and D. R. McCreath, 1997. Damage initation through extension fracturing in a moderately jointed brittle rock mass. *Int. J. Rock Mech. Min. Sci. & Geomech. Abstr.*, **34**(3-4).

[23] Castro, L. A. M., D. R. McCreath and P. Oliver, 1996. Rockmass damage initiation around the Sudbury Neutrino Observatory cavern. In *Proc. 2nd North American Rock Mechanics Symposium,* Montreal (Ed. M. Aubertin, F. Hassani and H. Mitri), vol. 2, pp. 1589–1595. A.A. Balkema, Rotterdam.

[24] Christiansson, R. and C. D. Martin, 2001. In-situ stress profiles with depth from site characterization programs for nuclear waste repositories. In *Proc. EUROCK 2001,* Espoo, Finland (Ed. P. Särkkä and P. Eloranta), pp. 737–742. A.A. Balkema, Rotterdam.

[25] Cook, N. G. W., 1965. A note on rockbursts considered as a problem of stability. *J. S. African Inst. Min. and Metall.*, **65**(8):436–528.

[26] Cook, N. G. W., 1967. The design of underground excavations. In *Proc. 8th U.S. Symp. on Rock Mechanincs,* Univ. of Minnesota (Ed. C. Fairhurst), pp. 167–193. Am. Inst. Min. Metall. and Petrol. Engins., New York.

[27] Cook, N. G. W., 1970. An experiment proving that dilatancy is a pervasive volumetric property of brittle rocks loaded to failure. *Rock Mech. and Rock Engin.*, **2**:181–188.

[28] Cook, N. G. W., E. Hoek, J. P. G. Pretorius, W. D. Ortlepp and M. D. G. Salamon, 1966. Rock mechanics applied to the study of rockbursts: a synthesis of the results of rockburst research in South Africa up to 1965. *J. S. African Inst. Min. and Metall.*, pp. 436–528.

[29] Cundall, P. A., D. O. Potyondy and C. A. Lee, 1996. Micromechanics-based models for fracture and breakout around the Mine-by tunnel. In *Proc. Int. Conf. on Deep Geological Disposal of Radioactive Waste,* Winnipeg (Ed. J. B. Martino and C. D. Martin), pp. 113–122. Canadian Nuclear Society, Toronto.

[30] Deere, D. U., 1980. Geological considerations. In *Rock Mechanics in Engineering Practice* (Ed. K. G. Stagg and O. C. Zienkiewicz), pp. 1–20. John Wiley & Sons, London.

[31] Detournay, E. and C. M. St. John, 1988. Design charts for a deep circular tunnel under non-uniform loading. *Rock Mech. and Rock Engin.*, **21**(2):119–137.

[32] Diederichs, M. S., 1999. *Instability of Hard Rockmasses: The Role of Tensile Damage and Relaxation.* Ph.D. thesis, Dept. of Civil Engineering, University of Waterloo, Waterloo, Canada.

[33] Diederichs, M. S. and P. K. Kaiser, 1999. Tensile strength and abutment relaxation as failure control mechanisms in underground excavations. *Int. J. Rock Mech. Min. Sci.*, **36**(1):69–96.

[34] Fairhurst, C., 1993. Analysis and design in rock mechanics–The general context. In *Comprehensive Rock Engineering – Rock Testing and Site Characterization* (Ed. J. A. Hudson), vol. 2, pp. 1–29. Pergamon Press, Oxford.

[35] Griffith, A. A., 1924. Theory of rupture. In *Proc. First International Congress on Applied Mechanics,* Delft, pp. 55–63.

[36] Grimstad, E. and R. Bhasin, 1997. Rock support in hard rock tunnels under high stress. In *Proc. Int. Symp. on Rock Support–Applied Solutions for Underground Structures,* Lillehammer (Ed. E. Broch, A. Myrvang and G. Stjern), pp. 504–513. Norwegian Society of Chartered Engineers, Oslo.

[37] Hajiabdolmajid, V., C. D. Martin and P. K. Kaiser, 2000. Modelling brittle failure. In *Proc. 4th North American Rock Mechanics Symposium, Narms 2000* Seattle (Ed. J. Girard, M. Liebman, C. Breeds and T. Doe), pp. 991–998. A.A. Balkema, Rotterdam.

[38] Hakala, M. and E. Heikkila, 1997. Summary report - Development of laboratory tests and the stress-strain behaviour of Olkiluoto mica gneiss. Tech. Rep. POSIVA-97-04, Posiva Oy, Helsinki, Finland.

[39] Hedley, D. G. F., 1992. Rockburst handbook for Ontario hardrock mines. CANMET

Special Report SP92-1E, Canada Centre for Mineral and Energy Technology.

[40] Hedley, D. G. F. and F. Grant, 1972. Stope-and-pillar design for the Elliot Lake Uranium Mines. *CIM Bull.*, **65**:37–44.

[41] Hedley, D. G. F., J. W. Roxburgh and S. N. Muppalaneni, 1984. A case history of rockbursts at Elliot Lake. In *Proc. 2nd Int. Conf. on Stability in Underground Mining,* Lexington, pp. 210–234. American Institute of Mining, Metallurgical and Petrolem Engineers, Inc., New York.

[42] Herget, G., 1974. Ground stress determinations in Canada. *Rock Mech. and Rock Engin.*, **10**(3-4):37–51.

[43] Herget, G., 1987. Stress assumptions for underground excavations in the Canadian Shield. *Int. J. Rock Mech. Min. Sci. & Geomech. Abstr.*, **24**(1):95–97.

[44] Herget, G., 1993. Rock stresses and rock stress monitoring in Canada. In *Comprehensive Rock Engineering - Rock Testing and Site Characterization* (Ed. J. A. Hudson), vol. 3, chap. 19, pp. 473–496. Pergamon Press, Oxford.

[45] Herget, G. and B. Arjang, 1990. Update on ground stresses in the Canadian Shield. In *Proc. Stresses in Underground Structures,* Ottawa (Ed. G. Herget, B. Arjang, M. Bétournay, M. Gyenge, S. Vongpaisal and Y. Yu), pp. 33–47. Canadian Government Publishing Centre, Ottawa, Canada.

[46] Hoek, E. and E. T. Brown, 1980. *Underground Excavations in Rock*. The Institution of Mining and Metallurgy, London.

[47] Hoek, E. and E. T. Brown, 1997. Practical estimates of rock mass strength. *Int. J. Rock Mech. Min. Sci.*, **34**(8):1165–1186.

[48] Hoek, E., P. K. Kaiser and W. F. Bawden, 1995. *Support of Underground Excavations in Hard Rock*. A. A. Balkema, Rotterdam.

[49] Hudson, J. A., E. T. Brown and C. Fairhurst, 1972. Shape of the complete stress-strain curve for rock. In *Proc. 13th U.S. Symp. on Rock Mechanics,* Urbana (Ed. E. Cording), pp. 773–795. American Society of Civil Engineers, New York.

[50] Hutchinson, D. J. and M. S. Diederichs, 1996. *Cablebolting in Underground Mines*. BiTech Publishers Ltd., Richmond.

[51] Hyett, A. J., C. G. Dyke and J. A. Hudson, 1986. A critical examination of basic concepts associated with the existence and measurement of *in situ* stress. In *Proc. Int. Symp. on Rock Stress and Rock Stress Measurements* (Ed. O. Stephansson), pp. 687–694. Centek, Lulea.

[52] Johansson, E. and M. Hakala, 1995. Rock mechanical aspect on the critical depth of kbs-3 type repository based on brittle rock strength criterion developed at URL iin

Canada. Arbets Rapport AR D-95-014, Swedish Nuclear Fuel and Waste Management Company, Stockholm, Sweden.

[53] Kaiser, P. K., D. R. McCreath and D. D. Tannant, 1997. Rockburst support. In *Canadian Rockburst Research Program 1990-95*, vol. 2, p. 342. Canadian Mining Industry Research Organization (CAMIRO), Sudbury.

[54] Linkov, A. M., 1992. Dynamic phenomena in mines and the problem of stability. Distributed by MTS Systems Corporation, 14000 Technology Drive, Eden Prairie, MN, USA, 55344. Notes from a course of lectures presented by Dr. Linkov as MTS Visiting Professor of Geomechanics at the University of Minnesota, Minneapolis, MN, USA.

[55] Ljunggren, C., 1998. Overcoring rock stress measurements in borehole KR6 at Hästholmen, Finland. Work Report 98-70, Posiva Oy, Helsinki, Finland.

[56] Ljunggren, C. and K. Klasson, 1996. Rock stress measurements at the three investigation sites, Kivetty, Romuvaara and Olkiluoto, Finland. Work Report PATU-96-26e, Posiva Oy, Helsinki, Finland.

[57] Lunder, P. J. and R. Pakalnis, 1997. Determination of the strength of hard-rock mine pillars. *CIM Bull.*, **90**(1013):51–55.

[58] Lundholm, B., 2000. Rock stress and rock stress measurements at Äspö. International Progress Report IPR-00-024, Swedish Nuclear Fuel and Waste Management Company, Stockholm, Sweden.

[59] Martin, C. D., 1990. Characterizing *in situ* stress domains at the AECL Underground Research Laboratory. *Can. Geotech. J.*, **27**:631–646.

[60] Martin, C. D., 1997. Seventeenth Canadian Geotechnical Colloquium: The effect of cohesion loss and stress path on brittle rock strength. *Can. Geotech. J.*, **34**(5):698–725.

[61] Martin, C. D. and N. A. Chandler, 1993. Stress heterogeneity and geological structures. *Int. J. Rock Mech. Min. Sci. & Geomech. Abstr.*, **30**(7):993–999.

[62] Martin, C. D. and N. A. Chandler, 1994. The progressive fracture of Lac du Bonnet granite. *Int. J. Rock Mech. Min. Sci. & Geomech. Abstr.*, **31**(6):643–659.

[63] Martin, C. D. and R. Christiansson, 1991. Overcoring in highly stressed granite – The influence of microcracking. *Int. J. Rock Mech. Min. Sci. & Geomech. Abstr.*, **28**(1):53–70.

[64] Martin, C. D., M. Diederichs and V. Hajiabdolmajid, 1998. Damage mechanisms in brittle rock masses. In *Proc. 51st Canadian Geotechnical Conference,* Edmonton, vol. 2, pp. 581–588.

[65] Martin, C. D., P. K. Kaiser and J. M. Alcott, 1996. Predicting the depth of stress-induced failure around underground openings. In *Proc. 49th Canadian Geotechnical Conference,* St. John's, vol. 1, pp. 105–114. C-CORE, St. John's.

[66] Martin, C. D., P. K. Kaiser and D. R. McCreath, 1999a. Hoek-Brown parameters for predicting the depth of brittle failure around tunnels. *Can. Geotech. J.*, **36**(1):136–151.

[67] Martin, C. D. and W. G. Maybee, 2000. The strength of hard-rock pillars. *Int. J. Rock Mech. Min. Sci.*, **37**(8):1239–1246.

[68] Martin, C. D., R. S. Read and N. A. Chandler, 1990a. Does scale influence *in situ* stress measurements?– Some findings at the Underground Research Laboratory. In *Proc. First Int. Workshop on Scale Effects in Rock Masses,* Loen, Norway (Ed. A. P. da Cunha), pp. 307–316. A.A. Balkema, Rotterdam.

[69] Martin, C. D., R. S. Read and E. J. Dzik, 1995. Near-face cracking and strength around underground openings. In *Proc. 2nd Int. Conf. on Mechanics of Jointed and Faulted Rock,* Vienna (Ed. H. P. Rossmanith), pp. 747–752. A.A. Balkema, Rotterdam.

[70] Martin, C. D., R. S. Read and P. A. Lang, 1990b. Seven years of *in situ* stress measurements at the URL - an overview. In *Proc. 31st U.S. Symp. on Rock Mechanicis,* Golden (Ed. W. Hustrulid and G. Johnson), pp. 15–25. A.A. Balkema, Rottterdam.

[71] Martin, C. D. and B. Stimpson, 1994. The effect of sample disturbance on laboratory properties of Lac du Bonnet granite. *Can. Geotech. J.*, **31**(5):692–702.

[72] Martin, C. D., D. D. Tannant, S. Yazici and P. K. Kaiser, 1999b. Stress path and instability around mine openings. In *Proc. 9th, ISRM Congress on Rock Mechanics,* Paris (Ed. G. Vouille and P. Berest), vol. 1, pp. 311–315. A. A. Balkema, Rotterdam.

[73] Martin, C. D., S. Yazici, R. P. Young and R. Murdie, 1997. Low stress damage mechanisms around underground openings in brittle rocks. In *Proc. 50th Canadian Geotechnical Conference,* Ottawa (Ed. G. E. Bauer), vol. 1, pp. 110–117.

[74] Maybee, W. G., 1999. *Pillar design in hard brittle rocks*. Master's thesis, School of Engineering, Laurentian University, Sudbury, ON, Canada.

[75] McGarr, A., 1978. State of stress in the earth's crust. *Ann. Rev. Earth Planet. Sci.*, **6**:405–436.

[76] Mogi, K., 1966. Pressure dependence of rock strength and transition from brittle fracture to ductile flow. *Bulletin Earthquake Res. Inst. (Japan)*, **44**:215–232.

[77] Myrvang, A. M., 1997. Evaluation of in-situ rock stress measurements at the ZEDEX test area. Progress Report HRL-97-22, Swedish Nuclear Fuel and Waste Management Company, Stockholm, Sweden.

[78] Nickson, S., D. Sprott, W. F. Bawden and A. Coulson, 1997. A geomechanical study for a shaft wall rehabilitation program. In *Proc. 99th CIM Annual General Meeting,* Vancouver, pp. 1–20. Canadian Institute of Mining, Montreal.

[79] Olsson, O., S. Emsley, C. Bauer, S. Falls and L. Stenberg, 1996. ZEDEX–A study of the

zone of excavation disturbance for blasted and bored tunnels. International Cooperation Report 96-03, Swedish Nuclear Fuel and Waste Management Company, Stockholm, Sweden. 3 Volumes.

[80] Olsson, O. L., 2000. Underground storage for nuclear waste in sweden. In *Proc. EUROCK 2000 Symposium,* Aachen (Ed. D. G. für Geotechnik e.V. (DGGT)), pp. 117–124. Verlag Glückauf GmbH, Essen.

[81] Ortlepp, W. D., 1992a. Assessment of rockburst risk in the Underground Research Laboratory, Pinawa, Manitoba, Canada. Tech. Rep. 195524, Overview Report for Atomic Energy of Canada Limited by Steffen, Robertson & Kirsten.

[82] Ortlepp, W. D., 1992b. The design of support for the containment of rockburst damage in tunnels – an engineering approach. In *Proc. Int. Symp. on Rock Support in Mining and Underground Construction,* Sudbury (Ed. P. K. Kaiser and D. R. McCreath), pp. 593–609. A. A. Balkema, Rotterdam.

[83] Ortlepp, W. D., 1992c. Note on fault-slip motion inferred from a study of micro-cataclastic particles from an underground shear rupture. *Pageoph*, **139**(3/4):167–195.

[84] Pettitt, W., 2001. Analysis of the in-situ principal stress field at the HRL using acoustic emission data. International Progress Report SKB-IPR-01-09, Swedish Nuclear Fuel and Waste Management Company, Stockholm, Sweden.

[85] Potyondy, D. O. and C. P. A., 1998. Modeling notch-formation mechanisms in the URL Mine-by Test Tunnel using bonded assemblies of circular particles. *Int. J. Rock Mech. Min. Sci. & Geomech. Abstr.*, **35**(4-5):510–511. Paper:067.

[86] Potyondy, D. O. and P. A. Cundall, 2000. Bonded-particle simulations of the in-situ failure test at Olkiluoto. Working Report 2000-29, Posiva Oy, Helskini, Finland. 76p.

[87] Potyondy, D. O., P. A. Cundall and C. A. Lee, 1996. Modelliing rock using bonded assemblies of circular particles. In *Proc. 2nd North American Rock Mechanics Symposium,* Montreal (Ed. M. Aubertin, F. Hassani and H. Mitri), vol. 2, pp. 1937–1944. A.A. Balkema, Rotterdam.

[88] Pritchard, C. J. and D. G. F. Hedley, 1993. Progressive pillar failure and rockbursting at Denison Mine. In *Proc. 3rd Int. Symp. on Rockbursts and Seismicity in Mines,* Kingston (Ed. R. P. Young), pp. 111–116. A.A. Balkema, Rotterdam.

[89] Read, R. S., 1996. Characterizing excavation damage in highly stressed granite at AECL's Underground Research Laboratory. In *Proc. Int. Conf. on Deep Geological Disposal of Radioactive Waste,* Winnipeg (Ed. J. B. Martino and C. D. Martin), pp. 35–46. Canadian Nuclear Society, Toronto.

[90] Read, R. S. and N. A. Chandler, 1997. Minimizing excavation damage through tunnel design in adverse stress conditions. In *Proceedings of the International Tunnelling Association World Tunnel Congress,* Vienna, vol. 1, pp. 23–28. A.A. Balkema, Rotterdam.

[91] Read, R. S. and C. D. Martin, 1996. Technical summary of AECL's Mine-by Experiment Phase 1: Excavation response. AECL Report AECL-11311, Atomic Energy of Canada Limited.

[92] Rhén, I., G. Gustafson, R. Stanfors and P. Wikberg, 1997. ÄSPÖ HRL – Geoscientific evaluation 1997/5: Models based on site characterization 1986-1995. SKB Technical Report TR97-06, Swedish Nuclear Fuel and Waste Management Company, Stockholm, Sweden.

[93] Salamon, M. D. G., 1984. Energy considerations in rock mechanics: fundamental results. *J. S. African Inst. Min. and Metall.*, **84**:233–246.

[94] Santarelli, F. J. and M. B. Dusseault, 1991. Core quality contol in petroleum engineering. In *Proc. 32nd U.S. Symp. on Rock Mechanics,* Norman (Ed. J.-C. Roegiers), pp. 111–120. A.A. Balkema, Rotterdam.

[95] Sharma, S. and W. R. Judd, 1991. Underground opening damage from earthquakes. *Engineering Geology*, **30**:263–276.

[96] Söder, P.-E. and N. Krauland, 1990. Determination of pillar strength by full scale pillar tests in the Laisvall mine. In *Proc. 11th Plenary Scientific Session of the Int. Bureau Strata Mechanics, World Mining Congress,* Novosibirsk (Ed. A. Kidybiński and J. Dubiński), pp. 39–59. A.A. Balkema, Rotterdam.

[97] Stacey, T. and C. H. Page, 1986. *Practical Handbook for Underground Rock Mechanics*, vol. 12 of *Series on Rock and Soil Mechanics*. Trans Tech Publications, Clausthal-Zerrerfeld, Germany.

[98] Stephansson, O., 1993. Rock stress in the Fennoscandian Shield. In *Comprehensive Rock Engineering - Rock Testing and Site Characterization* (Ed. J. A. Hudson), vol. 3, pp. 445–459. Pergamon Press, Oxford.

[99] Stephansson, O. and P. Ångman, 1984. Hydraulic fracturing stress measurements at Forsmark and Stidsvig, Sweden. Research Report TULEA 1984:30, Luleå University, Luleå, Sweden.

[100] Stille, H., 1992. Rock support in theory and practice. In *Proc. Int. Symp. on Rock Support in Mining and Underground Construction,* Sudbury (Ed. P. K. Kaiser and D. R. McCreath), pp. 421–438. A. A. Balkema, Rotterdam.

[101] Stille, H., 1996. Summary of rock mechanical results from the construction of Äspö Hard Rock Laboratory. Progress Report HRL-96-07, Swedish Nuclear Fuel and Waste Management Company, Stockholm, Sweden.

[102] Swan, G., 1985. Strength distributions and potential for multiple pillar collapse. Division Report MRP 85-127 (TR), Canada Centre for Mineral and Energy Technology (CANMET), Ottawa, Canada.

[103] Tapponnier, P. and W. F. Brace, 1976. Development of stress-induced microcracks in Westerly granite. *Int. J. Rock Mech. Min. Sci. & Geomech. Abstr.*, **13**:103–112.

[104] Vasak, P. and P. K. Kaiser, 1995. Tunnel stability assessment during rockbursts. In *Proc. CAMI'95: 3rd Canadian Conference on Computer Applications in the Mineral Industry,* Montreal (Ed. H. S. Mitri), pp. 238–247. McGill University, Montreal.

[105] Wagner, H., 1987. Design and support of underground excavations in highly stressed rock. In *Proc. 6th ISRM Int. Congress on Rock Mechanics,* Montreal (Ed. G. Herget and S. Vongpaisal), vol. 3, pp. 1443–1457. A.A. Balkema, Netherlands.

[106] Wiles, T. D. and P. K. Kaiser, 1990. A new approach for the statistical treatment of stress tensors. In *Proc. Stresses in Underground Structures,* Ottawa (Ed. G. Herget, B. Arjang, M. Bétournay, M. Gyenge, S. Vongpaisal and Y. Yu), pp. 62–76. Canadian Government Publishing Centre, Ottawa, Canada.

[107] Wiles, T. D. and P. K. Kaiser, 1994. *In situ* stress determination using the under-excavation technique—I. Theory. *Int. J. Rock Mech. Min. Sci. & Geomech. Abstr.*, **31**(5):439–446.

Appendices

A   Triaxial strength from Äspö samples

Table A1: *Summary of laboratory triaxial testing from Äspö samples.*

Borehole	σ_3	σ_1
KA3545G	5	258
KA3545G	20	350
KA3545G	20	327
KA3545G	50	528
KA3545G	50	523
KA3551G	5	239
KA3557G	5	272
KA3557G	20	326
KA3557G	40	434
KA3557G	50	455
KXZA4	11.3	216.8
KXZA4	15	311.8
KXZA5	29	162.8
KXZA5	30	346.1
KXZA6	3	152.1
KXZC4	10	244.5
KXZC4	25	254.8
KXZC4	29.5	356
KXZC5	17.5	202.7
KXZC5	19.1	115.9
KXZC5	20	331.9
KXZC6	12.5	200.8